Mechanics of morphogenesis

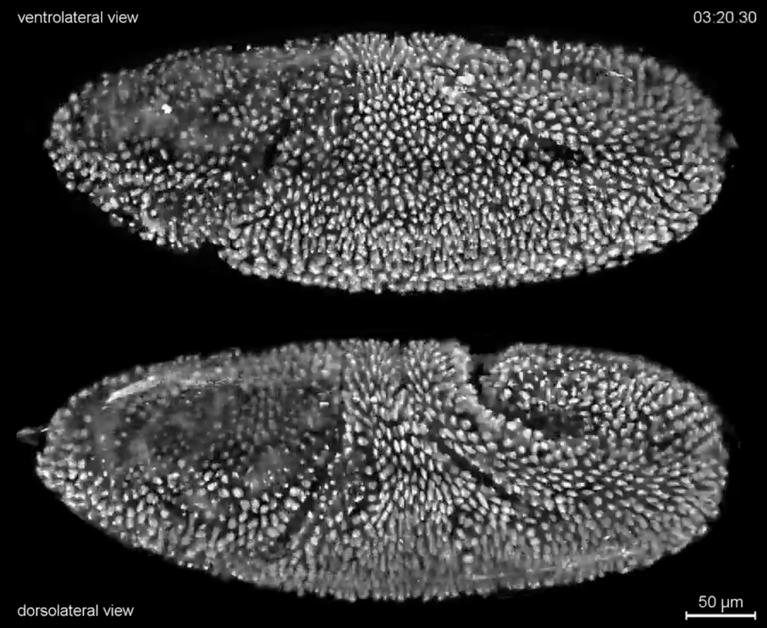

Tomer *et al* (2012)

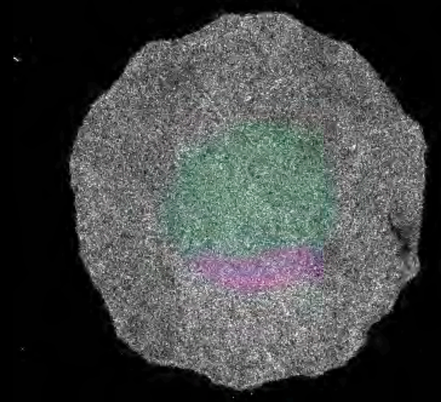

Saadhoui et al, 2018

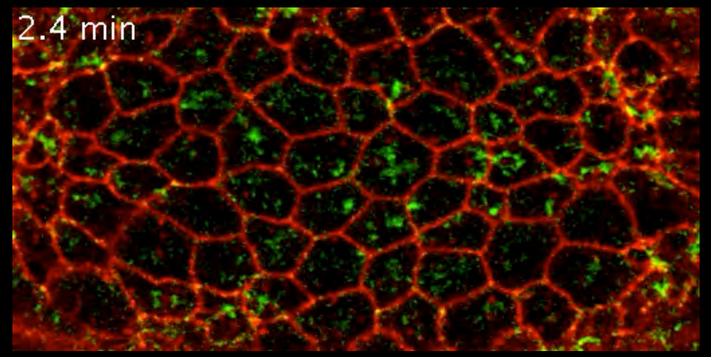

Martin *et al* (2009)

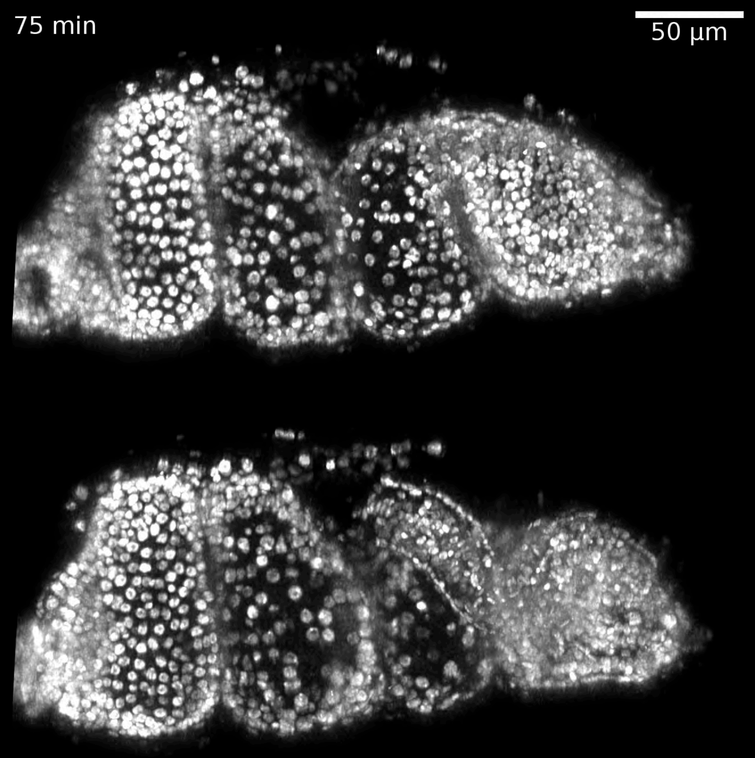

Mitchell *et al* (2022)

[On board]

Mechanics of morphogenesis

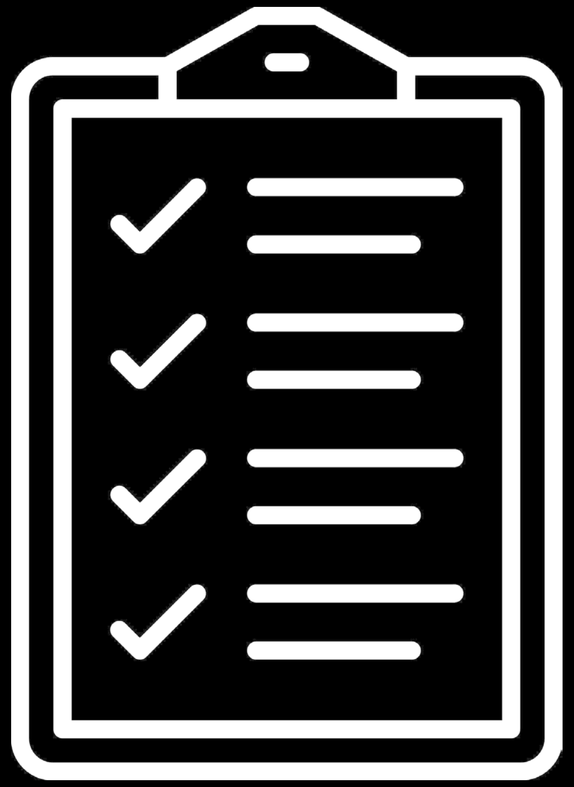

?

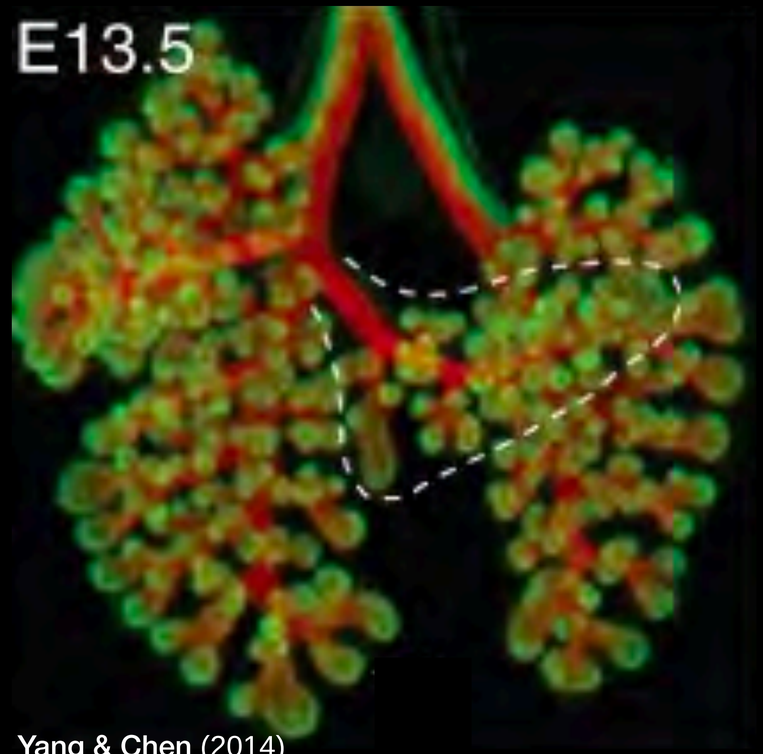

Yang & Chen (2014)

[On board]

Mechanics of morphogenesis

tissue engineering

in vitro

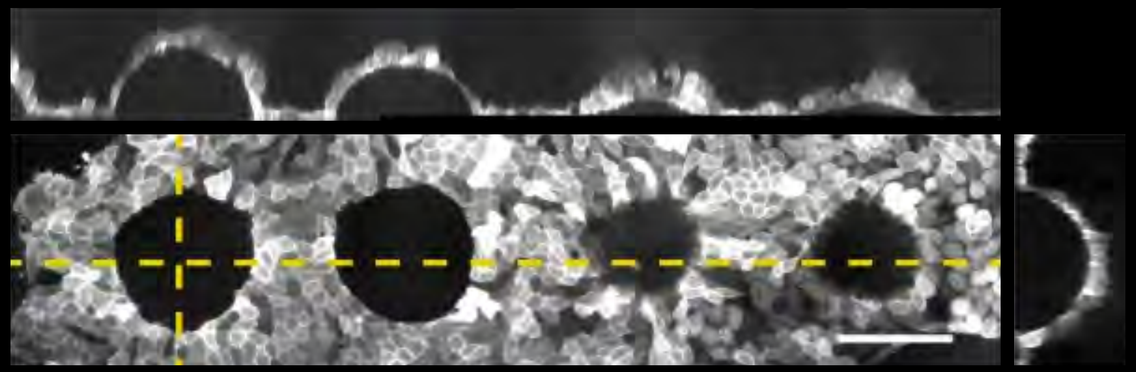

Latorre, et al Nature 2018

development & regeneration

in vivo / ex vivo

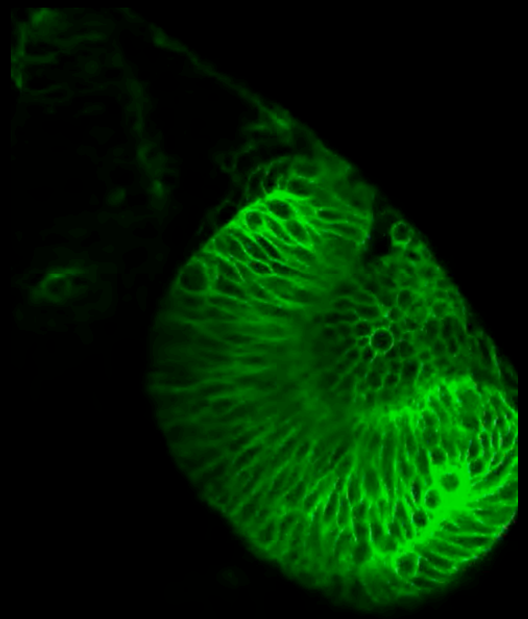

Heerman et al *eLife* 2015

[On board]

Mechanics of morphogenesis

Big space to explore

Focusing on specific models as examples

Patterning
- french flag & cell specification
- Reaction-diffusion

Gastrulation

Morphing tissues as active solids/fluids
- Cell mechanics in convergent extension
- Tissue-scale fluid flow
- Self-organization of convergent extension

Mechanics driving tissue curvature
- Bilayer bending & ventral furrow

Organogenesis

- Wrinkling & buckling
- Programmed shape changes

Mechanics of visceral organ morphogenesis
- Midgut tissue folding in flies
- Heart morphogenesis
- branching morphogenesis

Fridtjof Brauns [KITP, UCSB]

Development is a sequence of dynamic, self-organized geometric transformations

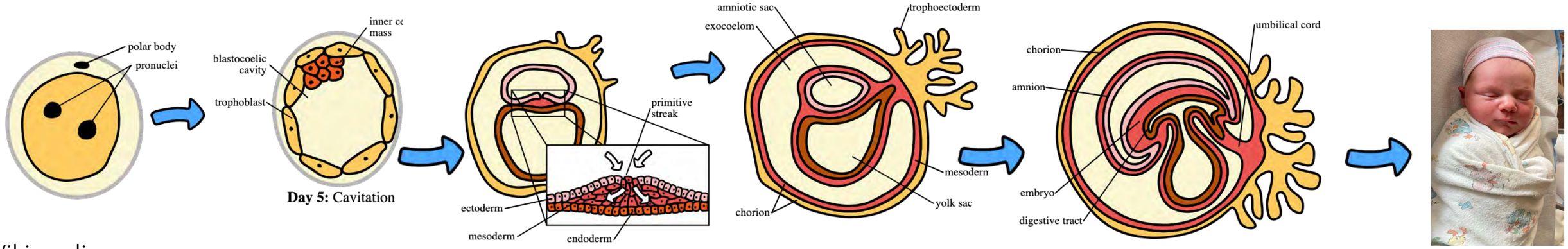

Wikimedia

gastrulation

organ morphogenesis

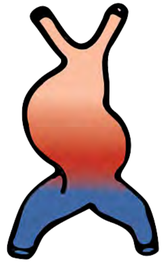

Morphogenesis: from genes to geometry

Patterns of genes

fly embryo
stained with fluorescent tags

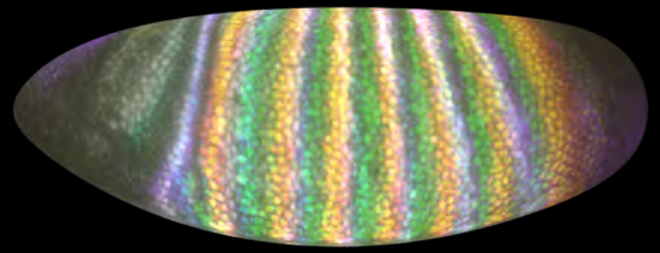

fly leg

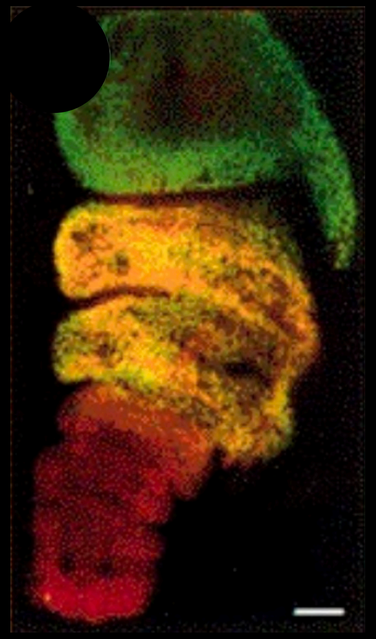

Lecuit & Cohen (1997)

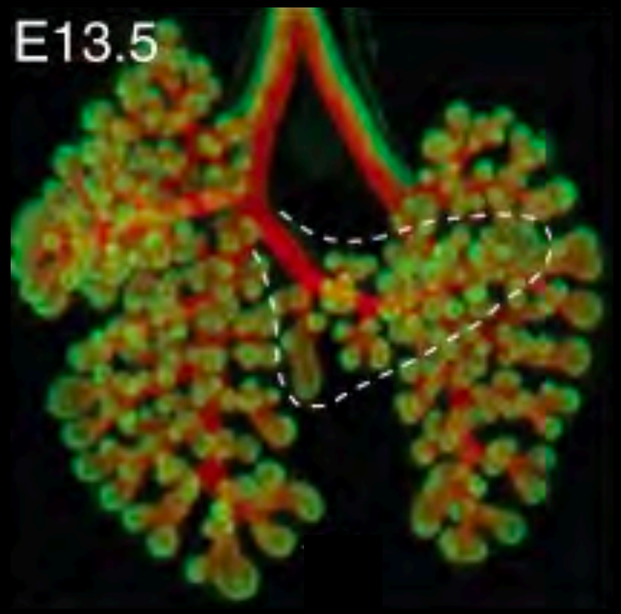

Yang & Chen (2014)

Lewis, Nüsslein-Volhard, Wieschaus, Levine, Gehring, Kaufman, Scott, Weiner, & others
Mitchell*, Lefebvre*, Jain-Sharma*, *et al* (2022)

Patterning is part of morphogenesis: two paradigmatic frameworks

Classic mechanisms of patterning:

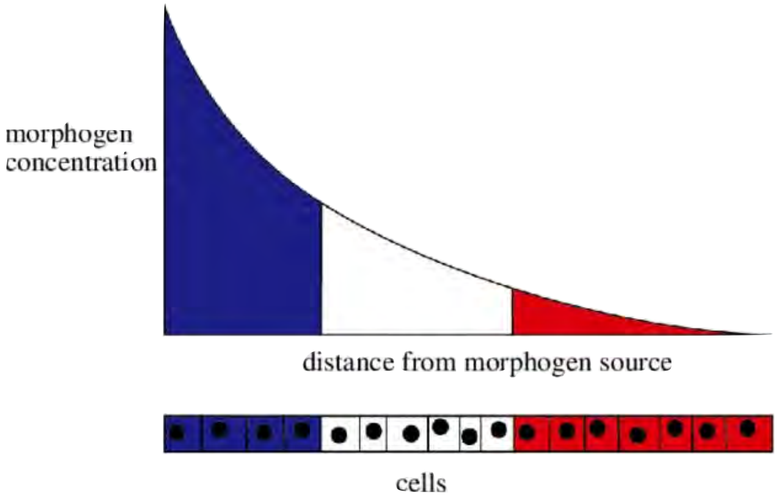

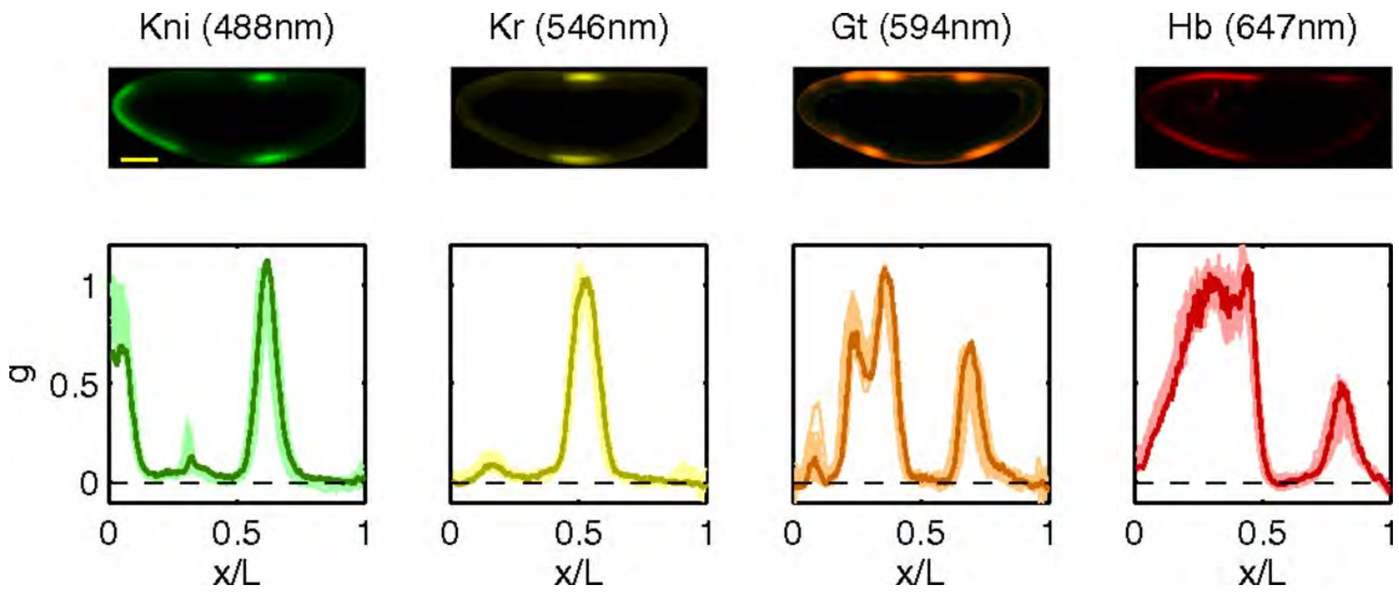

cells compute relative to a threshold

$$I_{g\to x} = \int dg\, P_g(g)\left(S[P_x(x)] - S[P(x|g)]\right)$$

Dubois et al *PNAS* 2012

See also Petkova et al *Cell* and David Bruckner et al *Nat Phys*

Patterning is part of morphogenesis: two paradigmatic frameworks

Classic mechanisms of patterning:

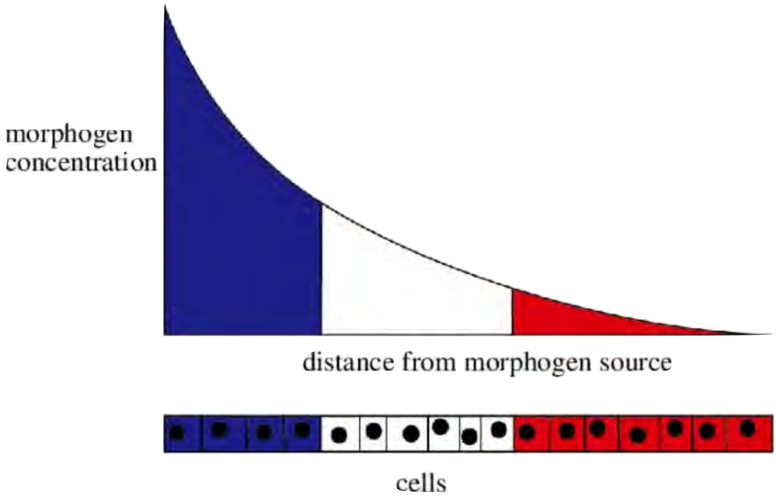

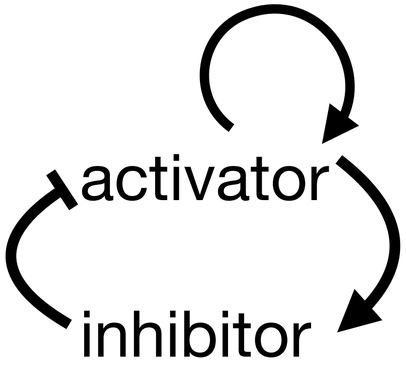

Turing, *Phil Trans Royal Soc of London B* 1952

cells compute relative to a threshold

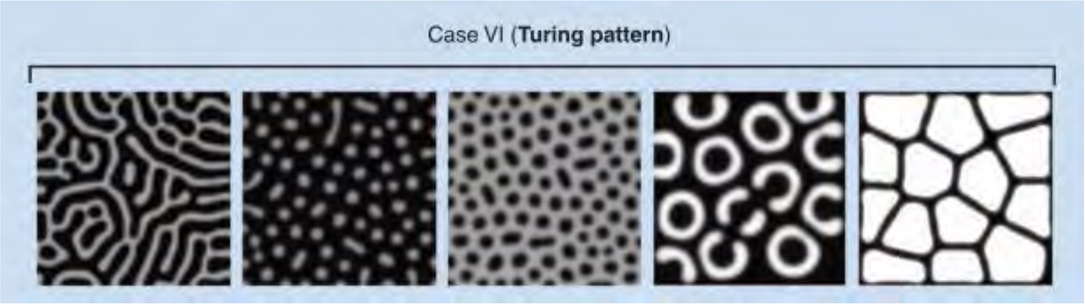

Kondo and Miura 2010

[On board]

Patterning is part of morphogenesis: two paradigmatic frameworks

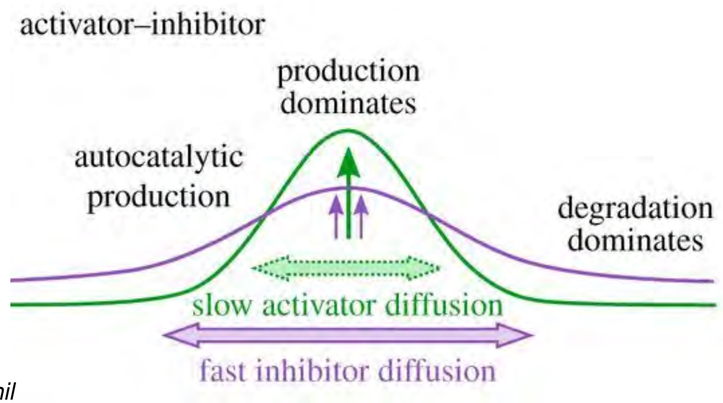

Halatek et al. *Phil Trans Royal Soc. B* 2018

$$\partial_t \boldsymbol{q} = \underline{\underline{\boldsymbol{D}}}\,\nabla^2 \boldsymbol{q} + \boldsymbol{R}(\boldsymbol{q})$$

$$\partial_t u = d_u^2\,\nabla^2 u + f(u) - \sigma v,$$
$$\tau \partial_t v = d_v^2\,\nabla^2 v + u - v$$

with $f(u) = \lambda u - u^3 - \kappa$

Morphogenesis: from genes to geometry

genes

Patterns of genes

fly embryo

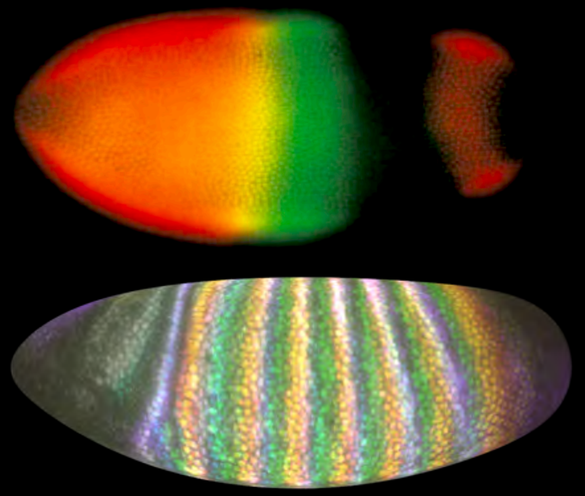

Hox genes

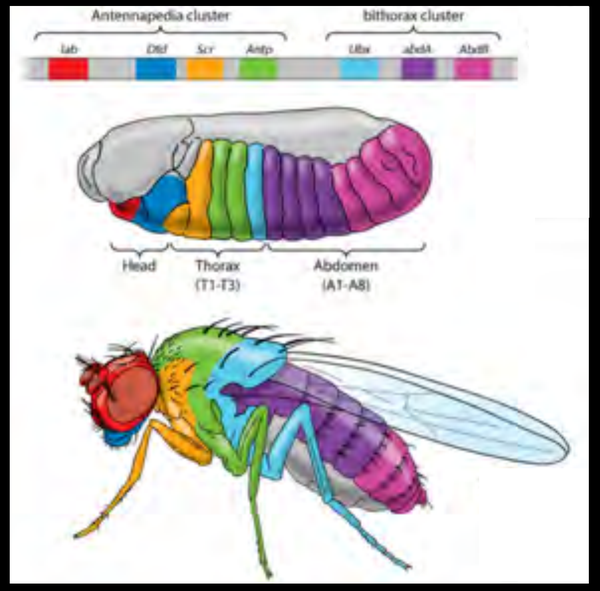

Ed Lewis

Caltech archives

Mitchell*, Lefebvre*, Jain-Sharma*, *et al* (2022)

Lewis, Nüsslein-Volhard, Wieschaus, Levine, Gehring, Kaufman, Scott, Weiner, & others

Morphogenesis: from genes to geometry

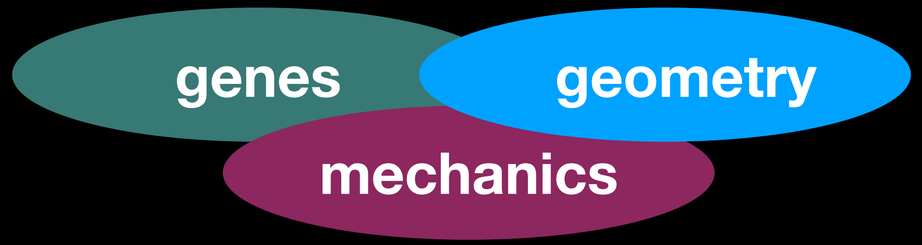

Patterns of genes

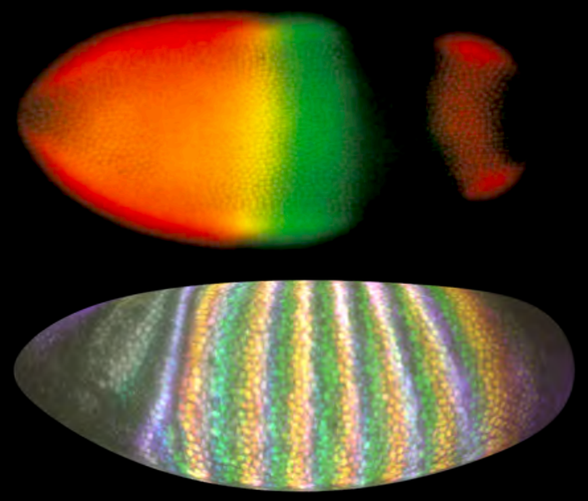

Hox genes

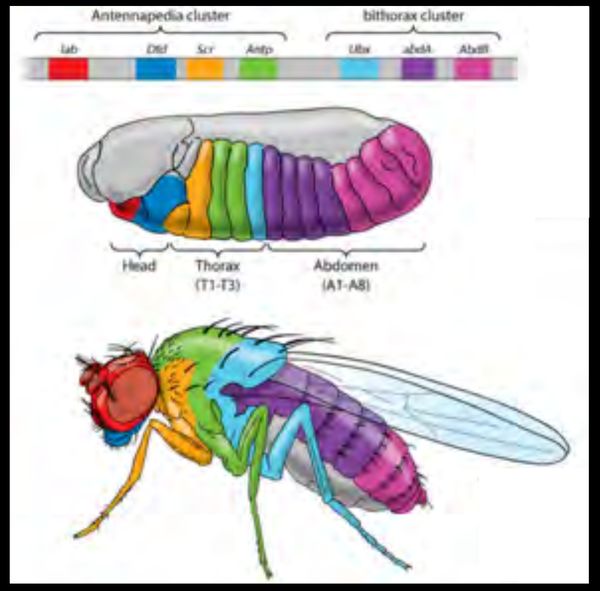

morphogenetic movements

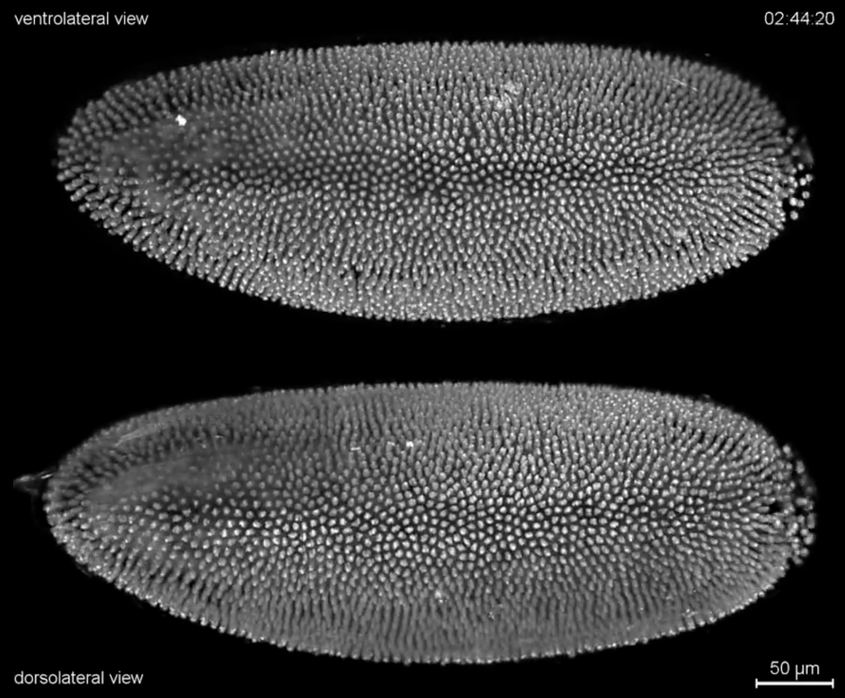

Mitchell*, Lefebvre*, Jain-Sharma*, *et al* (2022)

Lewis, Nüsslein-Volhard, Wieschaus, Levine, Gehring, Kaufman, Scott, Weiner, & others

Tomer *et al* (2012)

Morphogenesis: from genes to geometry … and back again

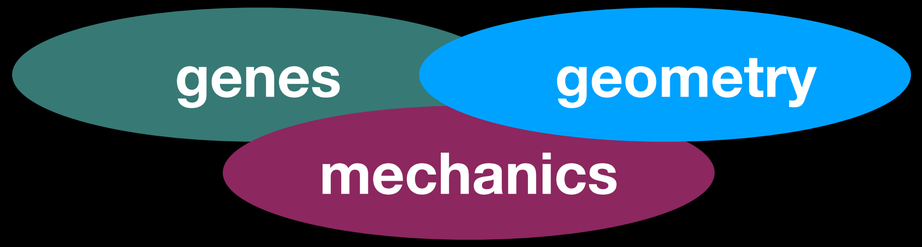

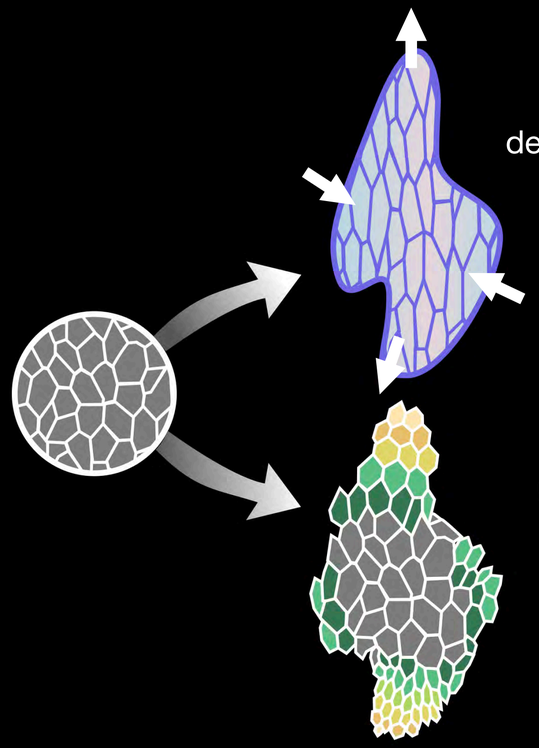

tissue deformation

- Cell area
- Cell shape
- Cell arrangement

tissue growth

Etournay *et al.* (2015), Jullicher + Eaton
Saadaoui *et al.* (2018), Corson + Gros
Lubensky, Martin, Heisenberg, Lecuit
Ghallager *et al.* (2022), Carthew
Lefebvre*, Claussen*, **Mitchell**, *et al.* (2022)
…and many others!

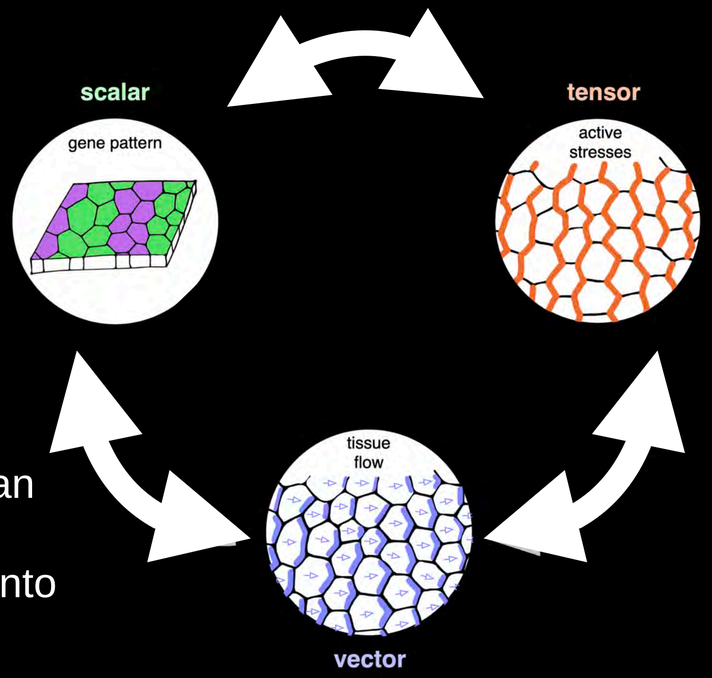

Feedback can arise:
shape feeds into patterning

[On board] Morphogenesis: from genes to geometry … and back again

Analogy to central dogma

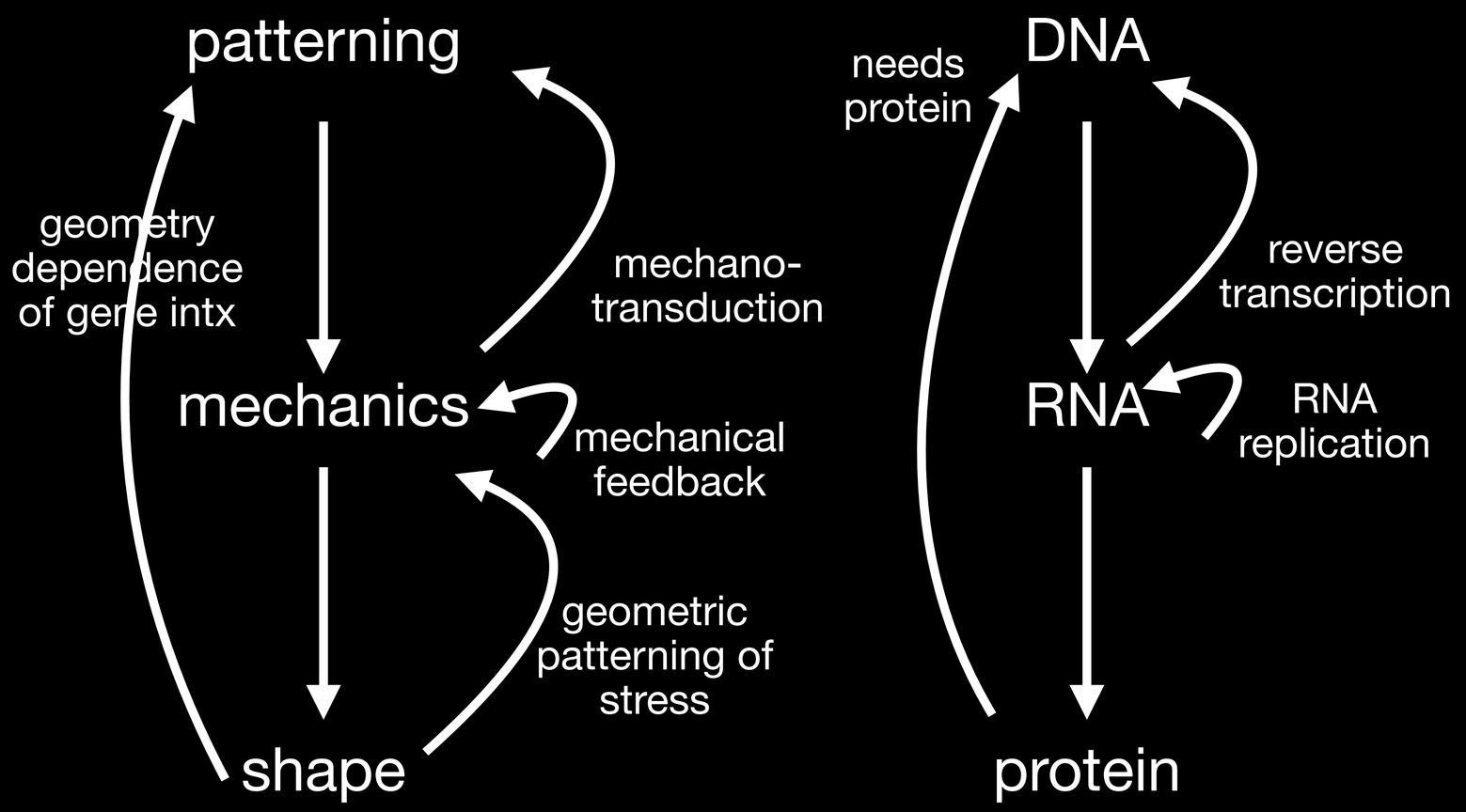

[On board]

From differentiation to morphogenesis
Example: gastrulation

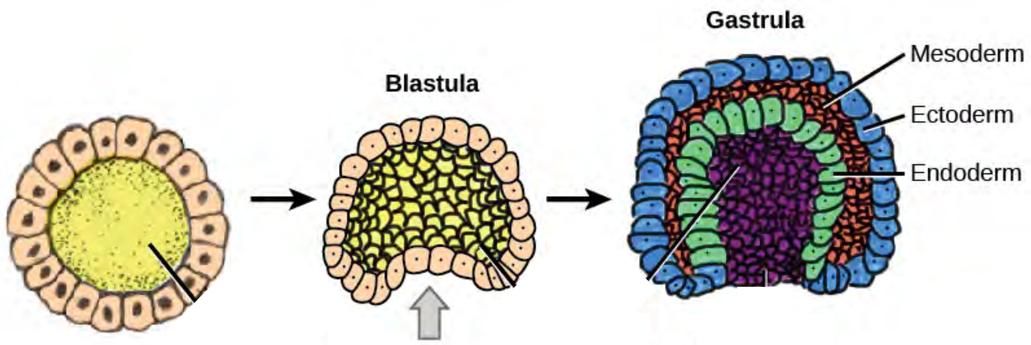

OpenTextBC & Abigail Pyne

"It is not birth, marriage, or death, but gastrulation which is truly the most important time in your life" – Lewis Wolpert 1986

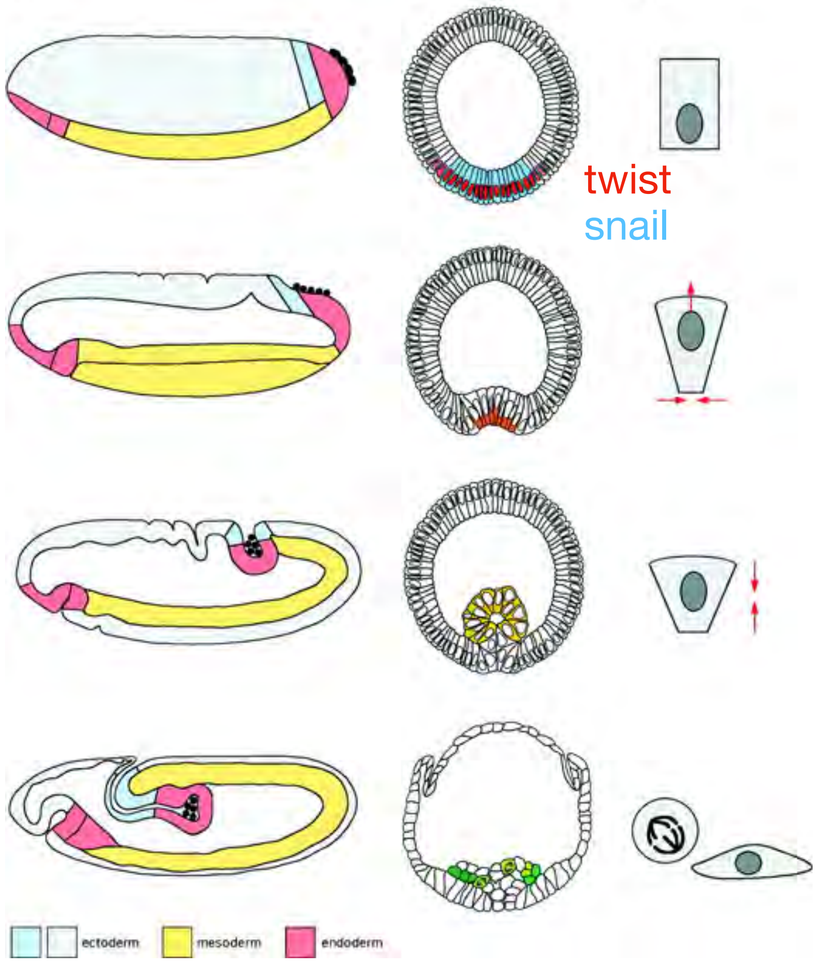

Leptin, *EMBO Journal* 1999

Tissue elongation by convergent extension

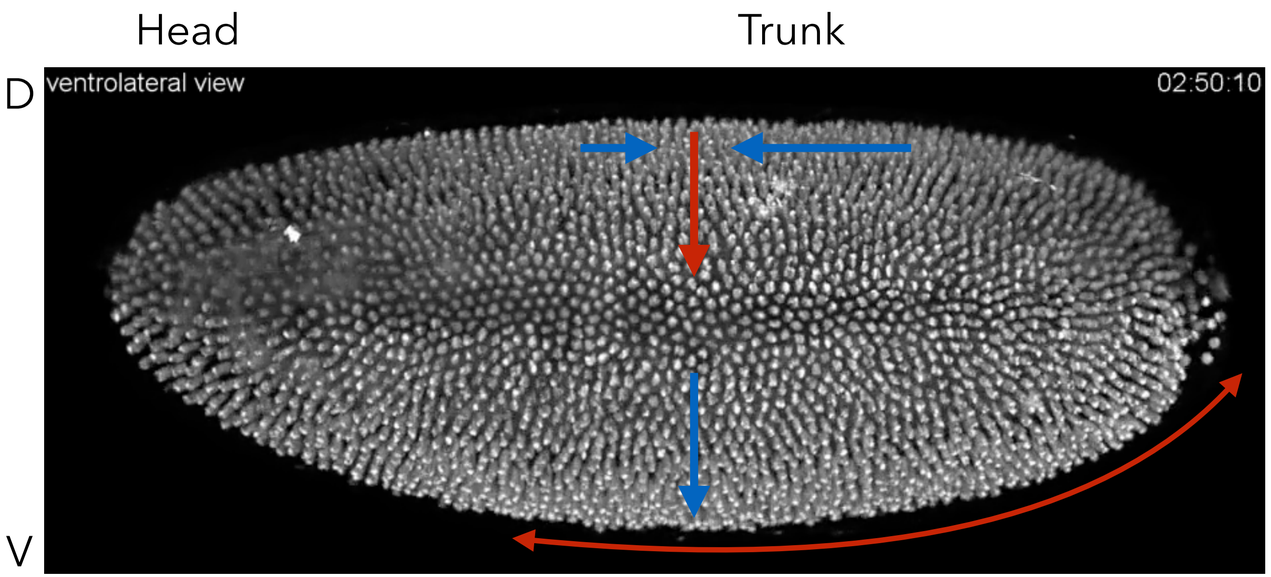

Drosophila gastrulation

Tomer et al. (2012)

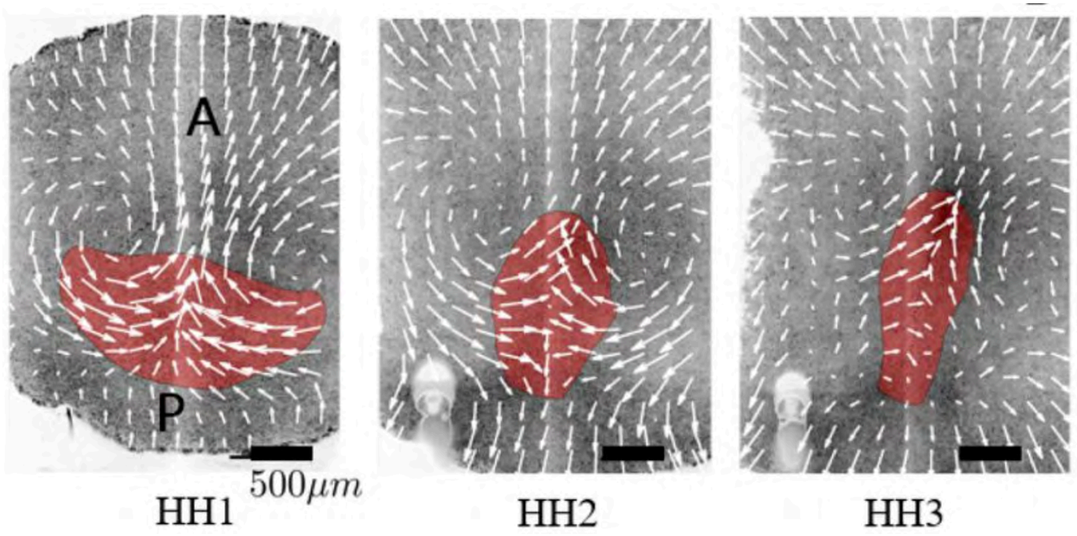

Primitive streak formation (chicken)

(Weijer Lab)

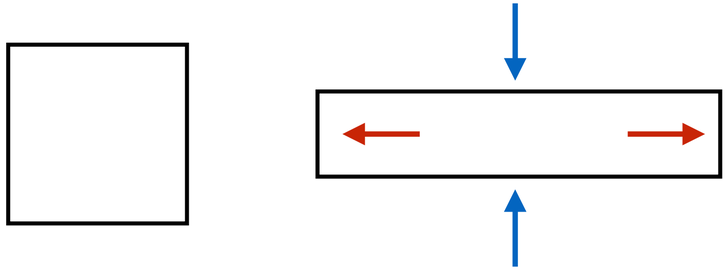

Tissue elongation (convergent–extension)

1. Where do the forces driving tissue flow originate? (local vs non-local)
2. How are the forces coordinated on the cellular scale?

Cell-scale ‘tissue tectonics’

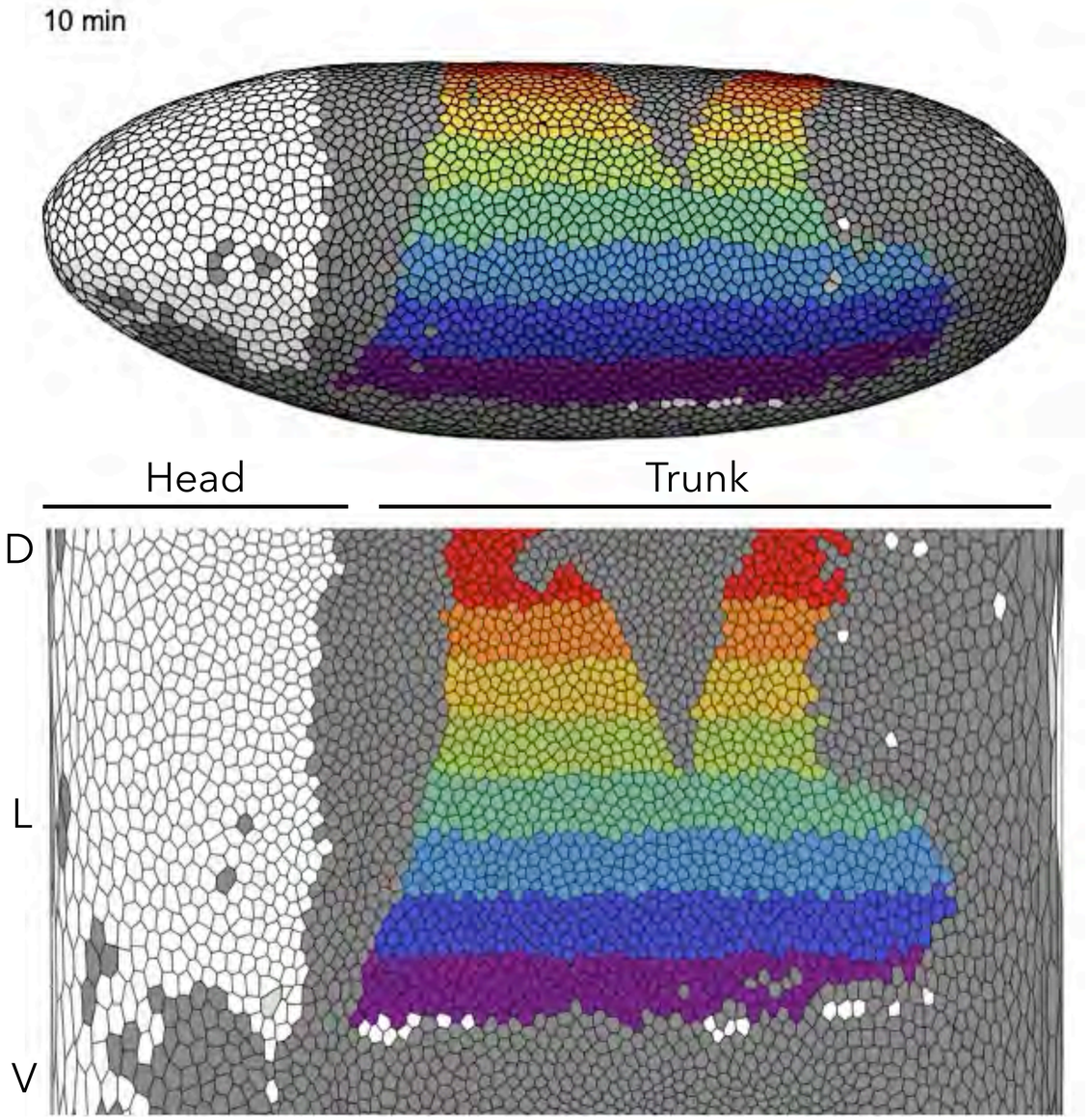

Tissue strain

=

Cell shape changes

+

Cell rearrangements

(T1 processes)

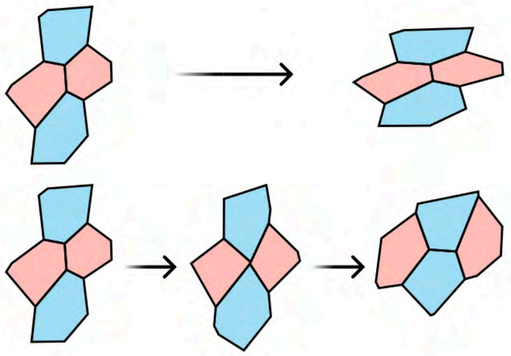

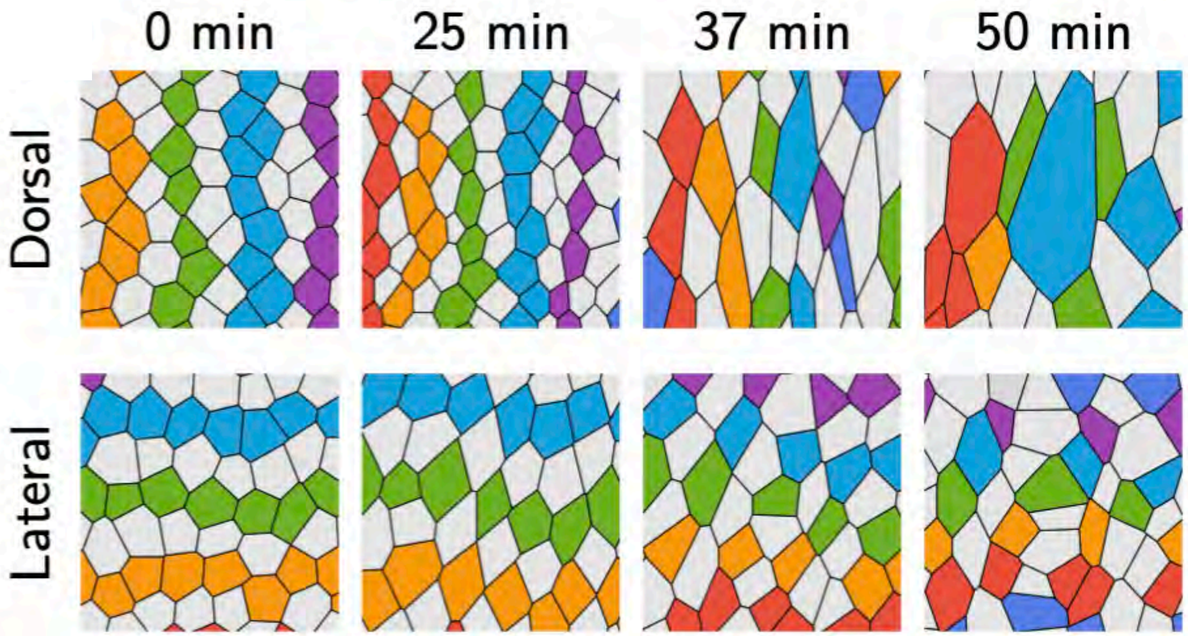

adapted from Fridtjof Brauns

Segmentation data from Stern et al., *Curr Biol.* (2022)

Brauns, Claussen, Wieschaus, & Shraiman, *eLife* (2024)

[On board]

Cell-cell mechanical interactions

Molecular interplay between cortical tension and adhesion.

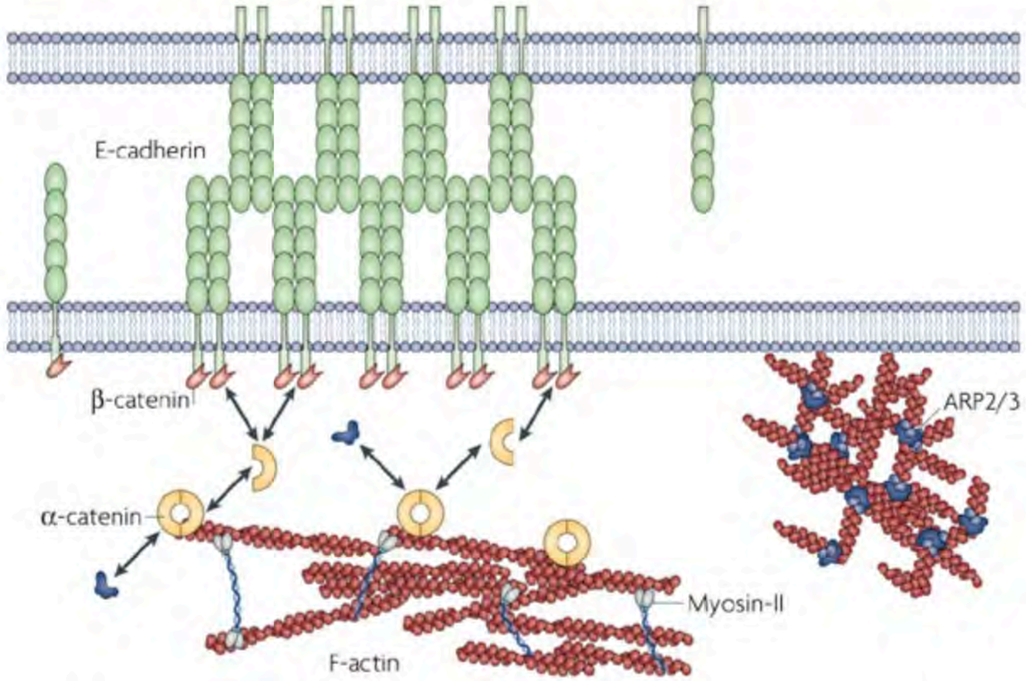

Intercellular adhesion is controlled by the *trans*-association of E-cadherin (green) *cis*-dimers that form homophilic complexes in the extracellular space. E-cadherin complexes are stabilized by cortical actin filaments (red). This stabilization requires α-catenin (yellow) shuttling between β-catenin (orange),

cytoskeleton & adherens junctions

Pasticity/viscosity from dynamic remodelling

Cortex is a bit like little muscles

Rest length is a variable!

Lecuit & Lenne, *Nat Rev Mol Cell Bio* 2007

Cell-cell mechanical interactions

Molecular interplay between cortical tension and adhesion.

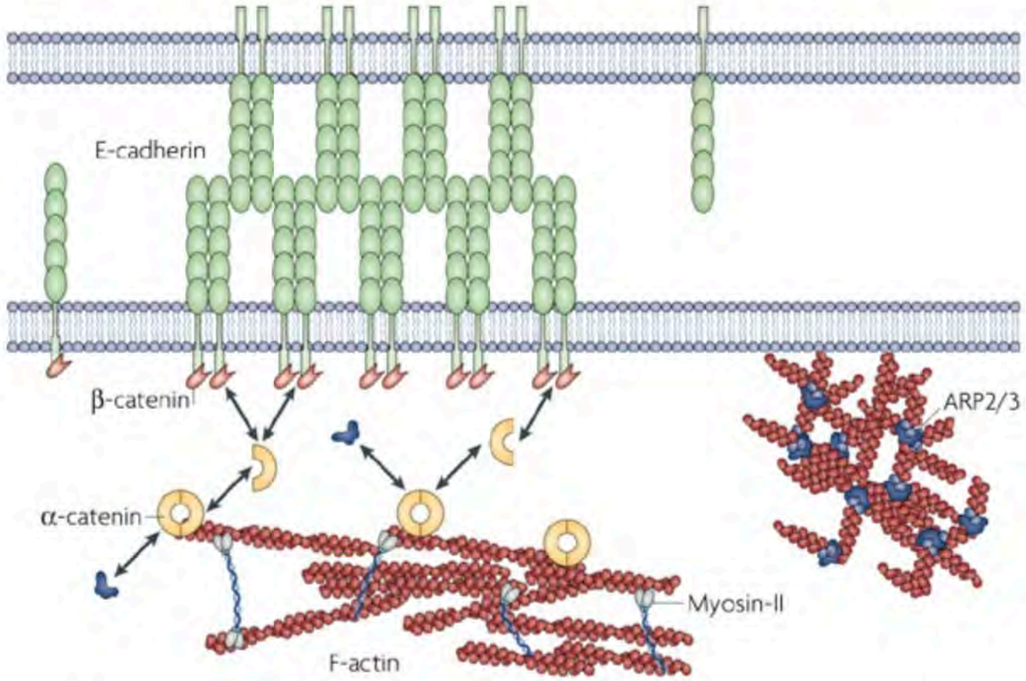

Intercellular adhesion is controlled by the *trans*-association of E-cadherin (green) *cis*-dimers that form homophilic complexes in the extracellular space. E-cadherin complexes are stabilized by cortical actin filaments (red). This stabilization requires α-catenin (yellow) shuttling between β-catenin (orange),

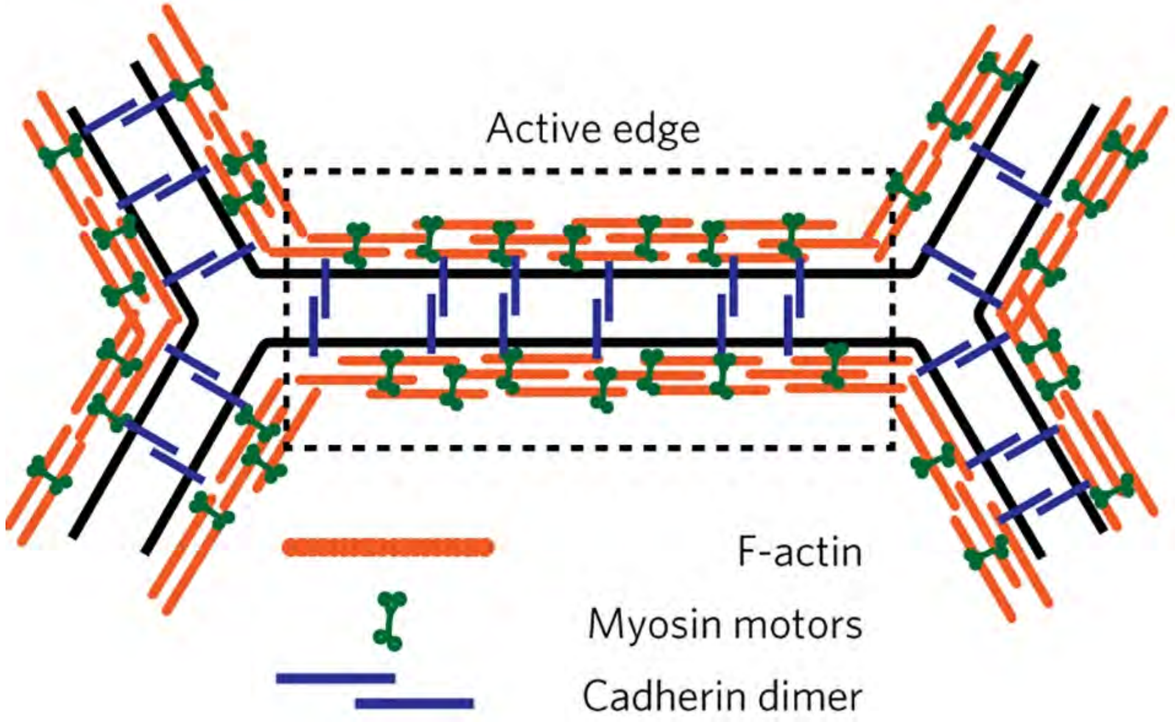

Noll et al, *Nat Phys* 2017

Lecuit & Lenne, *Nat Rev Mol Cell Bio* 2007

Tissue = tension net near force balance

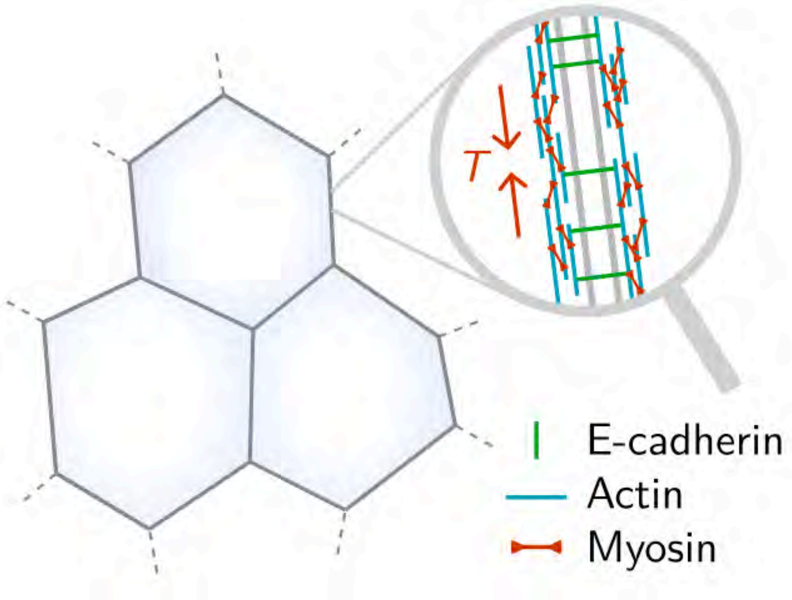

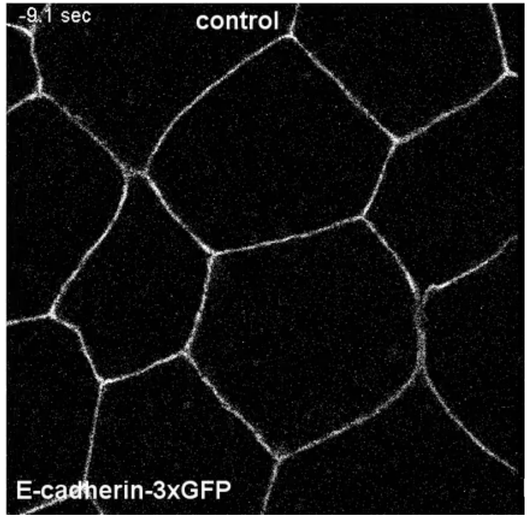

Arnold et al., *eLife* (2019)

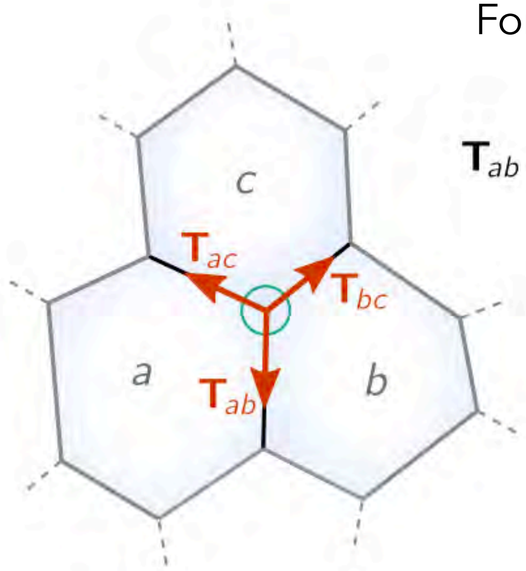

Force balance at a single vertex

$$\mathbf{T}_{ab} + \mathbf{T}_{bc} + \mathbf{T}_{ac} = 0$$

On the timescale of morphogenetic flow, the tissue is in quasi-stationary force balance.

Relative tensions can be inferred from observed geometry.

Force balance links geometry and mechanics:

Angles at vertices $\Leftrightarrow$ Junctional tensions

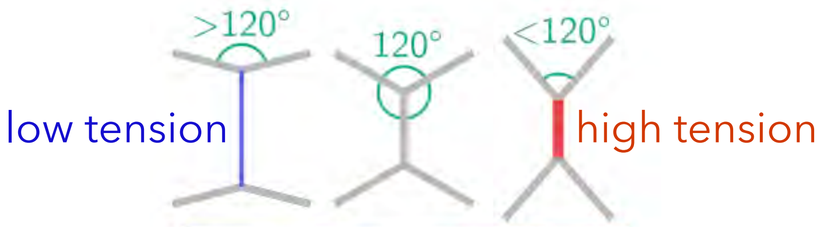

adapted from Fridtjof Brauns

Mechanical feedback: dynamical rules for tissues

t = 0 min

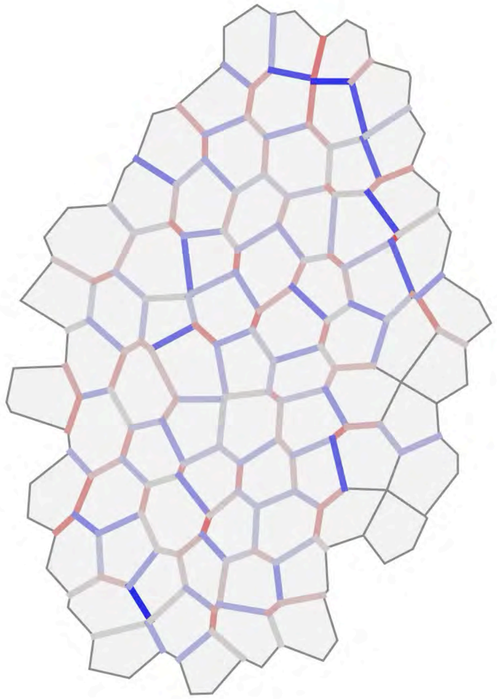

Feedback mechanisms are needed to maintain force balance in a network of active tensions

Theoretical prediction: rate of strain recruits myosin

Noll et al. *Nature Physics* (2017)

$$\frac{\dot{m}}{m} = \alpha \frac{\dot{\ell}}{\ell}$$

Experimental test

Optogenetic myosin recruitment to induce strain in adjacent tissue

Myosin is recruited in strained tissue

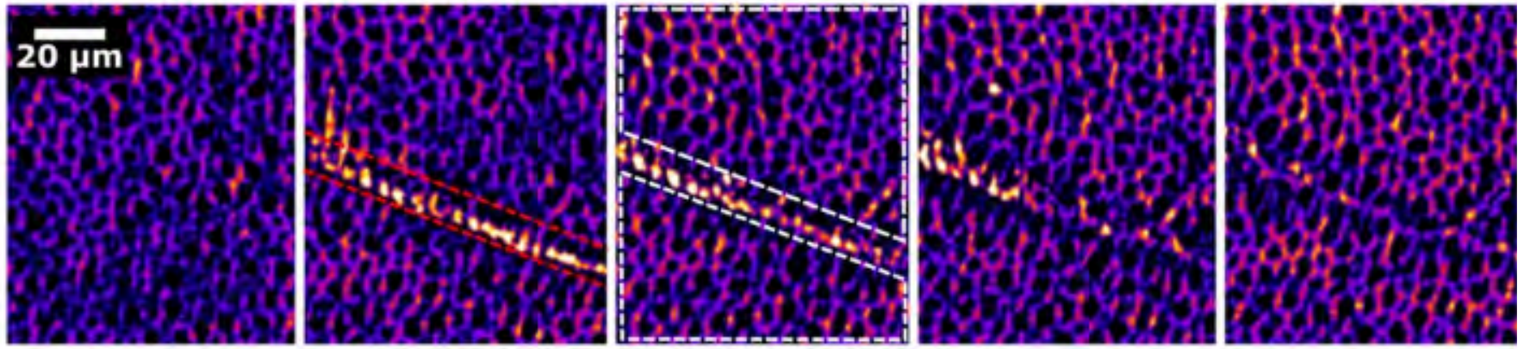

Gustafson et al. *Nature Communications* (2022)

adapted from Fridtjof Brauns

[On board]

Active solid behavior from strain-rate feedback

Elastic component $T = K(L - \ell)$

Remodeling $\frac{\dot{\ell}}{\ell} = \tau^{-1} W\left(\frac{T}{maT_s}\right)$

Feedback $\frac{\dot{m}}{m} = \alpha \frac{\dot{\ell}}{\ell}$

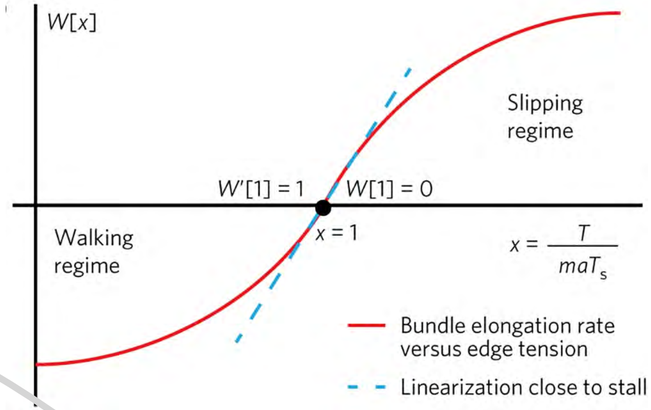

Noll et al. *Nature Physics* (2017)

myosins can walk, contracting the actin bundle, unless the load per myosin, T/am, reaches the 'stall force' level Ts. Above this, the filament elongates as motors slip. Here m is the average myosin line-density along the edge and a is the length scale over which motors share mechanical load.

The length L of the junction evolves according to $\gamma \partial_t L(t) = F - T$, with tension $T = k(L - l)$

We can solve the strain rate feedback equation finding $(m(t)/m_0) = (l(t)/l_0)^\alpha$

For the walking kernel, we use $W(x) = \tanh(x - 1)$ and set the remodeling timescale $\tau_l = 1$

adapted from Fridtjof Brauns

Active solid behavior from strain-rate feedback

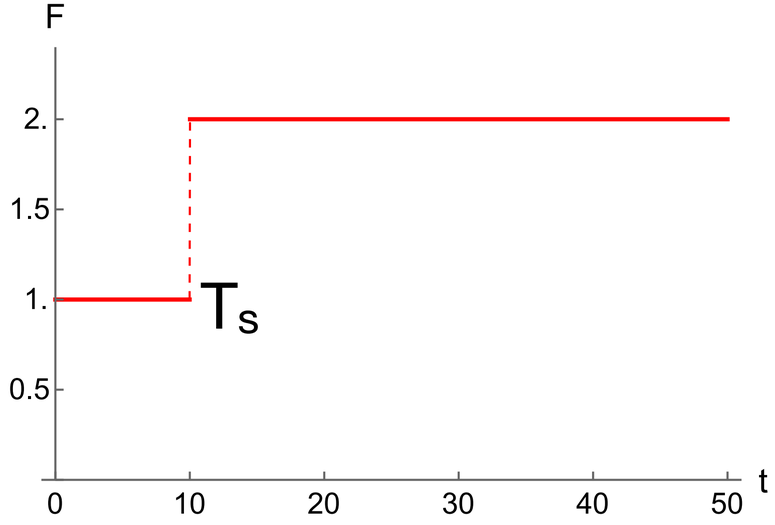

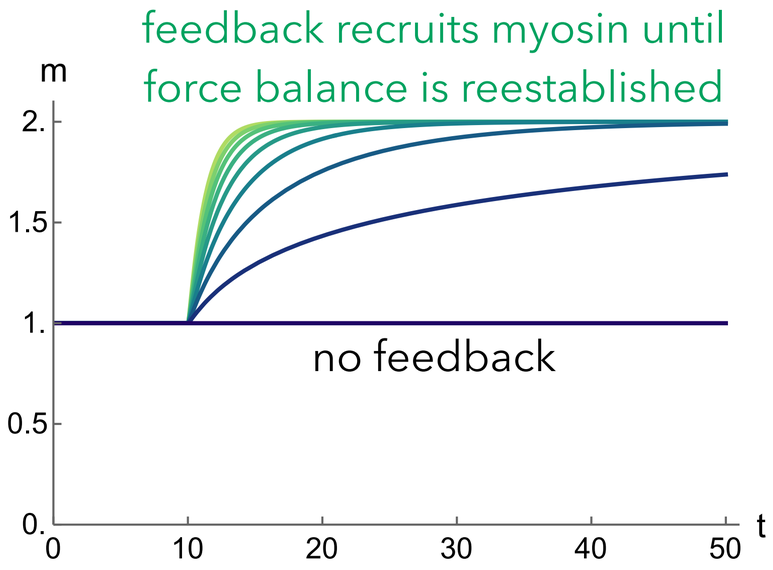

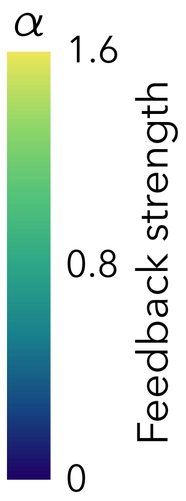

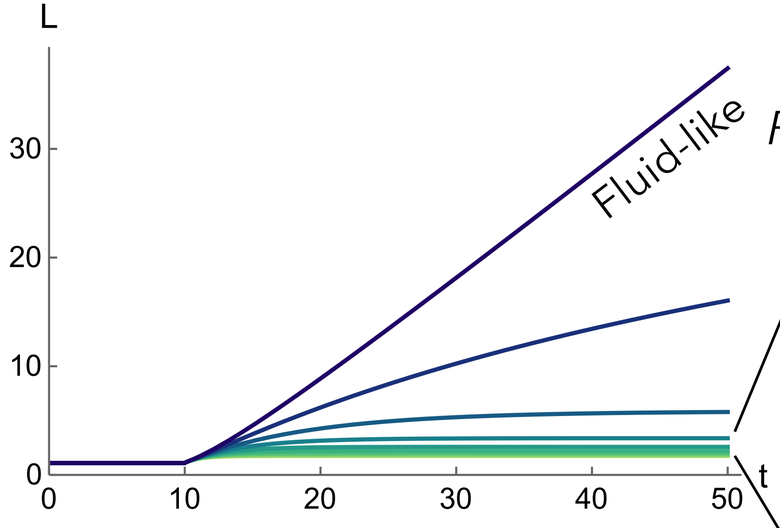

$F \sim \partial_t L / L_0$ the only resistance is the walking kernel

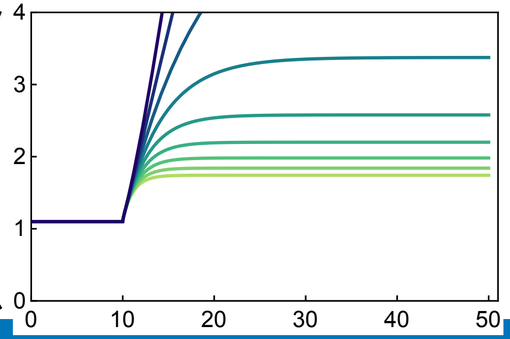

Solid-like (= "active" solid)

$F \sim (L - L_0)/L_0$

Short times: fluid-like behavior

If there is **negative** feedback, the system settles to a solid-like response

adapted from Fridtjof Brauns

[On board] Coarse-graining to 2D continuum mechanics

Viscoelastic: Kelvin-Voigt

$$\varepsilon_{\mathrm{S}} = \varepsilon_{\mathrm{D}}$$

$$\sigma = \sigma_{\mathrm{spring}} + \sigma_{\mathrm{dashpot}} = E\varepsilon + \eta\dot{\varepsilon}$$

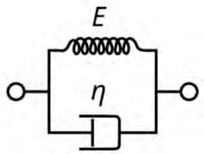

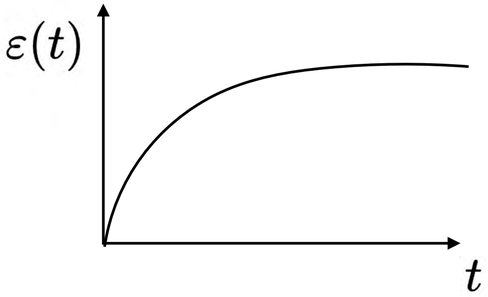

Sudden stress: $\varepsilon(t) = \dfrac{\sigma_0}{E}(1 - e^{-t/\tau_R})$

Dashpot resists sudden strain rate

Viscoelastic: Maxwell

$$\sigma_{\mathrm{dashpot}} = \sigma_{\mathrm{spring}}$$

$$\varepsilon_{\mathrm{total}} = \varepsilon_{\mathrm{spring}} + \varepsilon_{\mathrm{dashpot}}$$

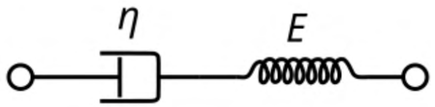

$$\frac{\dot{\sigma}}{E} + \frac{\sigma}{\eta} = \dot{\varepsilon}$$

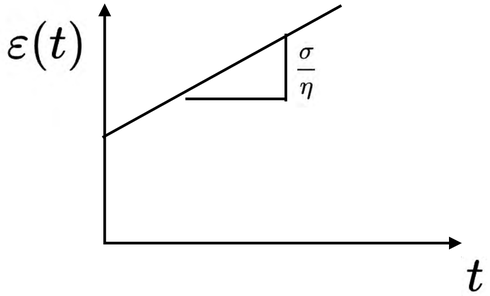

Spring suddely extends, dashpot flows under stress

Maxwell-Wiechert Model

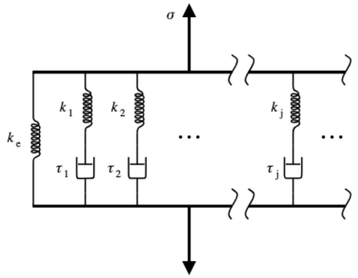

Tissue = tension net near force balance

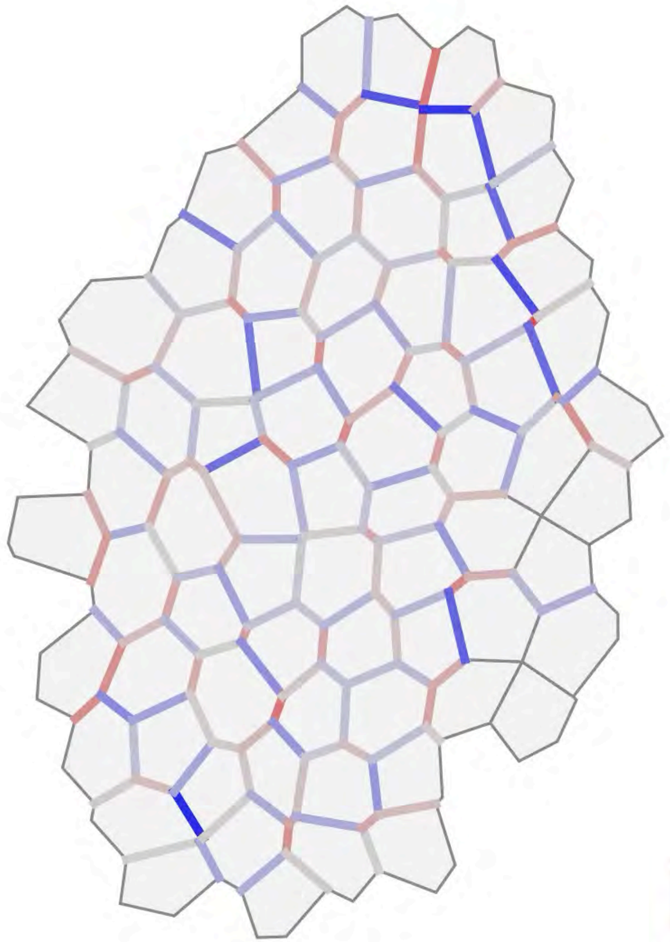

Local force inference: dynamic tensions.

Note the alternating pattern of low and high tensions that emerges before tissue flow starts.

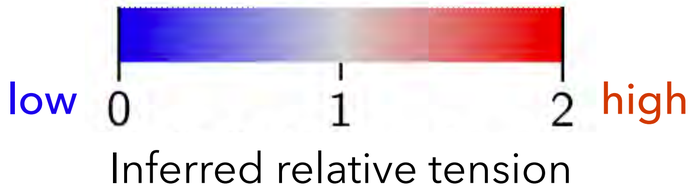

adapted from Fridtjof Brauns

Brauns, Claussen, Wieschaus, & Shraiman, *eLife* (2024)

Tissue = tension net near force balance

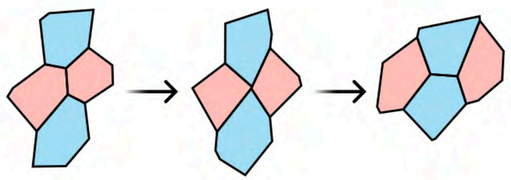

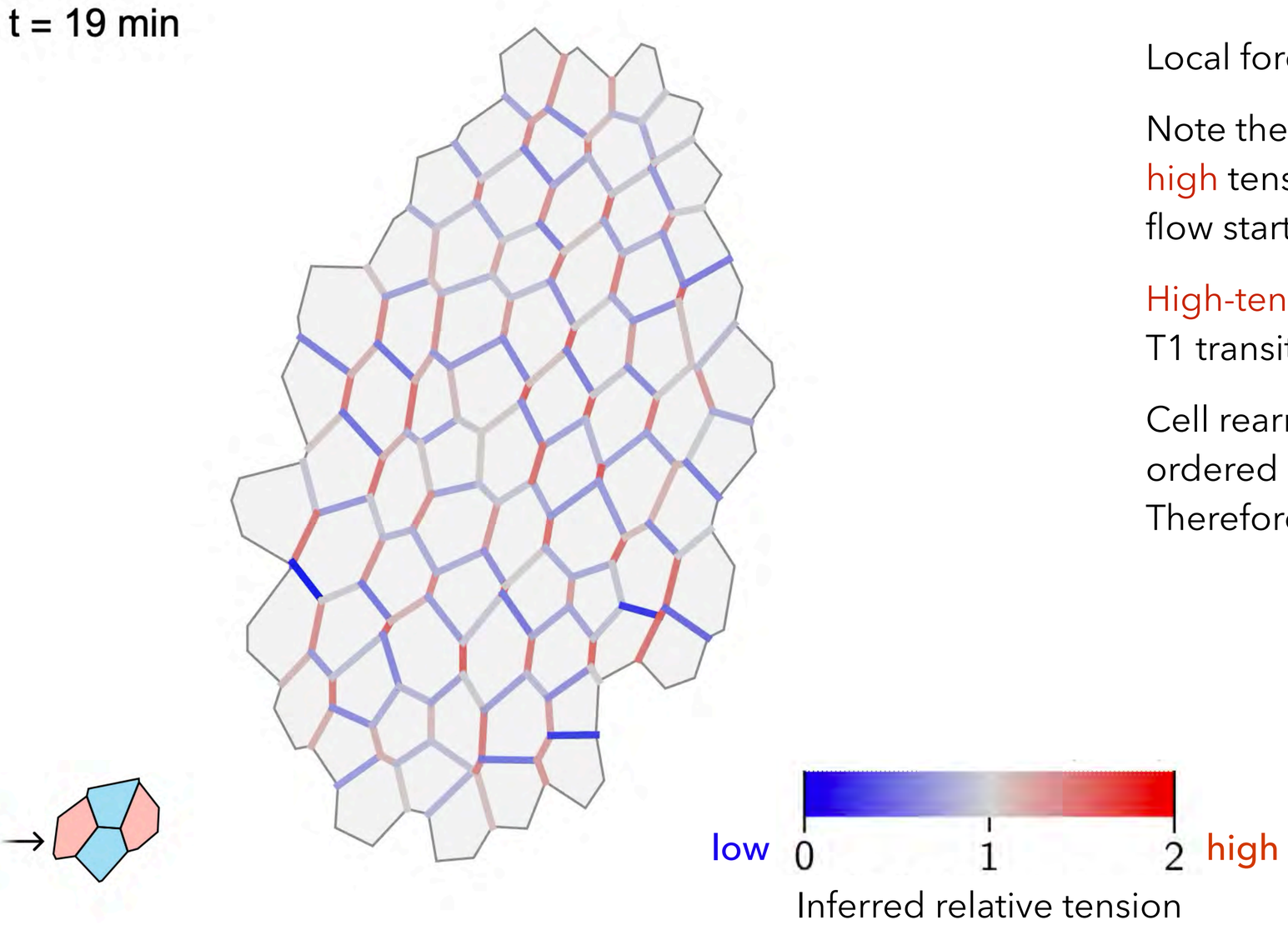

Local force inference: dynamic tensions.

Note the alternating pattern of low and high tensions that emerges before tissue flow starts.

High-tension junctions collapse, causing T1 transitions.

Cell rearrangements by T1s destroys the ordered pattern that coordinates them. Therefore, flow stalls.

adapted from Fridtjof Brauns

Brauns, Claussen, Wieschaus, & Shraiman, *eLife* (2024)

T1s are not simply a passive response to motility

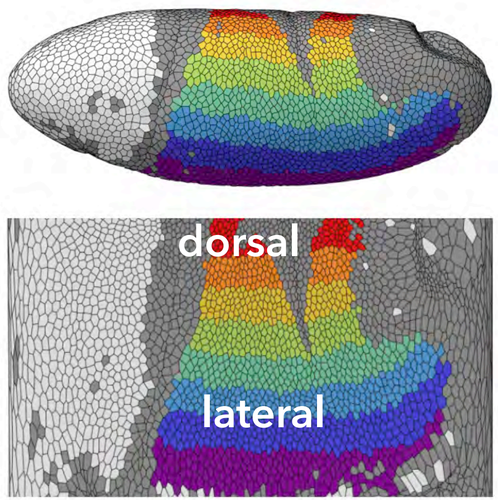

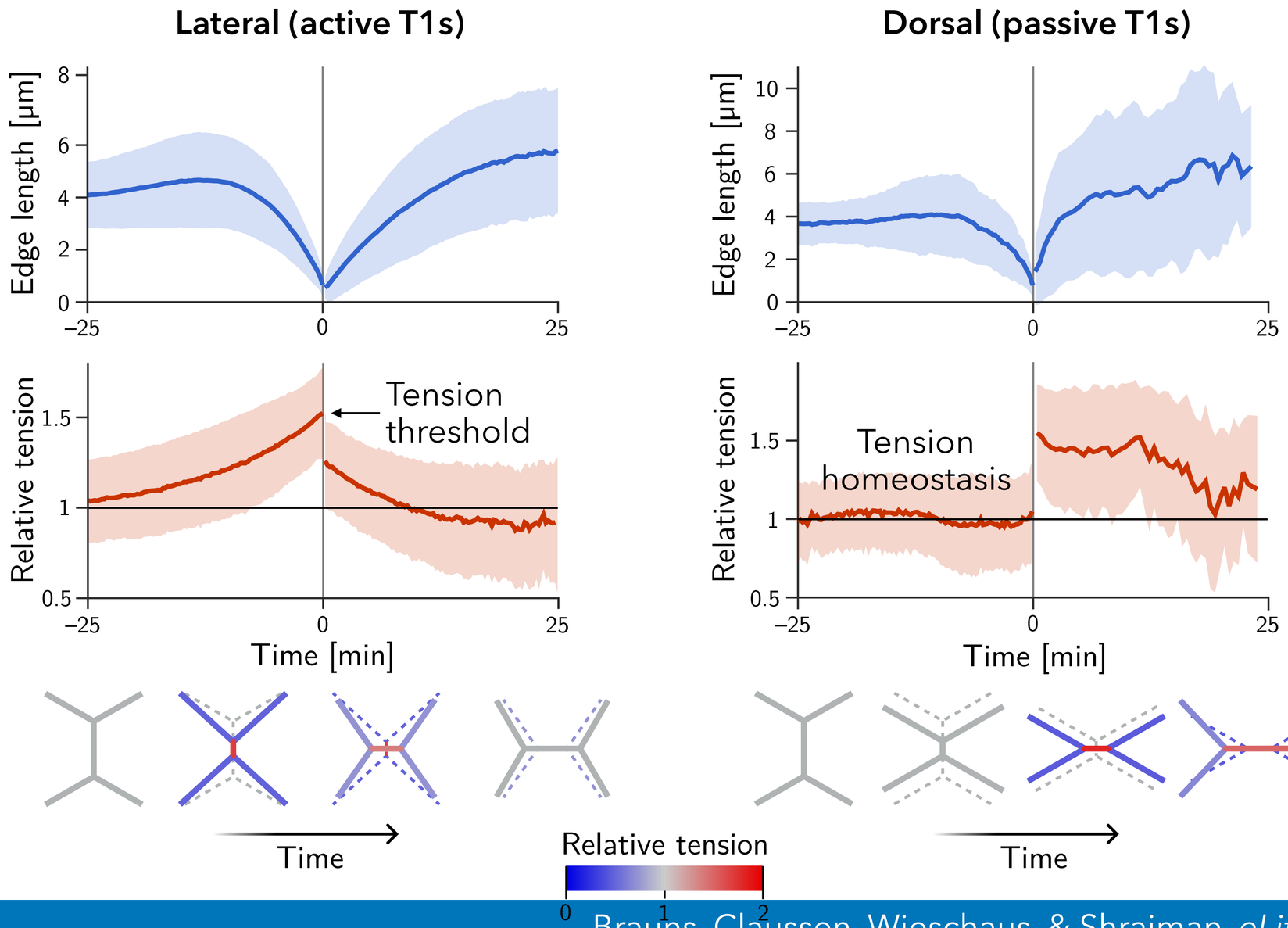

adapted from Fridtjof Brauns

Brauns, Claussen, Wieschaus, & Shraiman, *eLife* (2024)

[On board]

Yield stress & plasticity

Tension inference reveals difference between active and passive T1s.

Cell interfaces behave very differently from Hookean springs.
Junctions control tension independently of length (like muscles).

Yield stress and plasticity:

- small stress/strain > elastic (like for instance a foam)
- above a threshold > yield & flow.

Active T1s generate tissue flow through “active plasticity”, i.e. **internally driven plastic strain**

Epithelial tissue as a transcellular network of balanced tensions

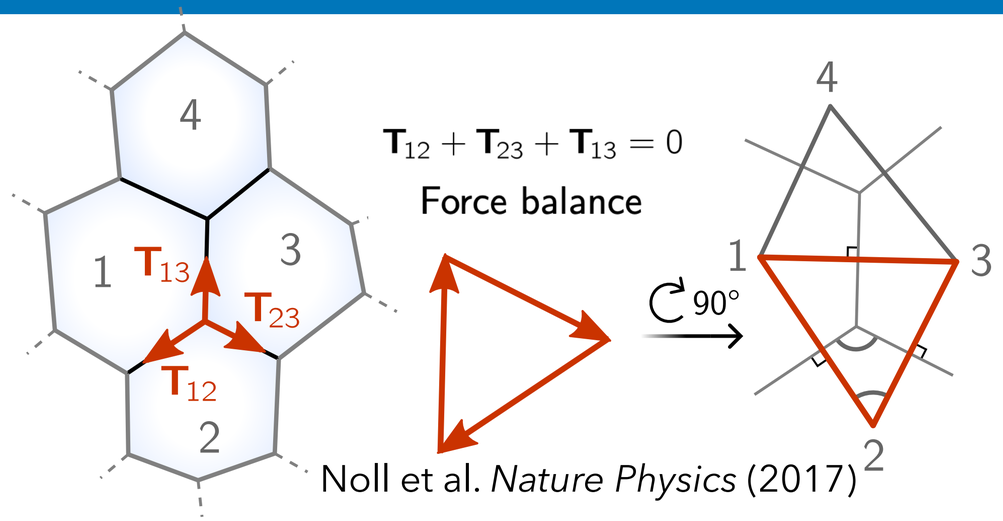

Noll et al. *Nature Physics* (2017)

Tensions triangles fit together forming a triangulation.

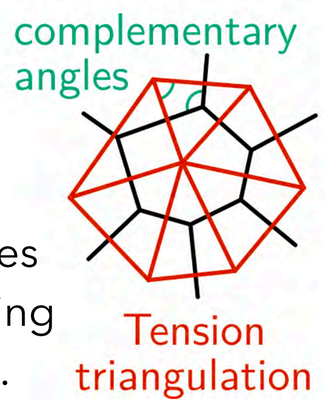

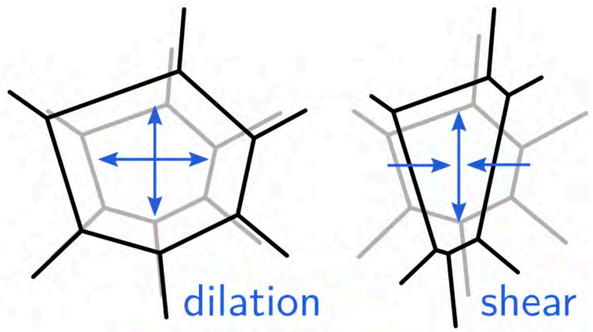

Tensions specify angles but leave *isogonal* (= angle preserving) d.o.f.s

- Tension triangulation can be used to formulate a model for tissue dynamics in **quasi-static force balance**.
- Tension triangulation provides geometric constraints on the cell tiling
- Remodeling drives tissue flow through the **dynamic constraints**. Remodeling is governed by biomechanical feedback mechanisms (negative + positive): **active plastic flow**

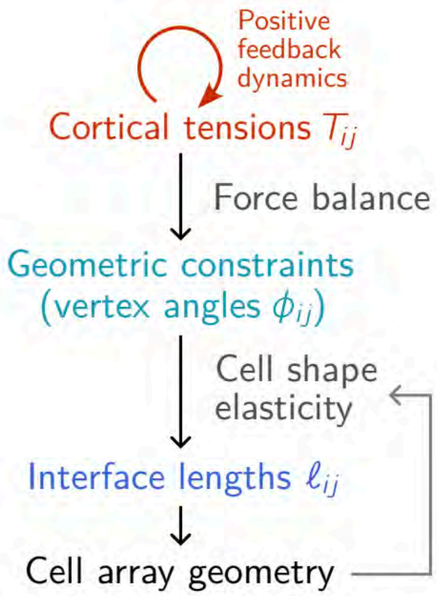

Claussen et al., *arXiv* (2024)

[On board] Epithelial tissue as a transcellular network of balanced tensions:

Energy terms

$$dE(\{\mathbf{r}_{ijk}\}|\{T_{ij}\}) = \sum_{ij} T_{ij} d\ell_{ij} - p \sum_i dA_i + \varepsilon \sum_i dE_{\mathcal{C}}(S_i)$$

Leading contribution — Uniform pressure — Prevents isogonal modes

$$\tau_{\mathrm{T}} \dot{\tilde{T}}_\alpha = T^n_\alpha - \frac{1}{3} \sum_\beta \tilde{T}^n_\beta$$

$$P = \sum_\alpha \tilde{T}_\alpha$$

Bulk elasticity

Bulk elasticity — Shear elasticity + some bulk contributions

$$E_{\mathcal{C}} = \lambda[\mathrm{Tr}(S_{\mathcal{C}} - S_0)]^2 + \mu \mathrm{Tr}[(S_{\mathcal{C}} - S_0)^2]$$

$$S_{\mathcal{C}} = \sum_i \frac{\mathbf{e}_i \otimes \mathbf{e}_i}{|\mathbf{e}_i|}$$

No floppiness (mu>0)

Tensions are balanced by uniform pressure, with subleading rigidity from elasticity

Initial anisotropy: winner-takes-all

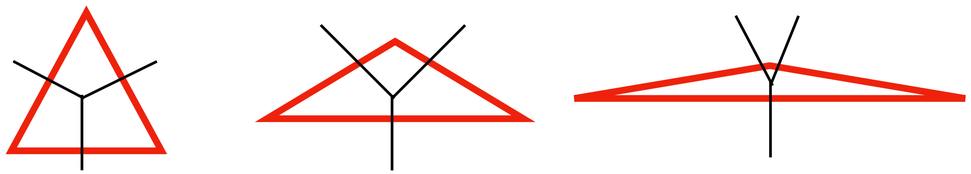

DAY 2

Mechanics of morphogenesis

Gastrulation

Morphing tissues as active solids/fluids
- Cell mechanics in convergent extension
- Tissue-scale fluid flow
- Self-organization of convergent extension

Mechanics driving tissue curvature
- Bilayer bending & ventral furrow

Organogenesis

- Wrinkling & buckling
- Programmed shape changes

Mechanics of visceral organ morphogenesis
- Midgut tissue folding in flies
- Heart morphogenesis
- branching morphogenesis

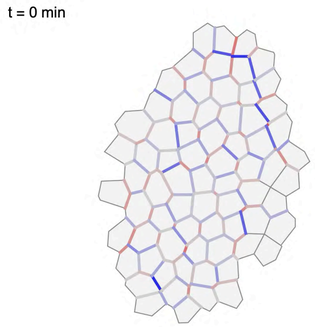

Negative strain rate feedback
Positive tension feedback

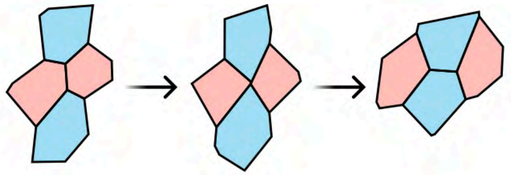

mechanical equilibrium + feedback
No energy barrier

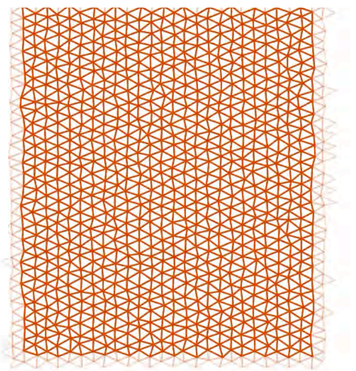

Time: 0 min

Fridtjof Brauns [KITP, UCSB]

Coarse-graining to 2D continuum mechanics

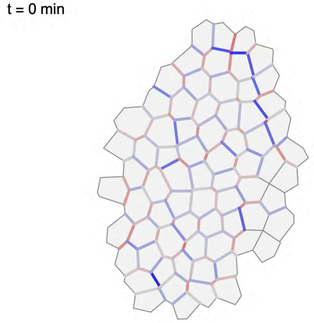

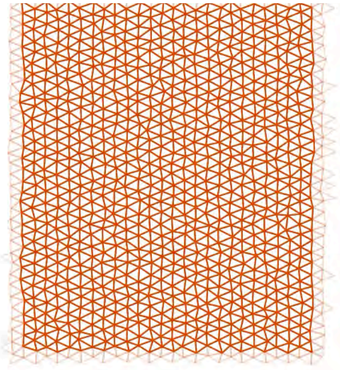

Negative strain rate feedback
Positive tension feedback

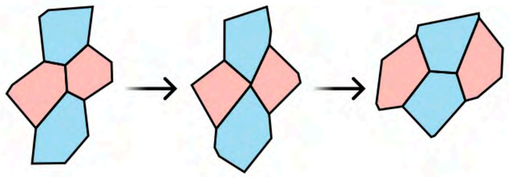

mechanical equilibrium + feedback
No energy barrier

2D active flows

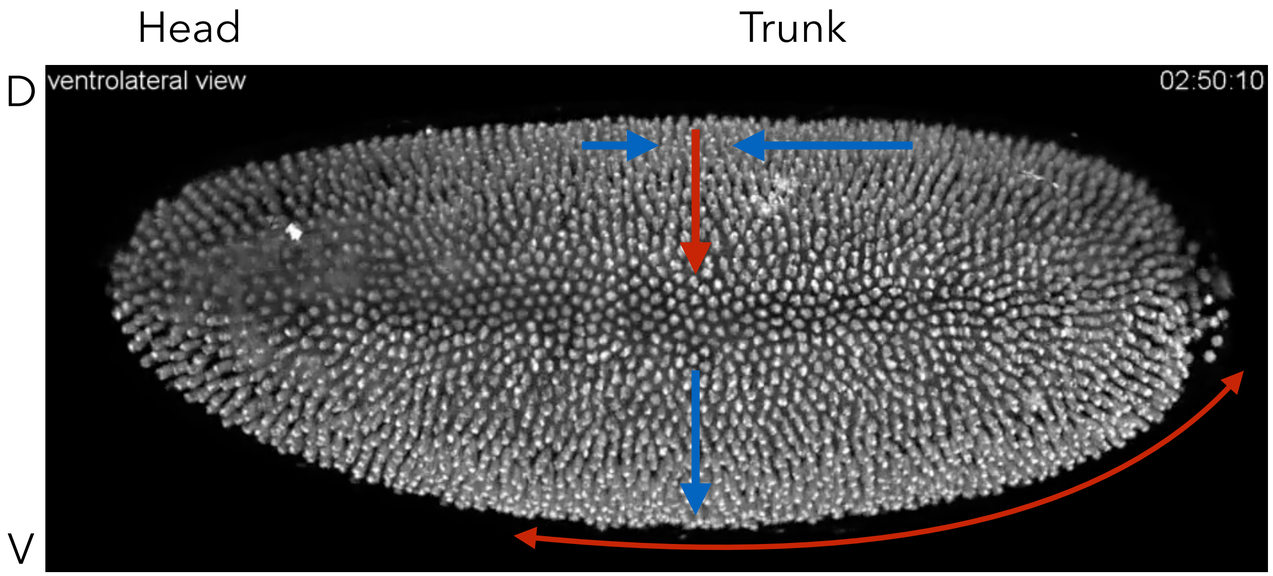

Tomer et al. *Nat Meth.* (2012)

Coarse-graining to 2D continuum mechanics

Definition of strain tensor

Decomposition: conformal + deviatoric components

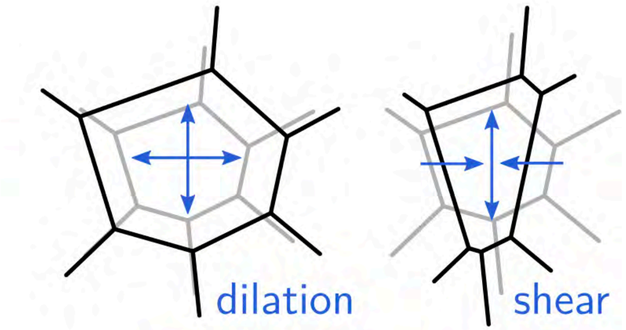

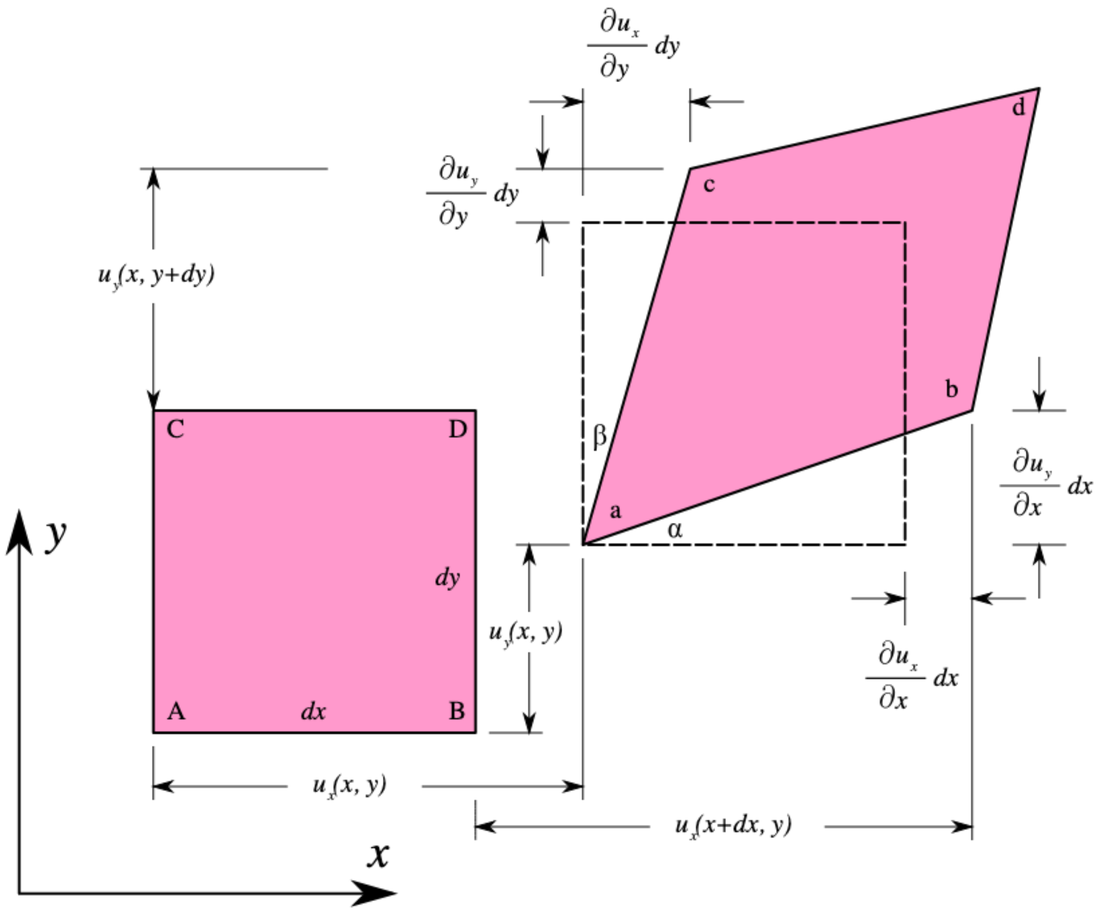

[On board] Coarse-graining to 2D continuum mechanics

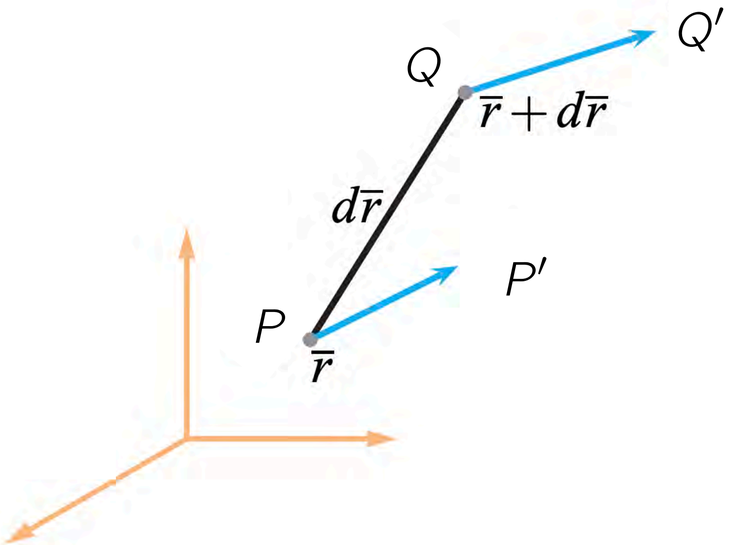

$$\mathbf{u}(\mathbf{r}+d\mathbf{r}) = \mathbf{u}(\mathbf{r}) + \nabla\mathbf{u}\cdot d\mathbf{r}$$

Gradient tensor

$$\nabla\mathbf{u} = \bar{\bar{\varepsilon}} + \bar{\bar{R}} = \begin{bmatrix} \frac{\partial u_x}{\partial x} & \frac{\partial u_x}{\partial y} \\ \frac{\partial u_y}{\partial x} & \frac{\partial u_y}{\partial y} \end{bmatrix}$$

$$\bar{\bar{\varepsilon}} = \frac{1}{2}\left(\nabla\vec{u} + (\nabla\vec{u})^T\right) = \begin{bmatrix} \frac{\partial u_x}{\partial x} & \frac{1}{2}\left(\frac{\partial u_x}{\partial y} + \frac{\partial u_y}{\partial x}\right) \\ \frac{1}{2}\left(\frac{\partial u_x}{\partial y} + \frac{\partial u_y}{\partial x}\right) & \frac{\partial u_y}{\partial y} \end{bmatrix}$$

$$\bar{\bar{R}} = \frac{1}{2}\left(\nabla\vec{u} - (\nabla\vec{u})^T\right) = \frac{1}{2}\begin{bmatrix} 0 & \frac{\partial u_x}{\partial y} - \frac{\partial u_y}{\partial x} \\ \frac{\partial u_y}{\partial x} - \frac{\partial u_x}{\partial y} & 0 \end{bmatrix}$$

[On board] Coarse-graining to 2D continuum mechanics

Strain Tensor (ε):

$$\varepsilon = \frac{1}{2}(\nabla u + (\nabla u)^T)$$

Deviatoric Strain ($\varepsilon_{\mathrm{dev}}$):

$$\varepsilon_{\mathrm{dev}} = \varepsilon - \frac{1}{n}(\mathrm{tr}(\varepsilon)I) \qquad = \begin{bmatrix} \varepsilon_{xx} - \frac{1}{2}(\varepsilon_{xx} + \varepsilon_{yy}) & \varepsilon_{xy} \\ \varepsilon_{xy} & \varepsilon_{yy} - \frac{1}{2}(\varepsilon_{xx} + \varepsilon_{yy}) \end{bmatrix}$$

Conformal Strain ($\varepsilon_{\mathrm{conf}}$):

$$\varepsilon_{\mathrm{conf}} = \frac{1}{n}(\mathrm{tr}(\varepsilon)I) \qquad = \frac{1}{2}(\varepsilon_{xx} + \varepsilon_{yy}) \begin{bmatrix} 1 & 0 \\ 0 & 1 \end{bmatrix}$$

[On board] Coarse-graining to 2D continuum mechanics

Solid

$$\sigma^{ij} = C^{ijkl}\varepsilon_{kl}$$ Hooke's law

$$K = \frac{\text{hydrostatic pressure}}{\text{volumetric strain}} = \frac{\frac{1}{2}(\sigma_{11} + \sigma_{22})}{\varepsilon_{11} + \varepsilon_{22}}$$

$$K = \lambda + \mu$$

$$\sigma_{ij} = \lambda\varepsilon_{kk}\delta_{ij} + 2\mu\varepsilon_{ij}$$ Isotropic linear elastic

Here, δ_{ij} is the Kronecker delta, and ε_{kk} represents the trace of the strain tensor

$$\sigma_{ij} = K\varepsilon_{kk}\delta_{ij} + 2\mu\left(\varepsilon_{ij} - \frac{1}{2}\delta_{ij}\varepsilon_{kk}\right)$$

Fluid

$$\sigma_{ij} = -p\delta_{ij} + 2\mu\dot{\varepsilon}_{ij}$$ Strain rate rather than strain: resistance to flow (viscosity)

- μ is the dynamic viscosity.

$$\mu = \nu\rho$$

- ν is the kinematic viscosity,

Tissue tectonics

$$\varepsilon = \varepsilon_{\text{cell shape}} + \varepsilon_{\text{T1}}$$

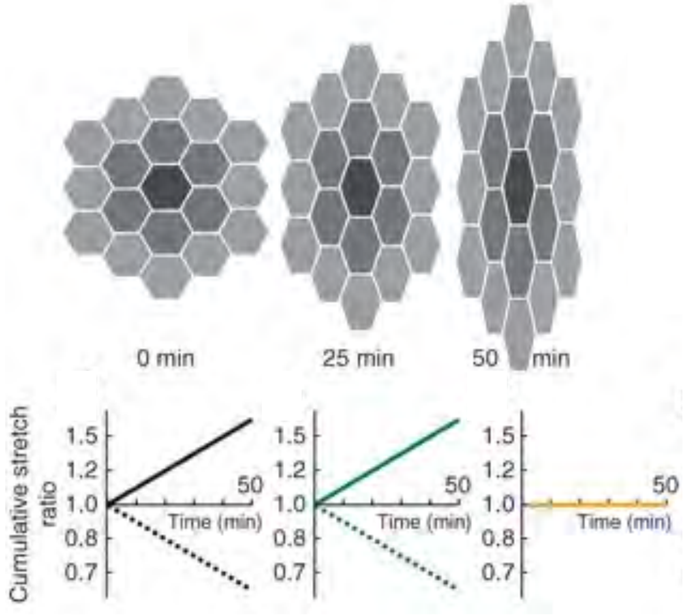

total stretch | cell shape | intercalations

$$\varepsilon = \varepsilon_{\text{cell shape}} + \varepsilon_{\text{T1}}$$

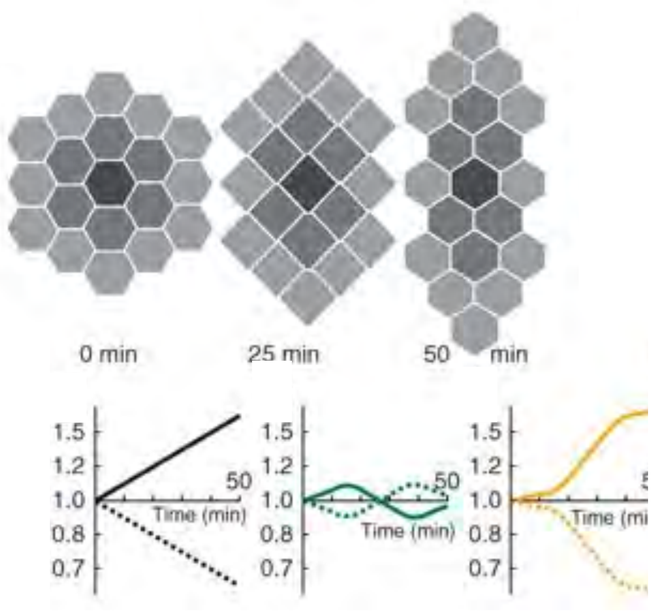

total stretch | cell shape | intercalations

$$\varepsilon = \varepsilon_{\text{cell shape}} + \varepsilon_{\text{T1}}$$

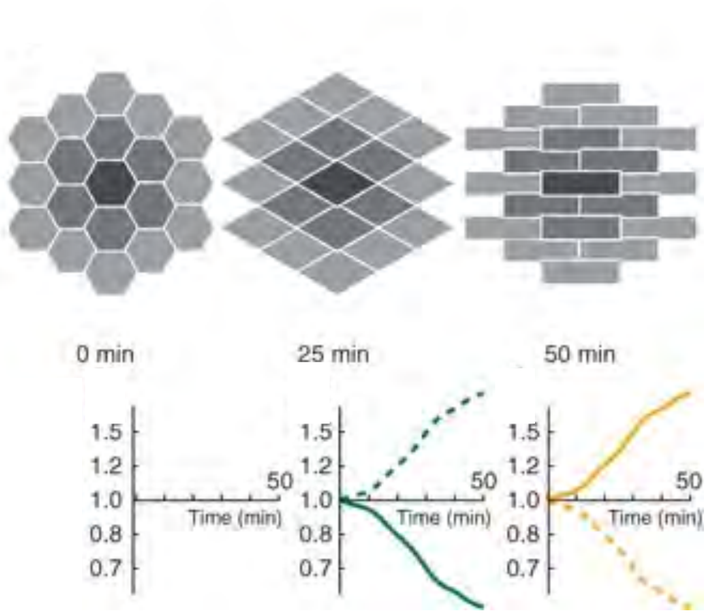

total stretch | cell shape | intercalations

Blanchard et al *Nat Meth* 2009

Tissue tectonics

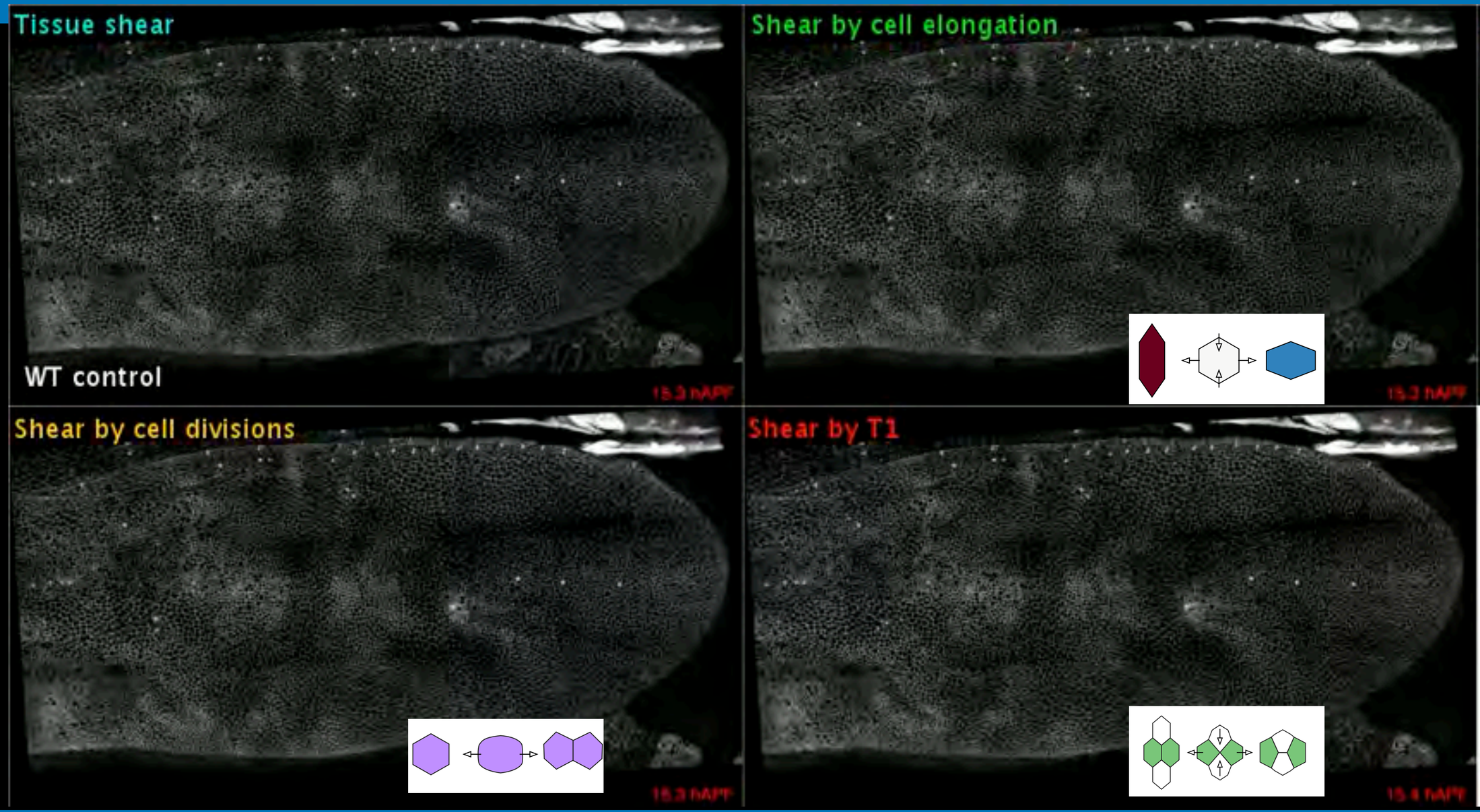

Etournay et al *eLife* 2015

Morphing tissues as viscous fluids

From active solids to active fluids

Long timescales:
many rearrangements

Embryo proper

Primitive streak

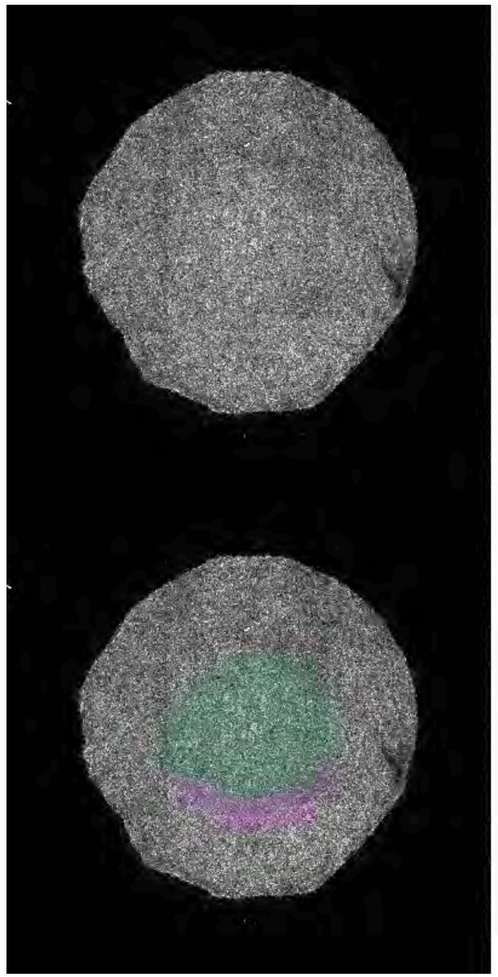

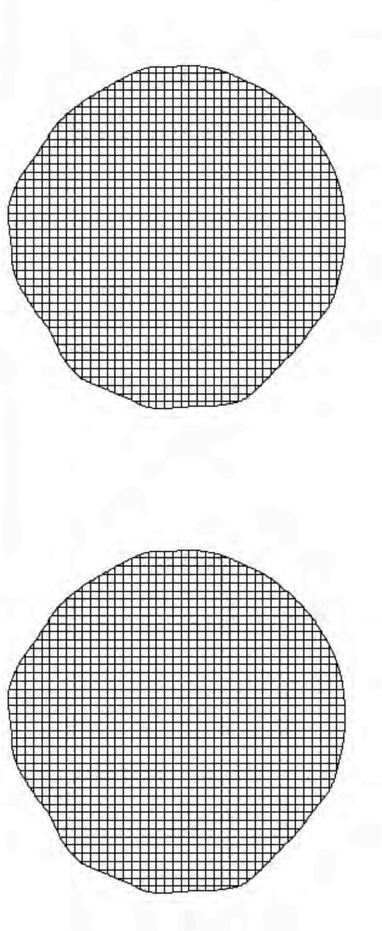

coarse-grained fluid: Streichan et al, *eLife* 2018; Saadhoui et al, *Science* 2018
coarse-grained solid: Brauns et al, *eLife* 2024; Claussen et al *bioRxiv* 2023
Similar models connecting chick & frog gastrulation via Serra, Maha, Weijer

Saadhoui et al, *Science* 2018

[On board] Active viscous fluids

Recall strain definition

$$\dot{\varepsilon}_{ij} = \frac{1}{2}\left(\partial_i u_j + \partial_j u_i\right)$$

ie

$$\bar{\bar{\dot{\varepsilon}}} = \frac{1}{2}\left(\nabla\vec{u} + \nabla\vec{u}^T\right)$$

and fluid const. rel.

$$\bar{\bar{\sigma}}_{\text{viscous}} = -p\bar{\bar{I}} + \mu\bar{\bar{\dot{\varepsilon}}}$$

Force balance

$$\vec{f} = \nabla\cdot\bar{\bar{\sigma}}_{\text{viscous}} - \nabla p$$

substituting

$$\nabla\cdot\bar{\bar{\sigma}}_a = \mu\nabla\cdot\bar{\bar{\dot{\varepsilon}}} - \nabla p$$

$$\nabla\cdot\bar{\bar{\sigma}}_a = \mu\nabla^2\vec{u} - \nabla p$$

Normally pressure is a Lagrange multiplier on incompressibility, but here we have divisions.

Morphing tissues as viscous fluids

From active solids to active fluids

$$-\boldsymbol{\nabla} p + \mu \nabla^2 \boldsymbol{u} = \boldsymbol{\nabla} \cdot \boldsymbol{\sigma}_a$$

$$\boldsymbol{\nabla} \cdot \boldsymbol{u} = \gamma$$

Lagrangian γ: property of material points in the tissue

model: boundary-driven 2D Stokes flow

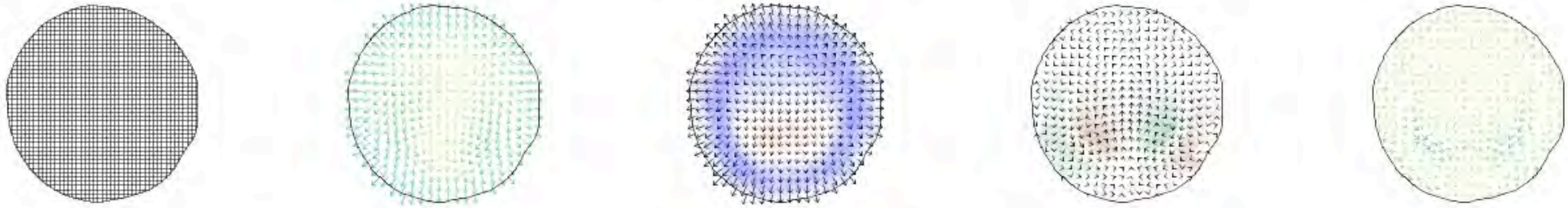

deformation map | velocity field | divergent component | rotational component | apparent forces

–> apparent forces are localized in a ring

Saadhoui et al, *Science* 2018

Morphing tissues as viscous fluids

From active solids to active fluids

$$-\boldsymbol{\nabla} p + \mu \nabla^2 \boldsymbol{u} = \boldsymbol{\nabla} \cdot \boldsymbol{\sigma}_a$$

$$\boldsymbol{\nabla} \cdot \boldsymbol{u} = \gamma$$

model: boundary-driven 2D Stokes flow

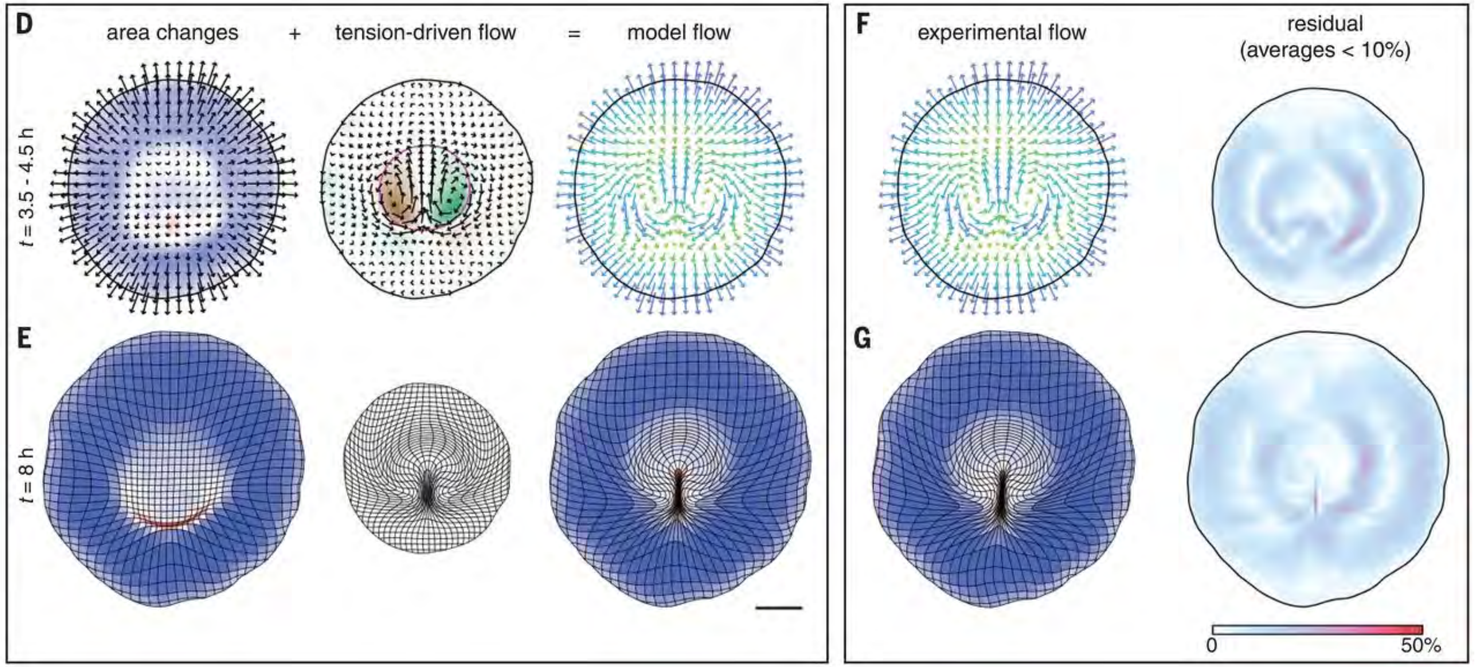

–> apparent forces are localized in a ring

coarse-grained fluid: Streichan et al, *eLife* 2018; Saadhoui et al, *Science* 2018
coarse-grained solid: Brauns et al, *eLife* 2024; Claussen et al *bioRxiv* 2023
Similar models connecting chick & frog gastrulation via Serra, Maha, Weijer

Saadhoui et al, *Science* 2018

Morphing tissues as viscous fluids

off-centered cuts bring the border closer to one side of the EP

interaction between the EP and the border induces a rotation of the axis, leaving only one apparent vortex and resulting in a bent streak

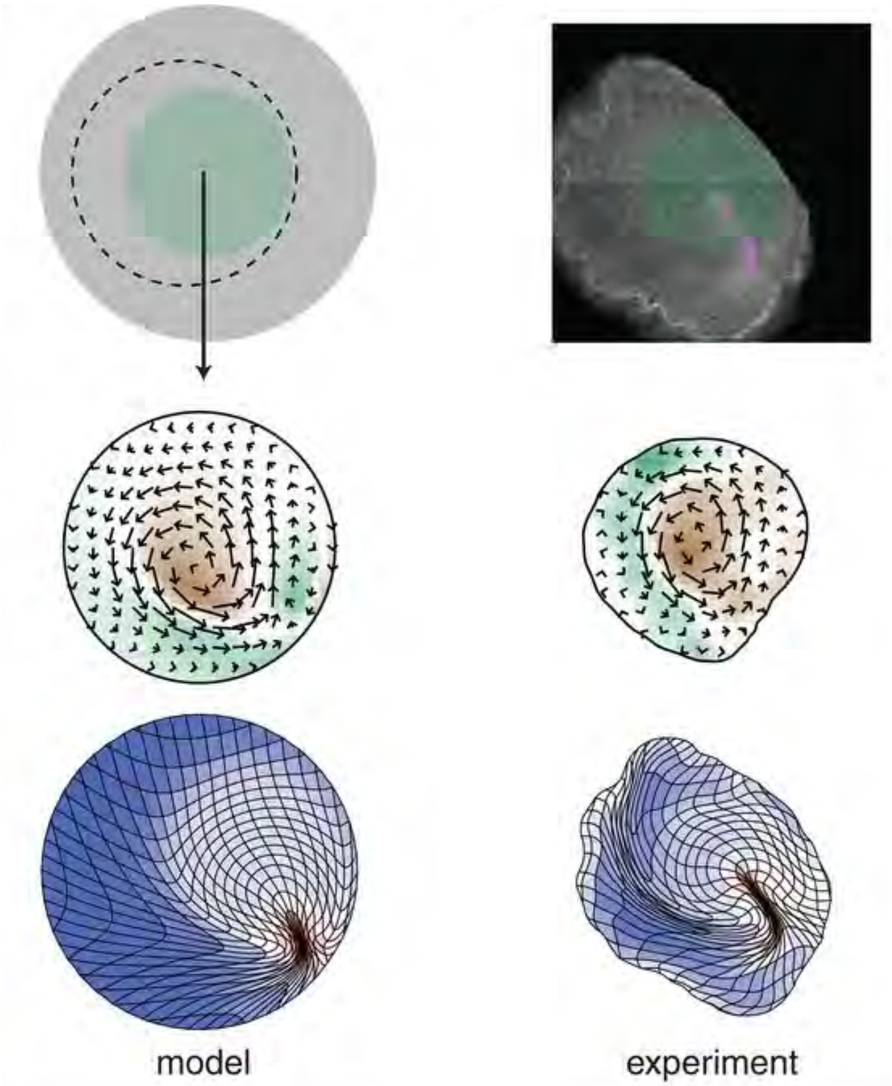

Saadhoui et al, *Science* 2018

Mechanical feedback in gastrulation

Experiments

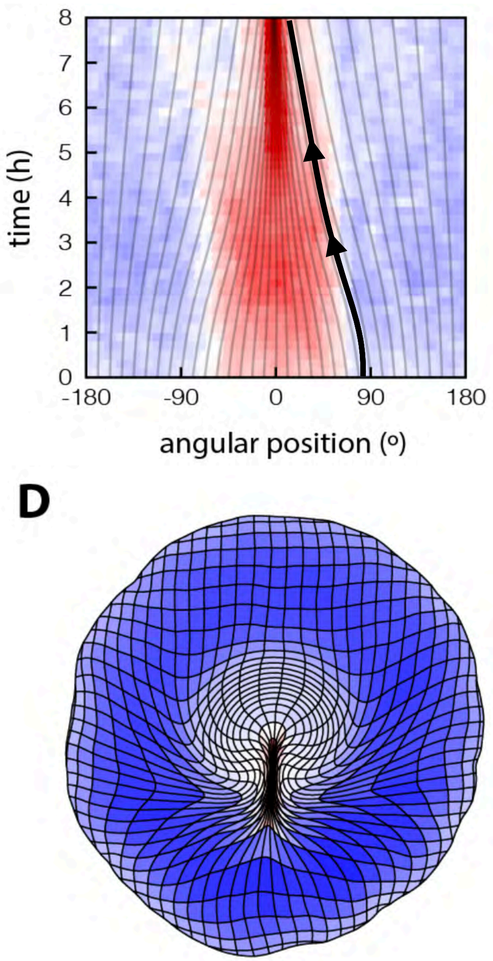

Model

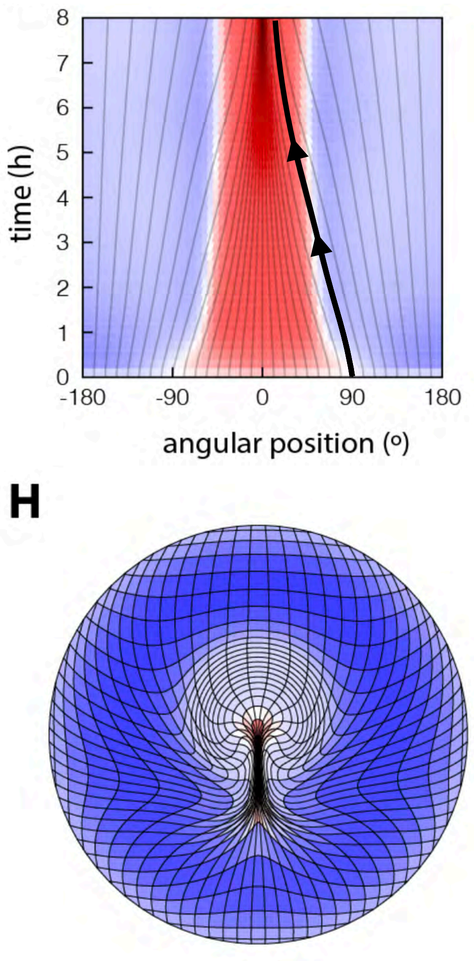

Contractile region is nearly stationary

ie **Eulerian**, not Lagrangian

Caldarelli et al *bioRxiv* 2021 [Gros & Corson Labs, Pasteur/ENS]

[On board]

Total tension T

Force balance: $\partial_x T = 0$

$\Rightarrow T = \text{const}$ for ring

$\Rightarrow T = 0$ for open curve

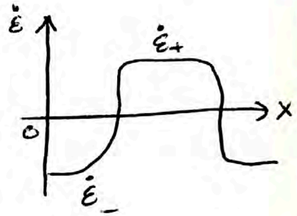

How does the pattern of $\dot\varepsilon$ self-organize?

Suppose active stress, driven by myosin, has + feedback, degrades, & diffuses

$$\underbrace{D_t m}_{\partial_t m + \partial_x (v m)} = \tilde f(\dot\varepsilon, m) - m + D\partial_x^2 m$$

$$\partial_t m + \partial_x (v m) = \partial_t m + v\partial_x m + m\underbrace{\partial_x v}_{\dot\varepsilon}$$

absorb dilation into $\tilde f$

$f \equiv \tilde f - \dot\varepsilon m$

and assume $f = f(\dot\varepsilon)$

[turnover on timescale of dil.]

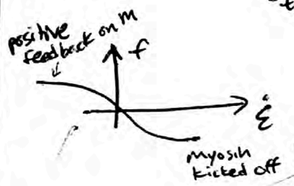

$$\partial_t m + v\partial_x m = f(\dot\varepsilon) - m - D\partial_x^2 m \quad *$$

Closed ring: $\int_0^L dx\, \dot\varepsilon = 0$

T will be a "Lagrange multiplier" for this constraint

Recast * as eq for $\dot\varepsilon$:

$T = T_a + \mu\dot\varepsilon = \text{const} \longrightarrow T_a = T - \mu\dot\varepsilon$

$$\partial_t \dot\varepsilon + v\partial_x \dot\varepsilon = -\frac{1}{\mu} f(\dot\varepsilon) - \dot\varepsilon + T + D\partial_x^2 \dot\varepsilon$$

Stationary (domain wall) soln: $T = \dot\varepsilon + f(\dot\varepsilon)/\mu$ in plateaus

where $\partial_x \dot\varepsilon \approx 0$, $\partial_x^2 \dot\varepsilon \approx 0$

add to $\dot\varepsilon$ to $f(\dot\varepsilon)$

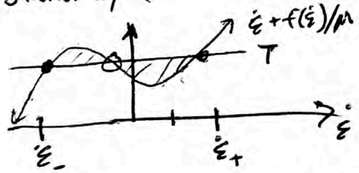

To find T, we use the closed ring constraint.

This becomes an equal area condition.

The velocity of the front can be shown to be $\approx$ zero.

Mechanical feedback in gastrulation

Same as before but scaled down by 2x

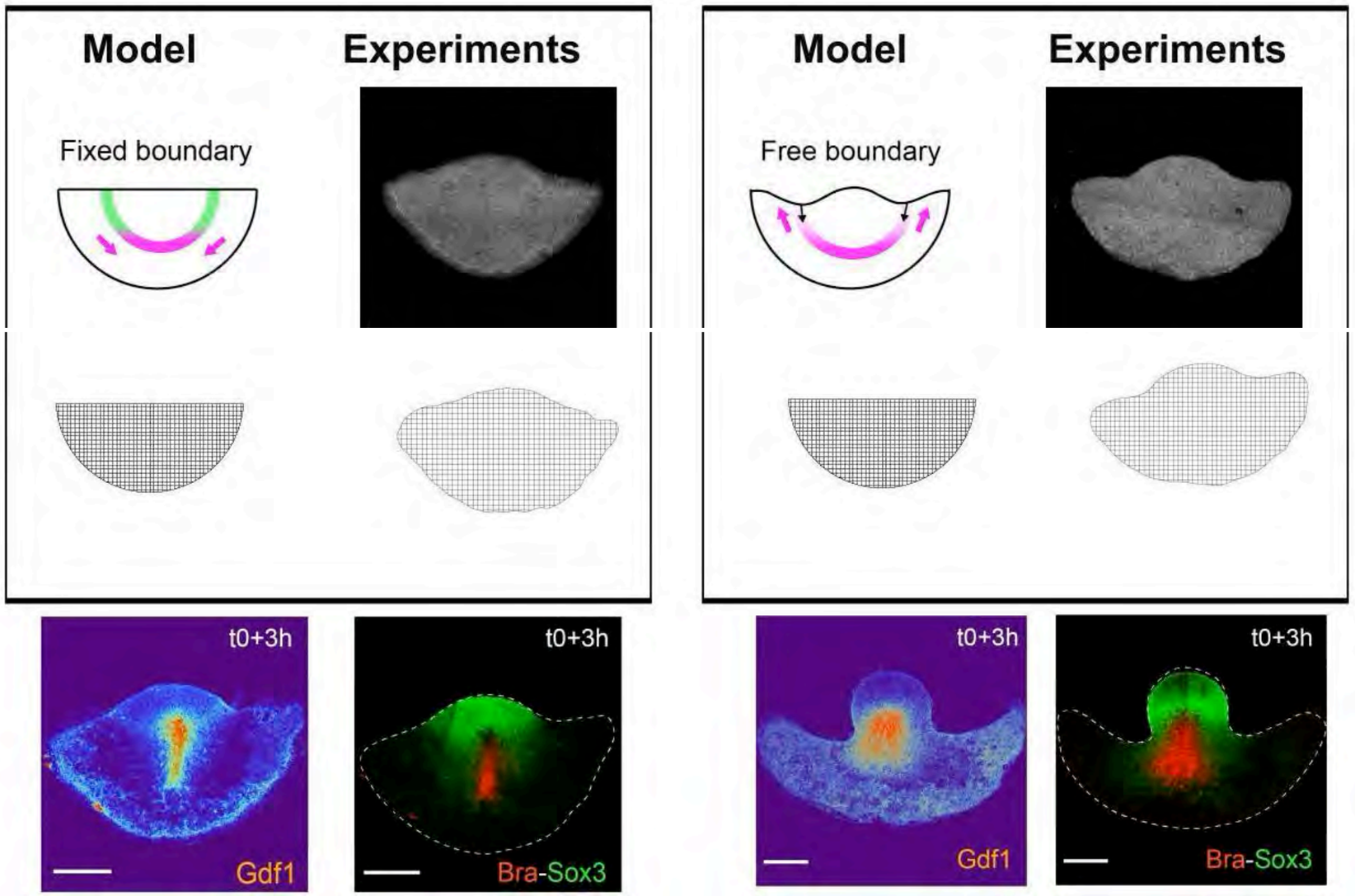

Constraint of vanishing average strain is gone!

Now the whole tissue can become contractile.

Caldarelli et al *bioRxiv* 2021 [Gros & Corson Labs, Pasteur/ENS]

Counter-rotational cell flows in morphogenesis across systems: mammalian hair follicle polarization

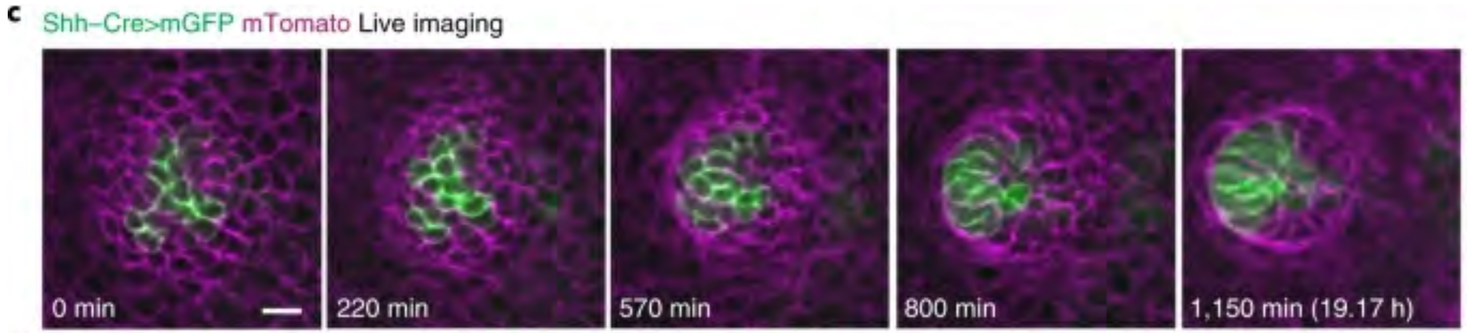

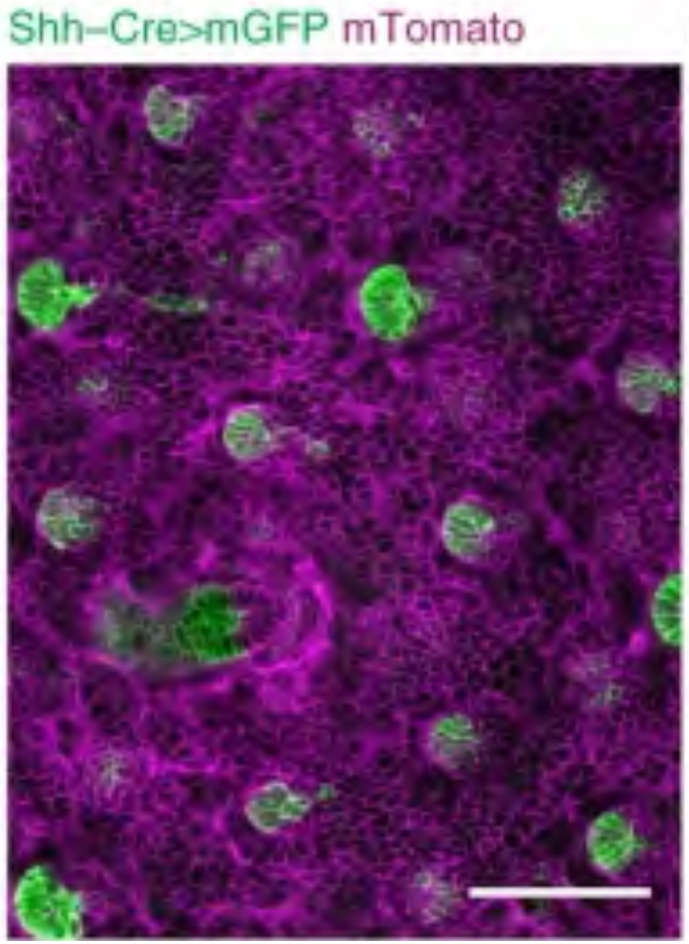

Cetera et al *Nat Cell Bio* 2018
Devenport Lab, Princeton

Counter-rotational cell flows in morphogenesis across systems: mammalian hair follicle polarization

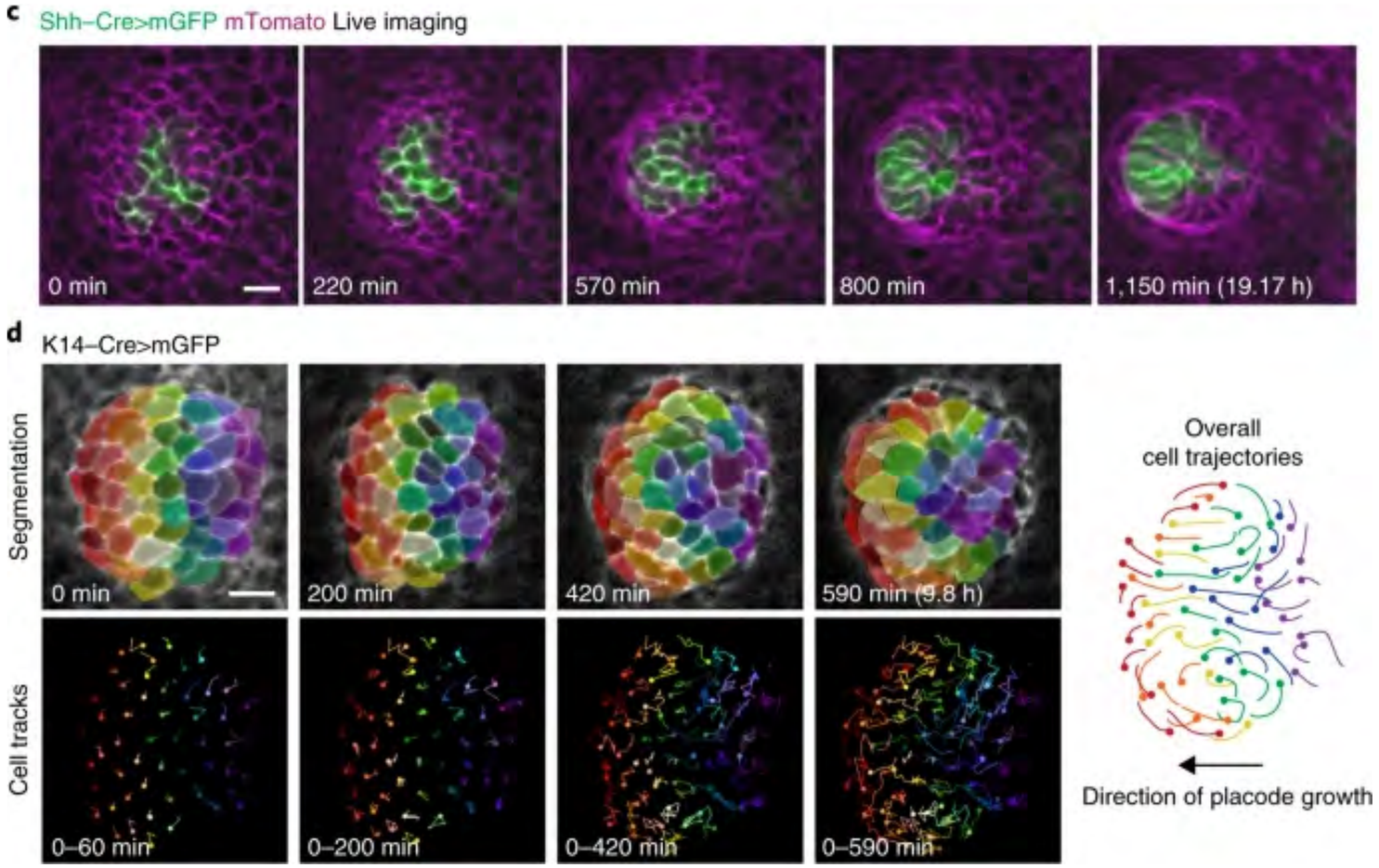

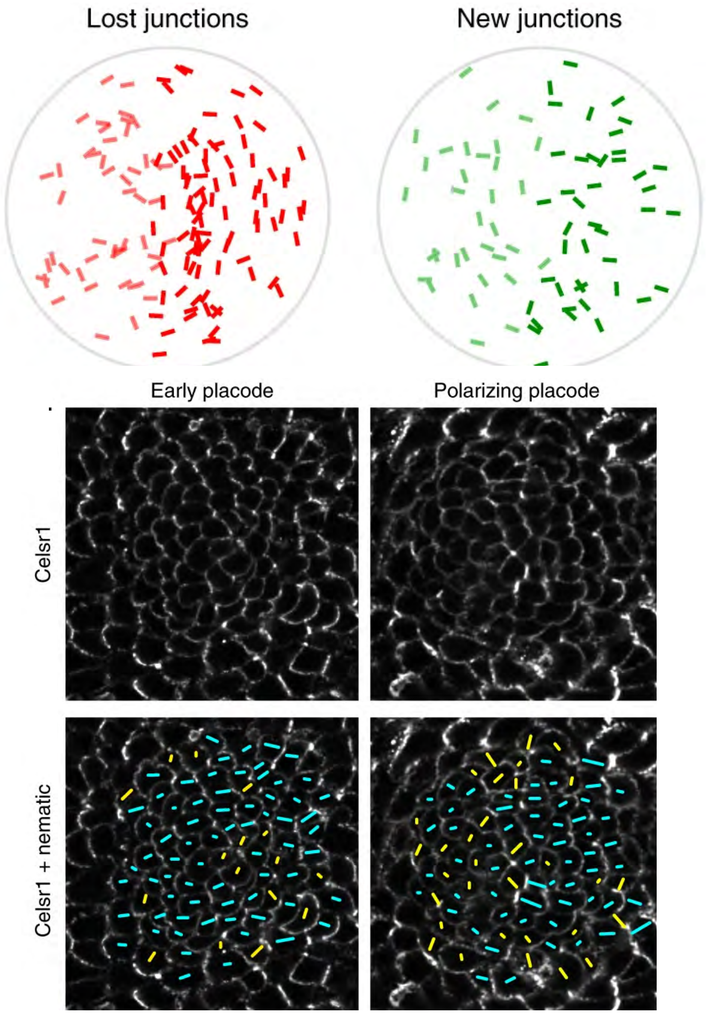

Cetera et al *Nat Cell Bio* 2018
Devenport Lab, Princeton

Counter-rotational cell flows in morphogenesis across systems: mammalian hair follicle polarization

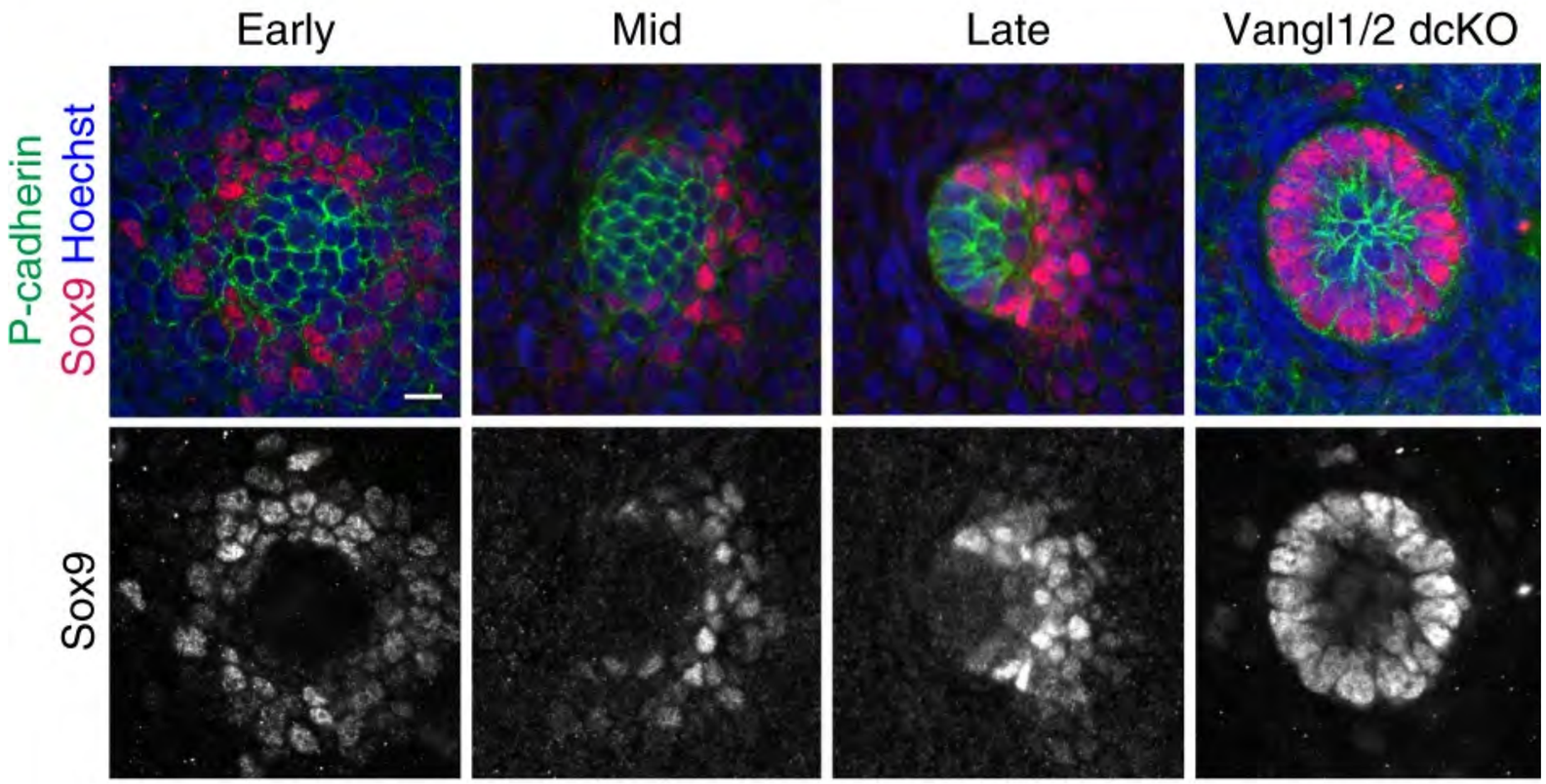

Requires planar cell polarity > Rho kinase + myoII

Linked to cell fate patterning

Cetera et al *Nat Cell Bio* 2018
Devenport Lab, Princeton

Counter-rotational cell flows in morphogenesis, part 3: cranial neural crest migration

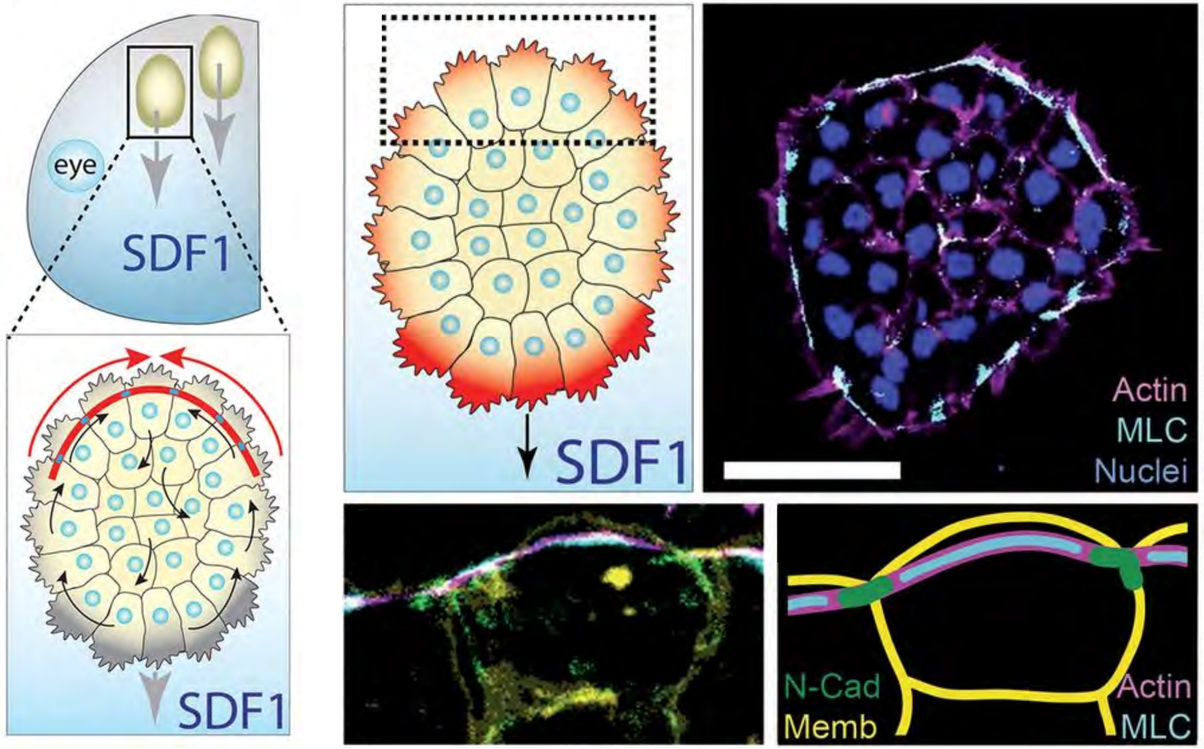

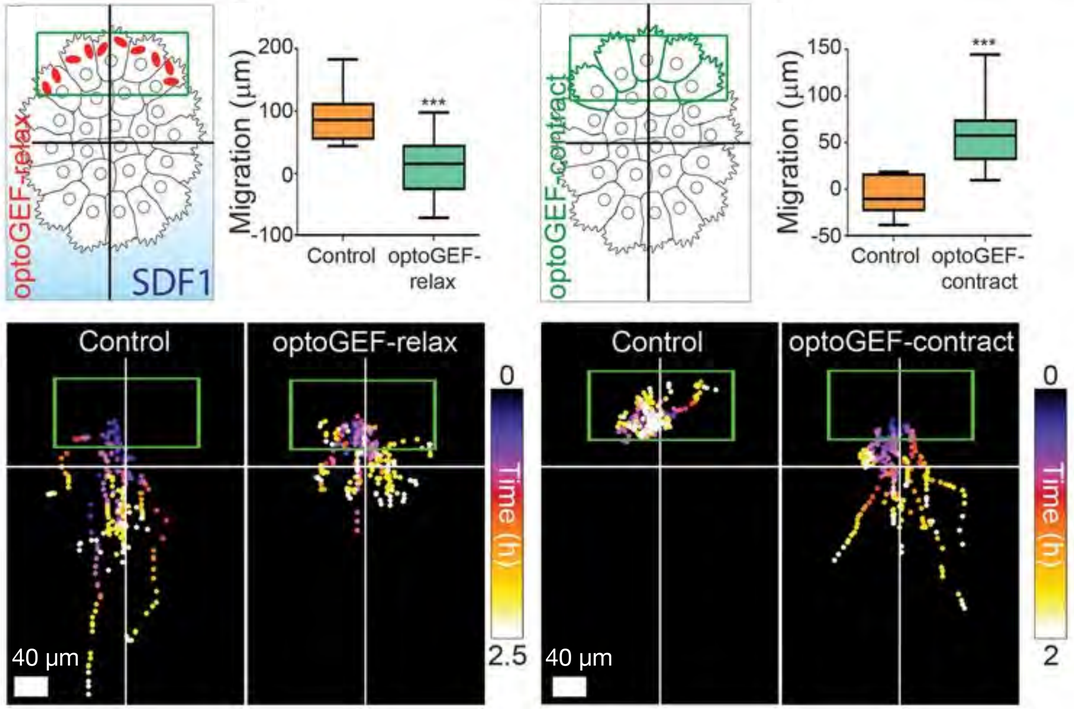

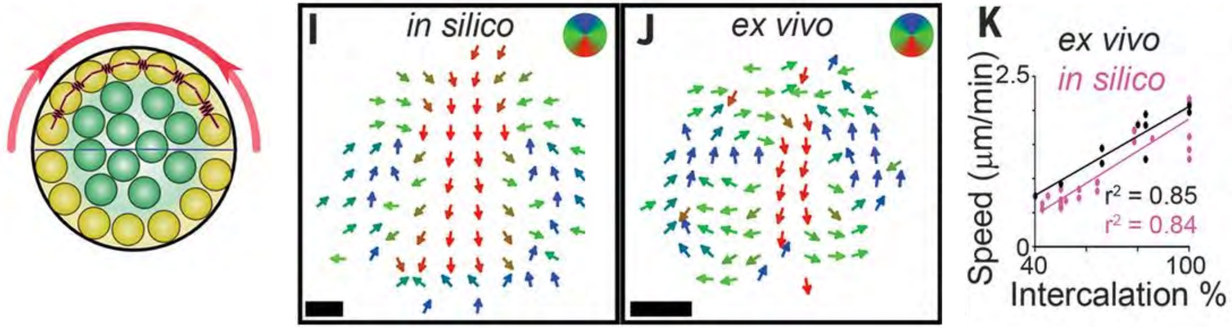

Shellard et al *Science* 2018
Mayor Lab, UCL

Polonaise motions in convergent extension across diverse systems

Different scales

Different motility mechanisms

Amniote gastrulation

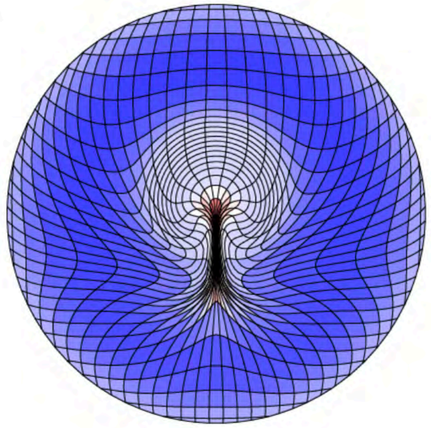

Saadhoui et al, *Science* 2018

Mouse hair follicle

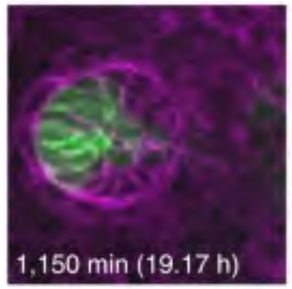

Cetera et al *Nat Cell Bio* 2018

Frog CNC migration

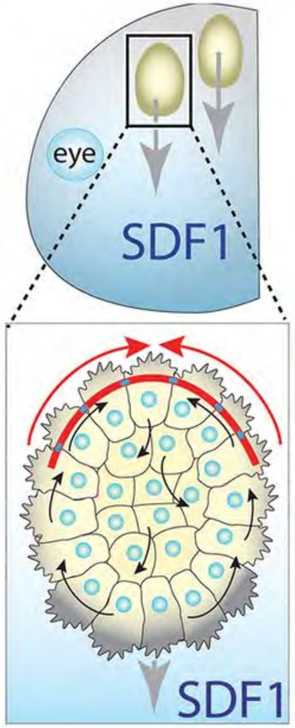

Shellard et al *Science* 2018

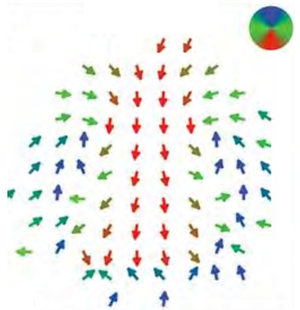

Active bending in gastrulation

a canonical example of tissue bending:
ventral furrow formation

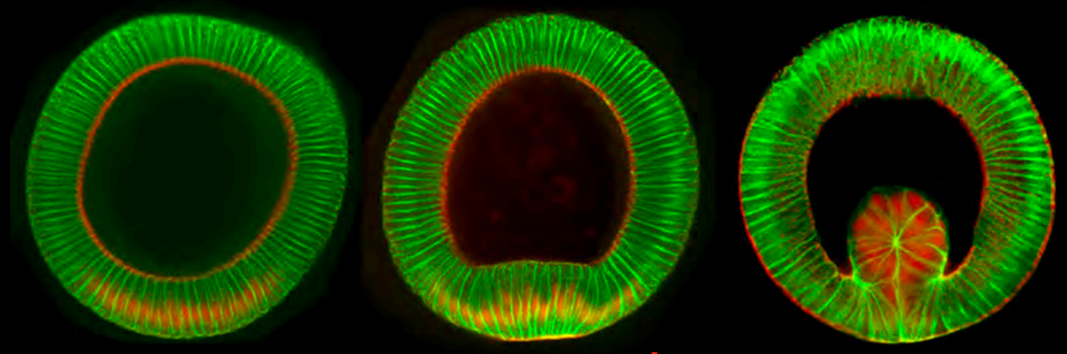

twist

Eric Wieschaus (Princeton)

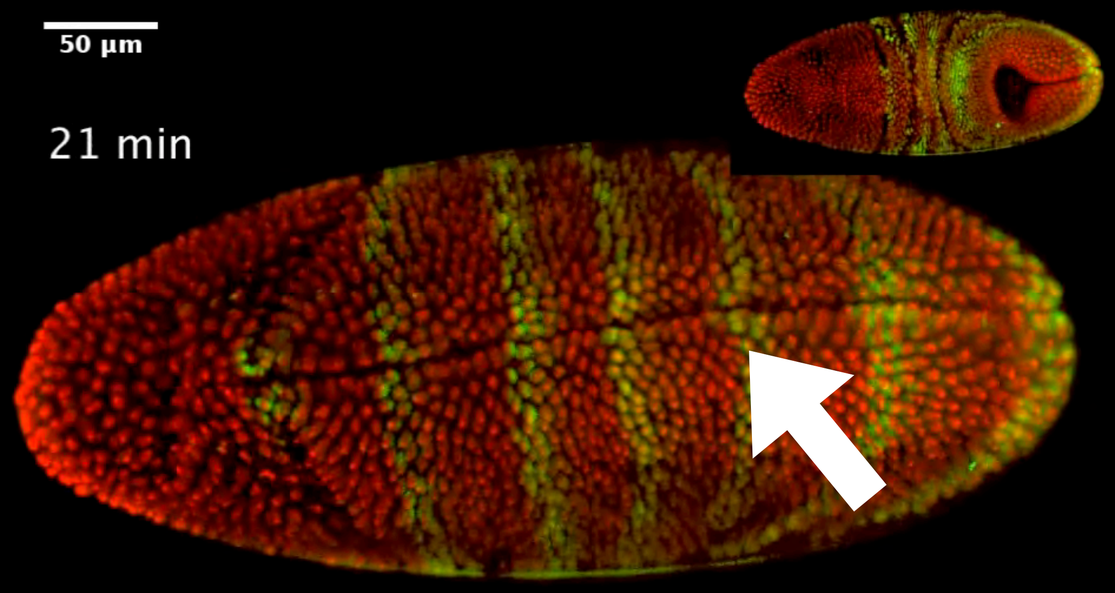

Internalized mesoderm

Streichan Lab (UCSB)

Bending (*a la* the bimetallic strip)

1D: curvature from difference in strains

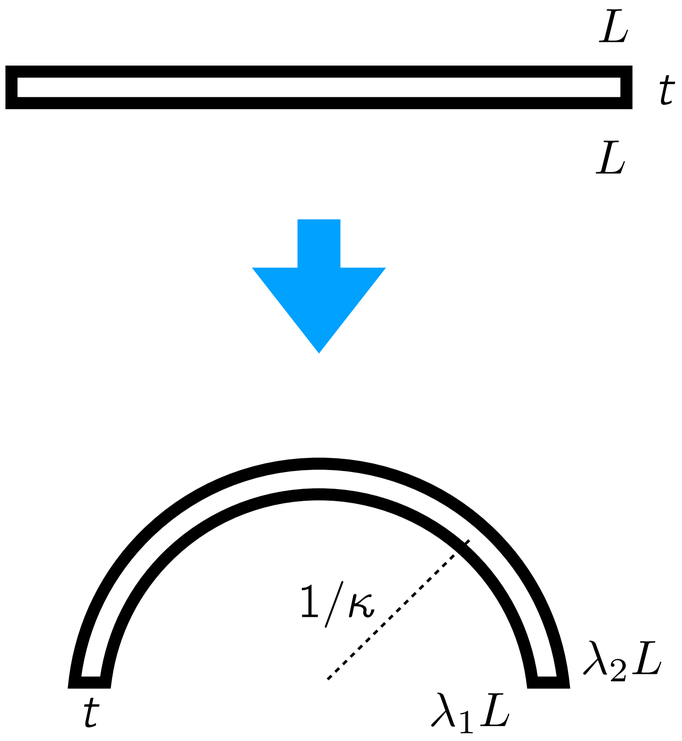

The length of the midline is the average stretch:

$$R\theta = \lambda L$$

Substituting into the expression for the length of the far edge gives the curvature:

$$\begin{aligned}
(R + t/2)\theta &= \lambda_2 L \\
(R + t/2)\theta &= \lambda_2 L \\
\theta &= \frac{2}{t}(\lambda_2 L - R\theta) \\
\frac{\lambda L}{R} &= \frac{2}{t}(\lambda_2 L - \lambda L) \\
\kappa\lambda &= \frac{2}{t}(\lambda_2 - \lambda) \\
\kappa &= \frac{\lambda_2 - \lambda_1}{\lambda t}.
\end{aligned}$$

Larger difference: more curved.
Thicker: less curved.
More average stretch: less curved.

Bending via **apical constriction** in epithelial morphogenesis

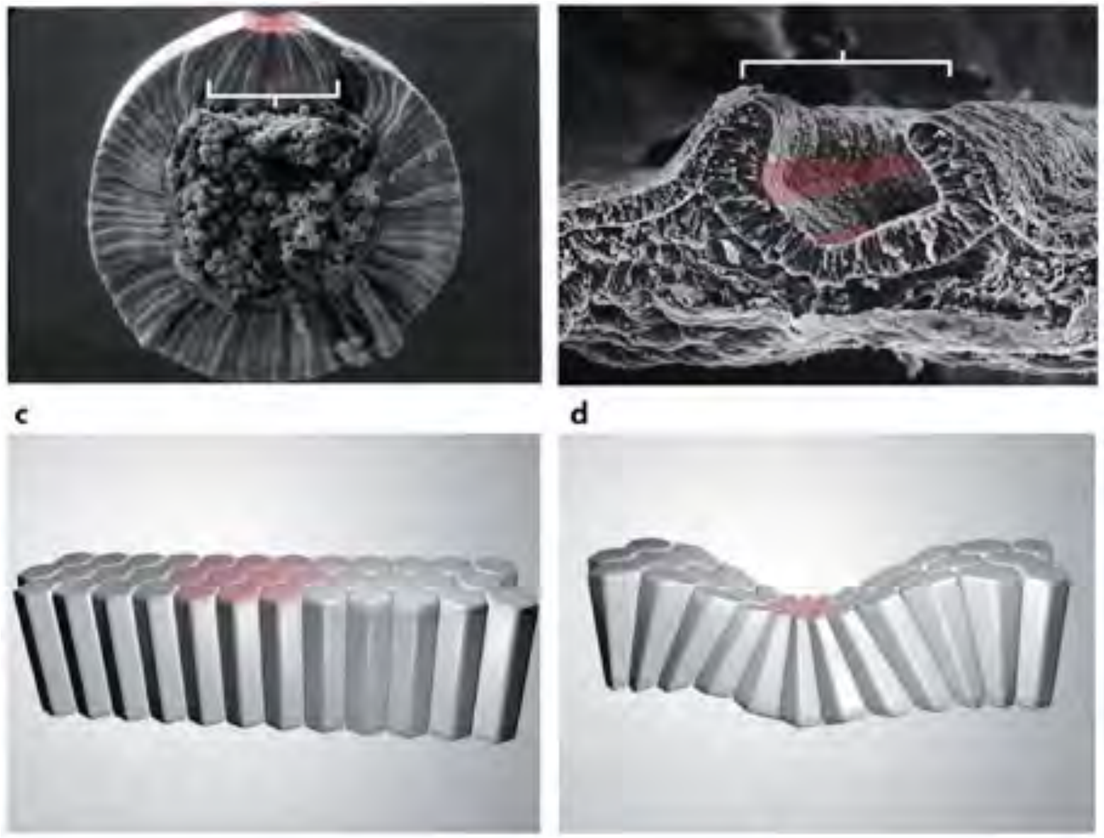

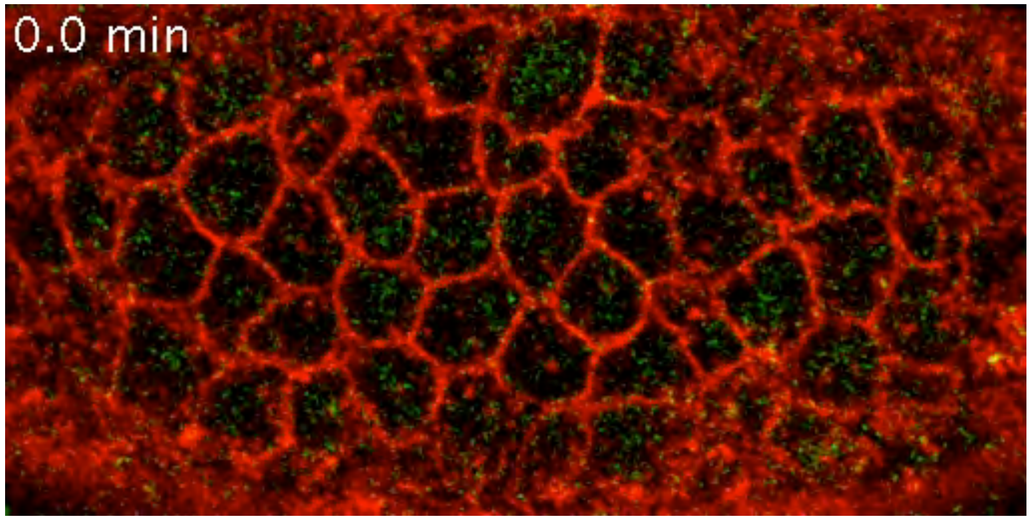

Myosin-mCherry
Spider-GFP

Martin *et al Nature* (2009)

Lecuit & Lenne, *Nat Rev Mol Cell Bio* 2007

Bending via **apical constriction** in epithelial morphogenesis

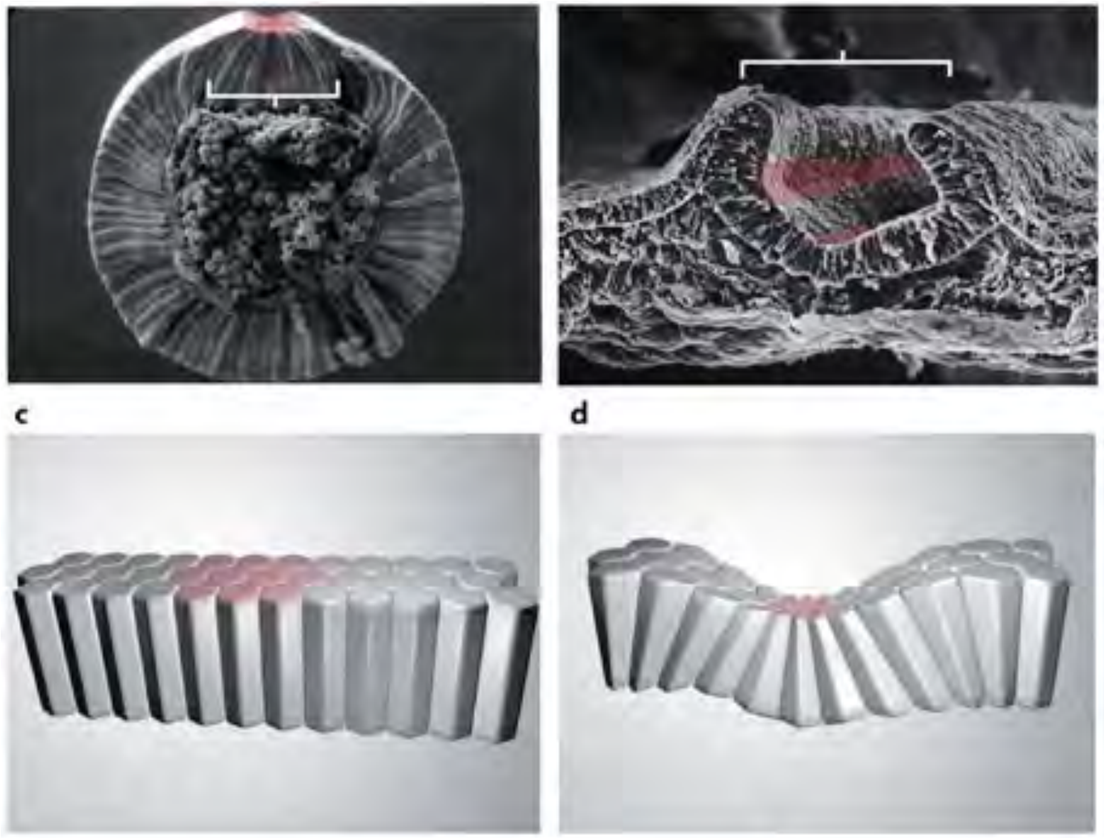

Conserved repertoire of structural motifs
Conserved cell mechanics

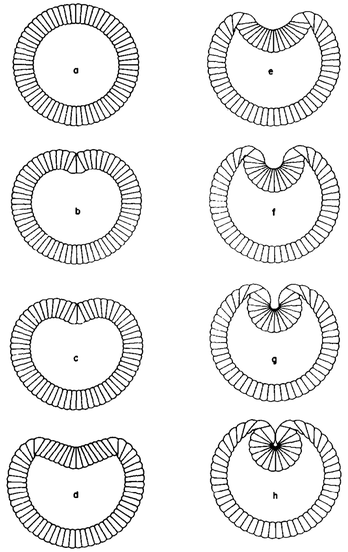

Drosophila ventral furrow formation

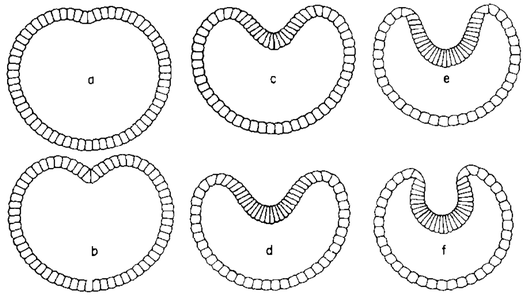

Sea urchin gastrulation

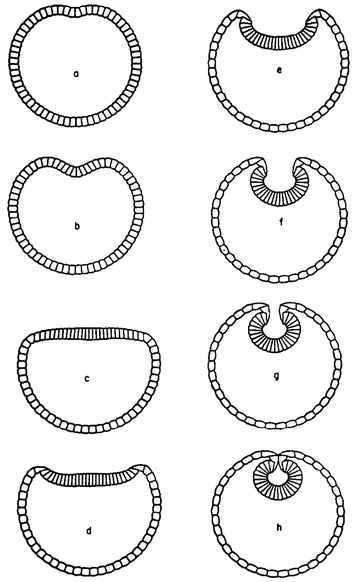

Frog neural tube formation

Odell, Oster, Alberch, & Burnside, *Dev Biol.* 1980

Bending via **apical constriction** in epithelial morphogenesis

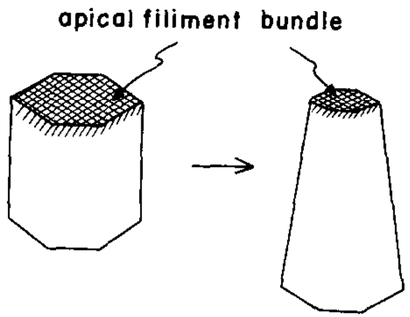

“purse-string” contraction in the apical cortex

Kelvin-Voigt = no turnover/internal remodeling, such that you have a fixed reference length. Viscosity is due to surrounding fluid, etc.

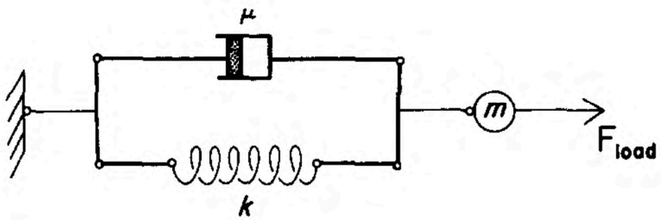

Viscoelastic units of the cell & cytoskeleton

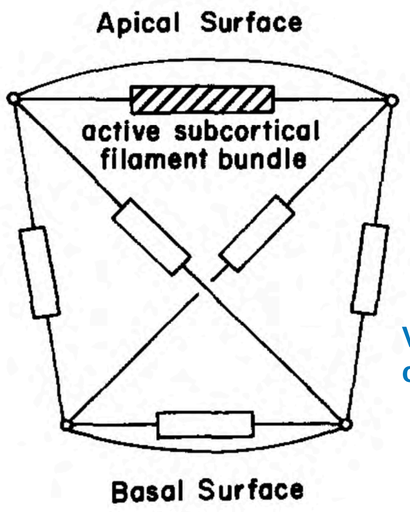

One excitable unit at the apical surface

Volume conservation

Mechanical feedback

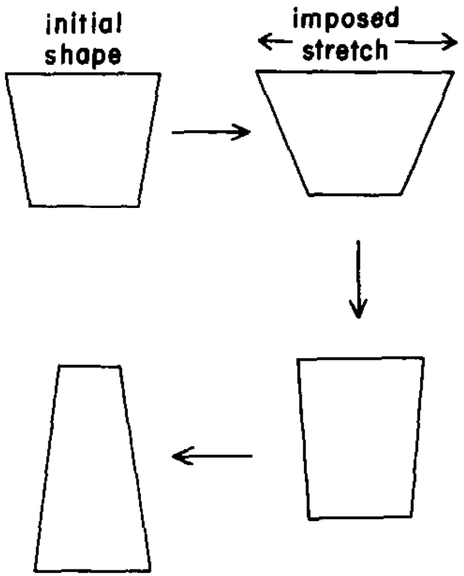

Shape dynamics under supercritical “trigger” of contraction and shortened rest length, with viscoelastic dynamics

Odell, Oster, Alberch, & Burnside, *Dev Biol.* 1980

Programmed curvature in ventral furrow

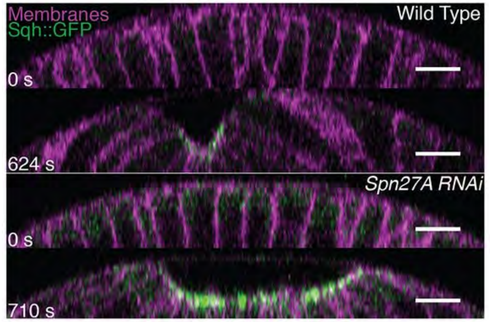

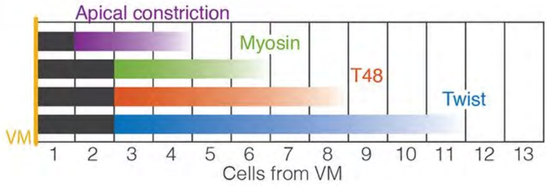

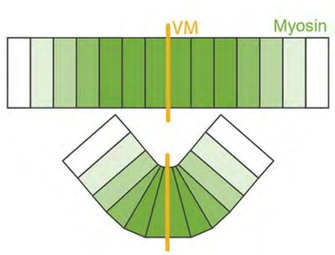

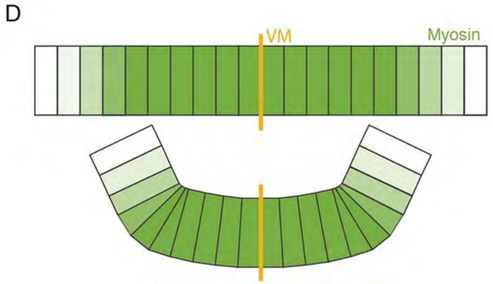

continuum picture

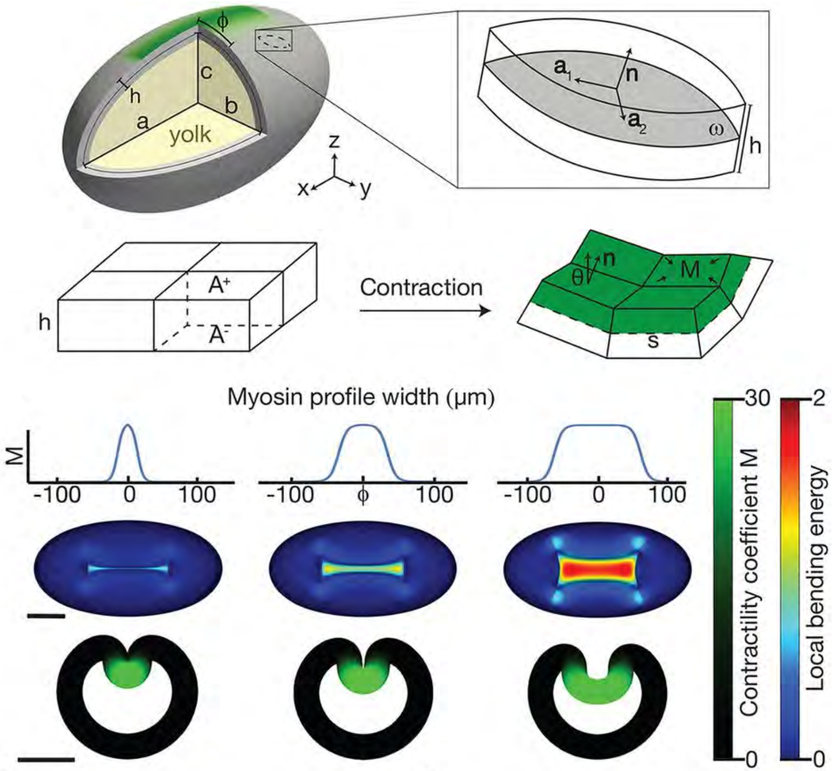

Heer et al *Development* 2017

[On board]

Some differential geometry for Koiter elasticity

Metric ('first fundamental form')

$$a_{\alpha\beta} = \boldsymbol{a}_\alpha \cdot \boldsymbol{a}_\beta = a_{\beta\alpha}$$

Example: flat space –> identity

surface tangent vectors $\mathbf{a}_\alpha(\mathbf{r})$

Surface normal

$$\mathbf{n} = \frac{\boldsymbol{a}_1 \times \boldsymbol{a}_2}{|\boldsymbol{a}_1 \times \boldsymbol{a}_2|}$$

Curvature tensor ('Second fundamental form')

$$b_{\alpha\beta} = \mathbf{n} \cdot \partial_\beta \mathbf{a}_\alpha = \frac{\partial^2 \mathbf{r}}{\partial^\alpha \partial^\beta} \cdot \mathbf{n}$$

how the surface curves within the ambient space

$$b_{ij} := -\mathbf{e}_i \cdot \partial_j \mathbf{n}$$

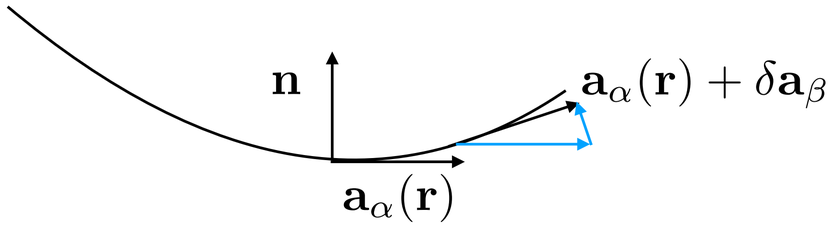

https://static-content.springer.com/esm/art%3A10.1038%2Fnmat4202/MediaObjects/41563_2015_BFnmat4202_MOESM12_ESM.pdf

[On board]

Active Koiter elasticity

The KS equations describe the equilibrium of a thin shell when the thickness *h* of the shell is small compared to its curvature in undeformed and deformed configurations.

$$\mathcal{E}_{KS} = \mathcal{E}_b + \mathcal{E}_s + \mathcal{E}_f$$

shear + bulk Linear change in area

$$\mathcal{E}_s = \frac{Yh}{8(1-\nu^2)} \int_{\bar{\omega}} S(M) \left[(1-\nu)\mathrm{Tr}[(a_{\alpha\beta} - \bar{a}_{\alpha\beta})^2] + \nu \mathrm{Tr}(a_{\alpha\beta} - \bar{a}_{\alpha\beta})^2 \right] d\bar{\omega}$$

$$\mathcal{E}_b = \frac{Yh^3}{24(1-\nu^2)} \int_{\bar{\omega}} S(M) \left[(1-\nu)\mathrm{Tr}[(b_{\alpha\beta} - \bar{b}_{\alpha\beta})^2] + \nu \mathrm{Tr}(b_{\alpha\beta} - \bar{b}_{\alpha\beta})^2 \right] d\bar{\omega}$$

$$\mathcal{E}_f = \mu_V (V - V_0)^2 + \mu_S \int_{\bar{\omega}} B(\mathbf{\Theta}) \mathbf{d}\bar{\omega}$$

volume constraint imposed by the enclosed yolk

boundary wall constraint imposed by the vitelline membrane on the embryo

Surface parameterization

$$\mathbf{S} = \mathbf{\Theta}(\eta_1, \eta_2)$$

Surface element

$$d\omega = \sqrt{|\det(a_{\alpha\beta})|} d\eta_1 d\eta_2$$

Gradients of $\mathcal{E}_{KS}$ give force.
Evolve with viscous damping.

Note

$$K_{2D} = \frac{E_{2D}}{2(1-\nu_{2D})}$$

[On board]

Active Koiter elasticity

$$E(A^+, A^-) = C_M \rho_M A^{+2} + K(A^+ - A^0)^2 + K(A^- - A^0)^2$$

Energy for a cell

$$M = C_M \rho_M / K$$

Contractility coefficient

- incompressibility of the cytoplasm, we assume a constant cell volume.
- cell is significantly stiffer against vertical compression than against horizontal, and treat the cell height as a fixed quantity *h*

$$A^+ + A^- + \sqrt{A^+ A^-} = 3A^0$$

$$\kappa(M) \approx \frac{\theta}{s}$$

$$\theta = \pi - 2\tan^{-1}\left[2h/(\sqrt{\bar{A}^-} - \sqrt{\bar{A}^+})\right]$$

$$s = (\sqrt{\bar{A}^+} + \sqrt{\bar{A}^-})/2$$

distance between cell centers on the middle-surface

Ventral furrow formation in *Drosophila*: pulsatile ratcheting contraction

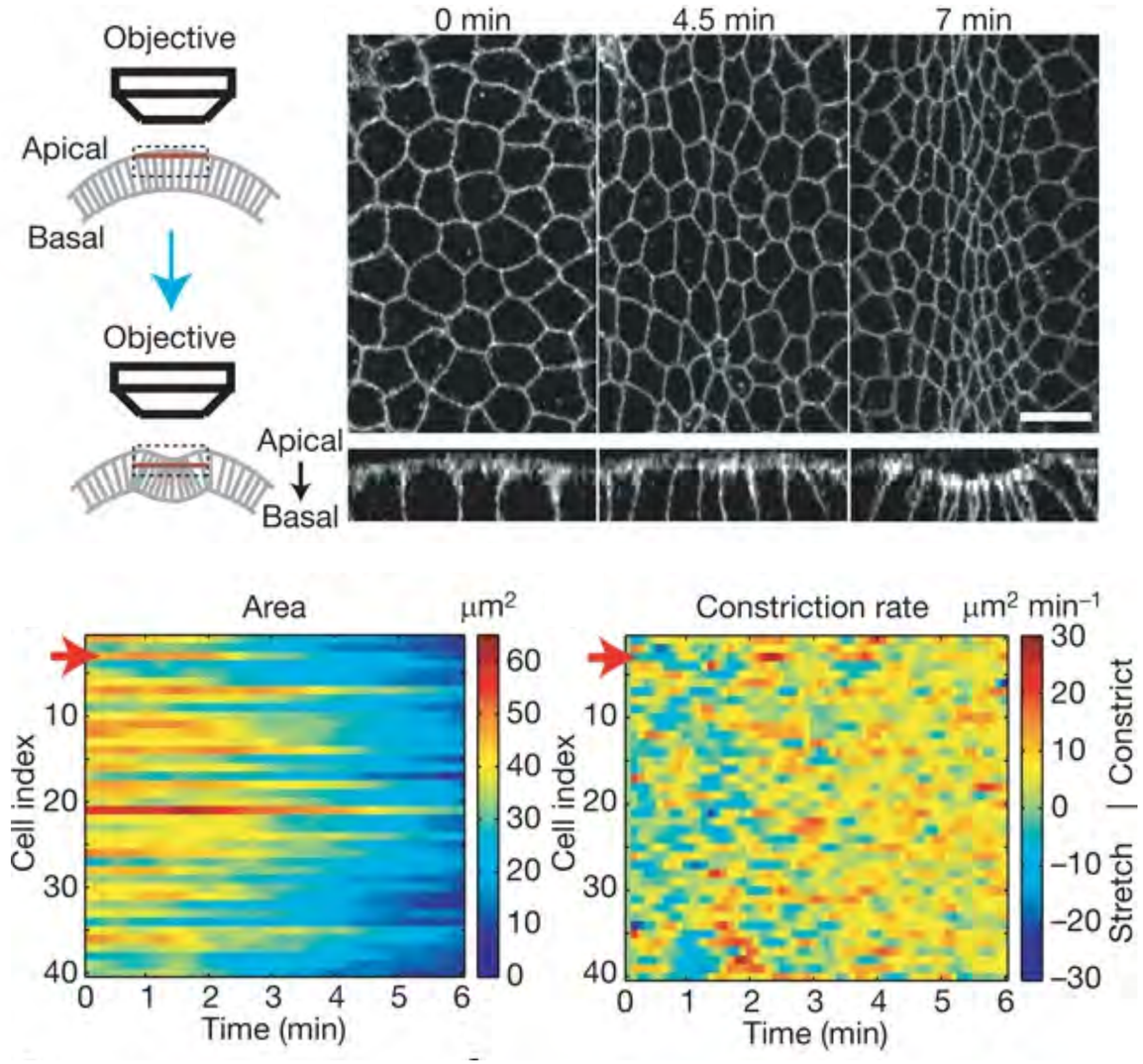

Future directions: coupling pulsatile/mechanical oscillators

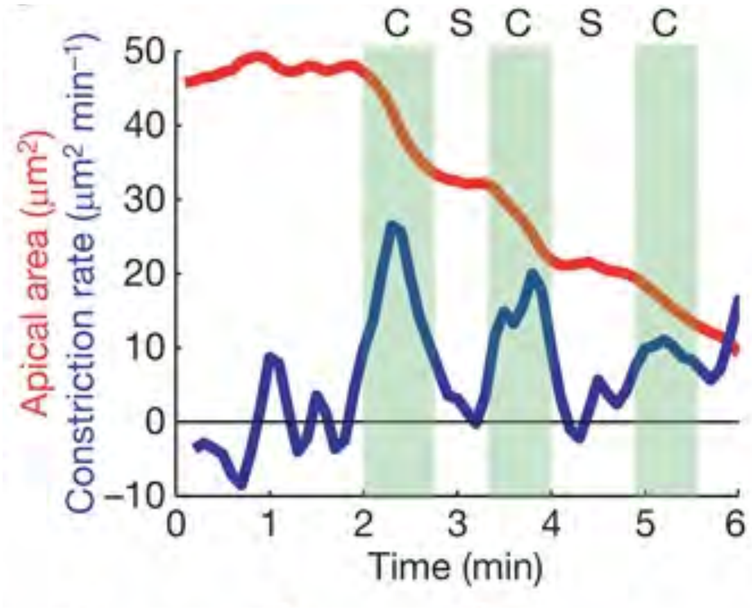

Martin et al *Nature* 2009

Ventral furrow formation in *Drosophila*: pulsatile ratcheting contraction

snail mutants *twist* mutants

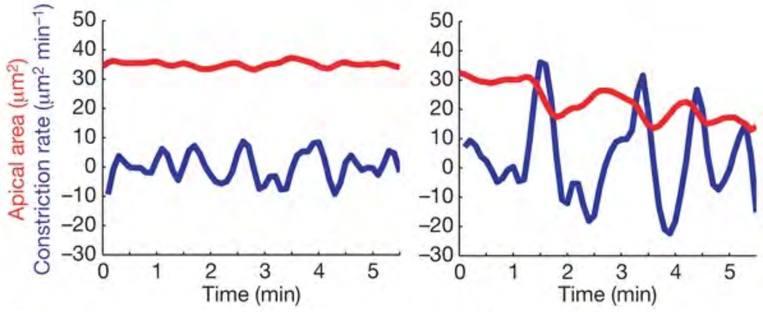

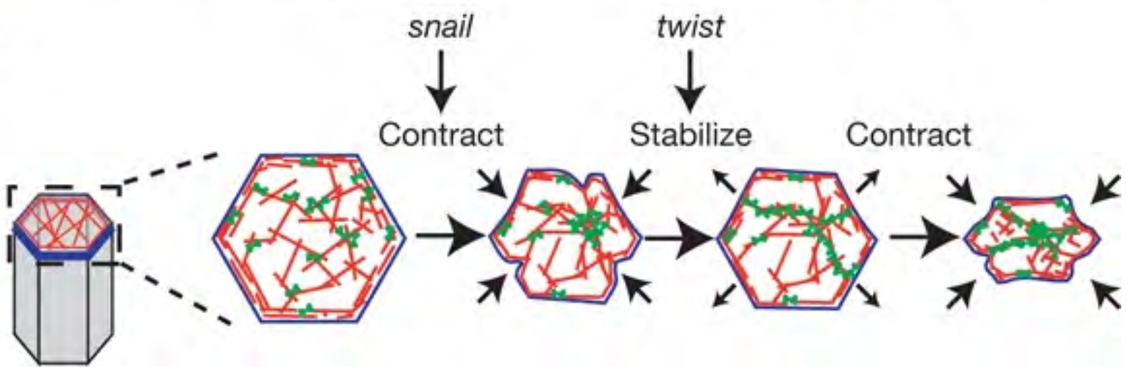

Future directions: coupling pulsatile/mechanical oscillators

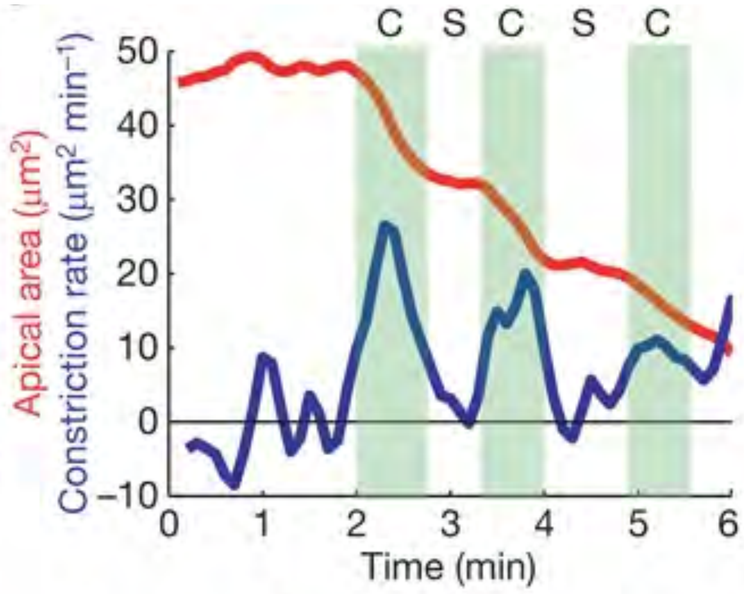

Martin et al *Nature* 2009

Mechanical cues in epithelial lung branching morphogenesis

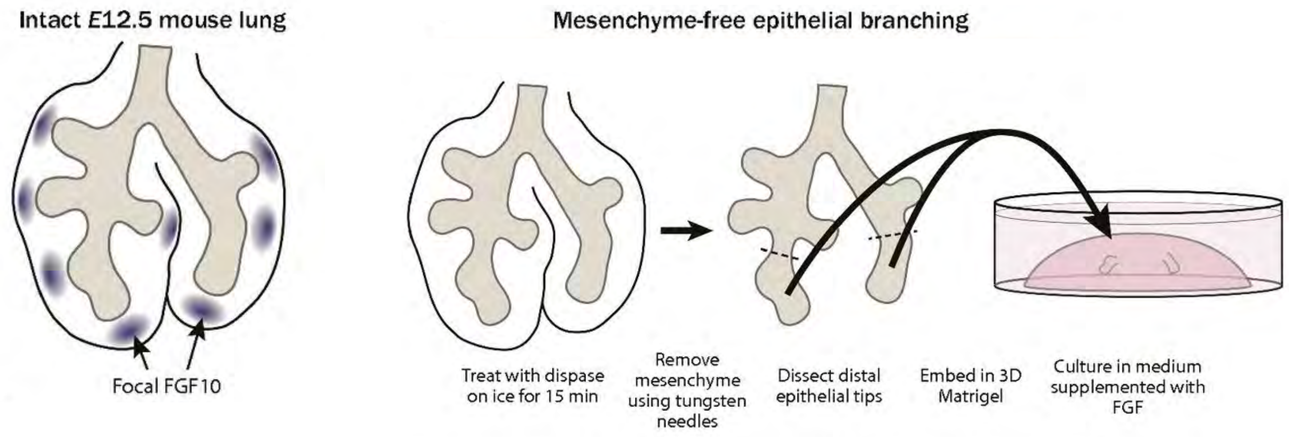

Lung branching stereotypy is in part due to biochemically patterned FGF (a la reaction-diffusion)

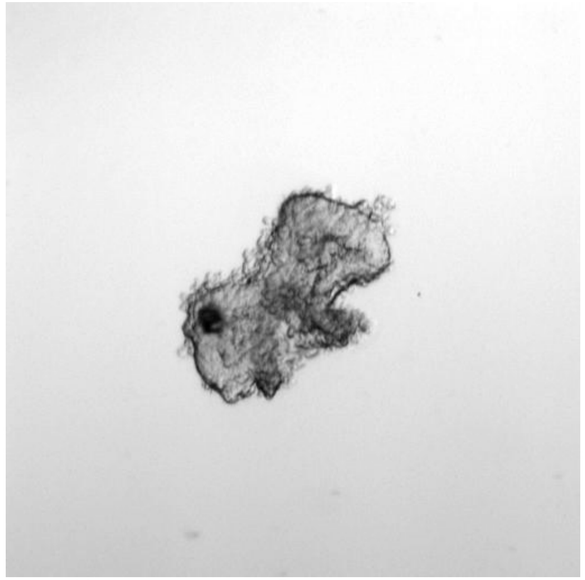

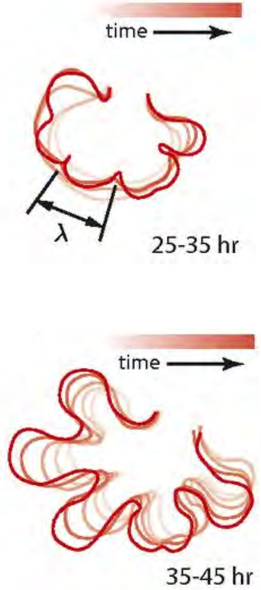

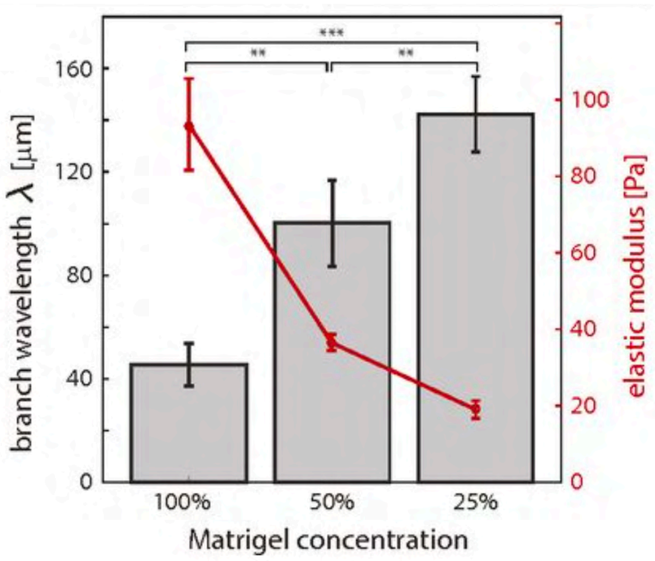

$$\lambda_{cr_e} = 2\pi h \sqrt[3]{B/3B_f},$$

B = elastic modulus of tissue

B_f = elastic modulus of matrigel

Spatial Patterns of Proliferation Do Not Appear Until Branches Have Already Formed.

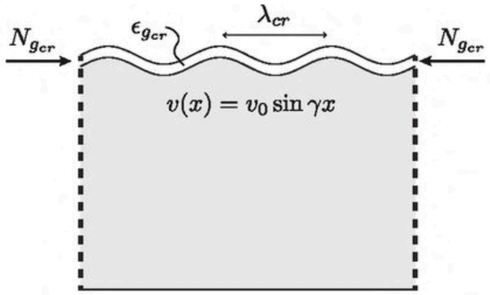

Varner et al, *PNAS* 2015

Self-organization vs genetic programming in branching morphogenesis

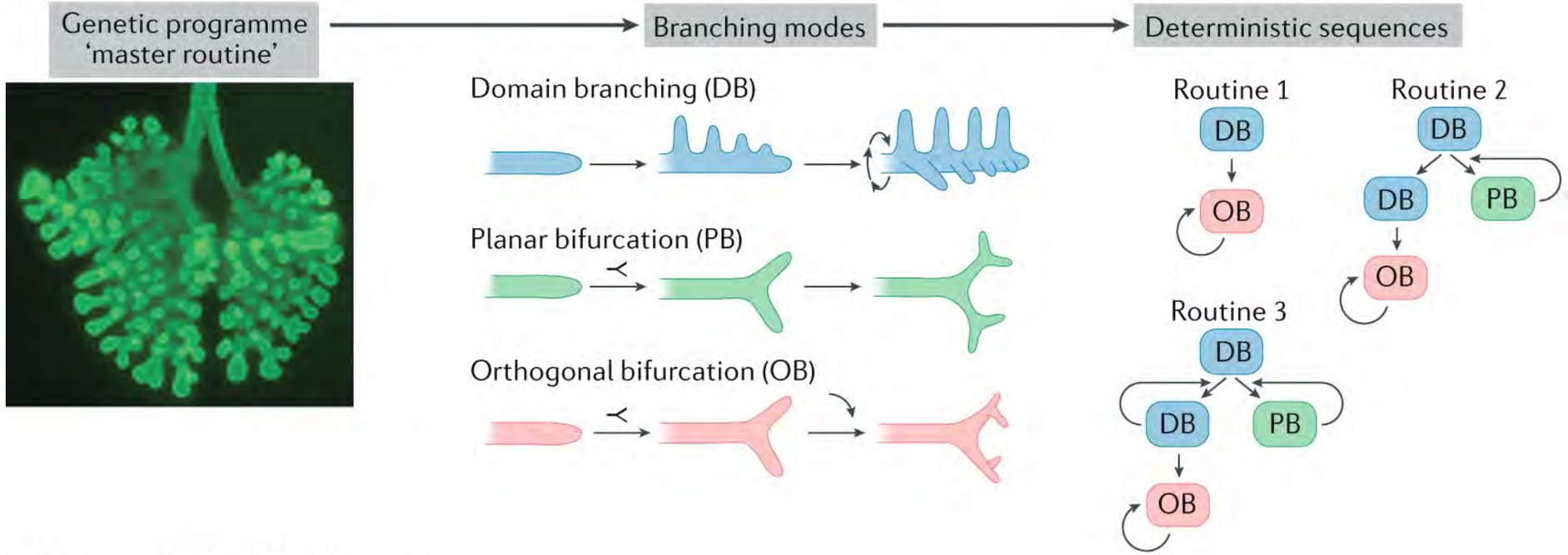

"…each mode of branching is controlled by a genetically encoded subroutine, a series of local patterning and morphogenesis operations, which are themselves controlled by a more global master routine."

- genetically tractable
- suited to evolution

Metzger, Klein, Martin. Krasnow. The branching programme of mouse lung development. *Nature* **453**, 745–750 (2008)

2D buckling as a mechanism for villi formation

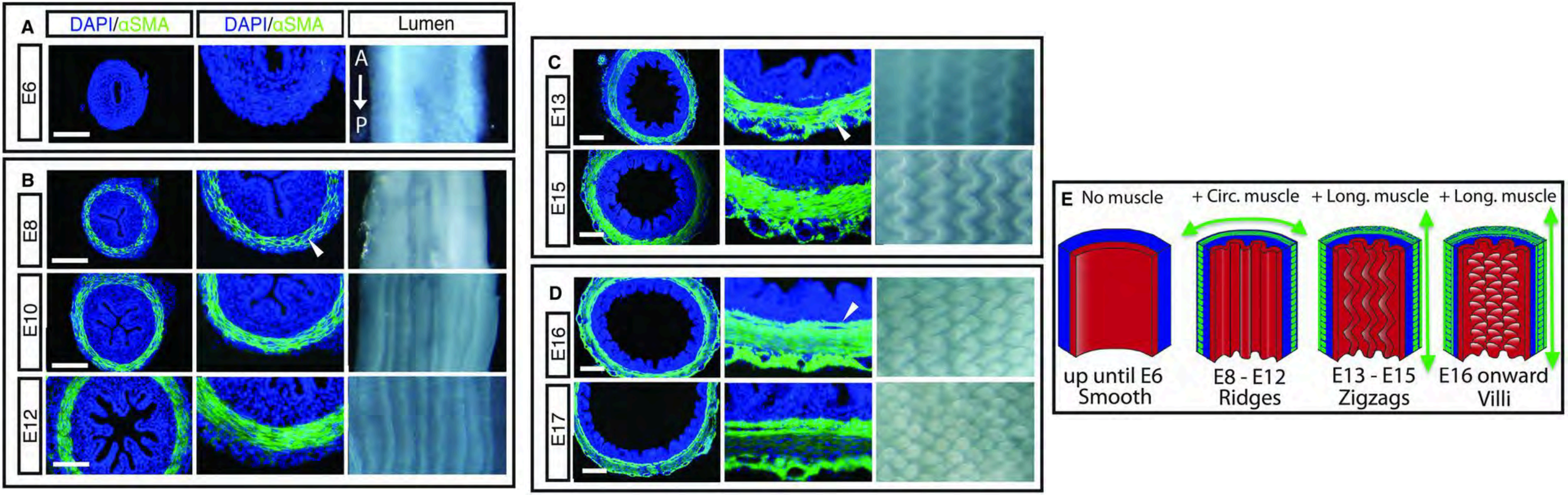

Shyer et al, *Science* 2013

2D buckling as a mechanism for villi formation

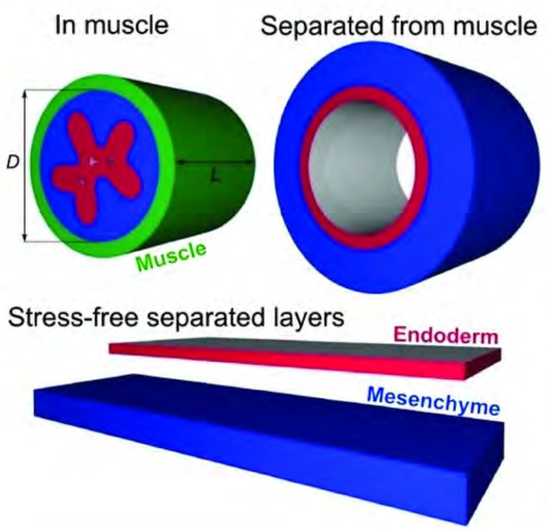

$$W = \frac{\mu}{2}\left[\overbrace{\mathrm{Tr}(\mathbf{F}\mathbf{F}^{\mathrm{T}})}^{\lambda_1^2+\lambda_2^2+\lambda_3^2}J^{-2/3} - 3\right] + K(J - \log J - 1)$$

$$dx_j = F_{jK}\, dX_K$$

$$J = \det(\boldsymbol{F}) = \lambda_1\lambda_2\lambda_3$$

neo-Hookean energy density

Highly non-linear – *forget analytics*

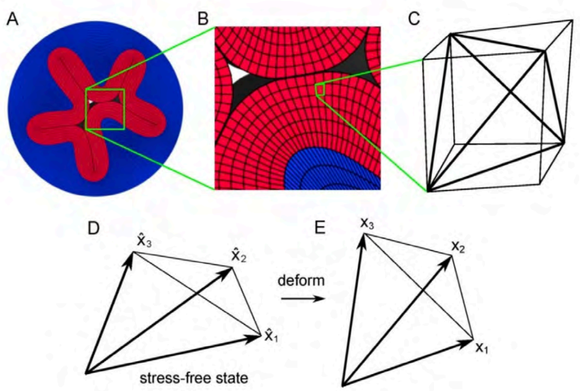

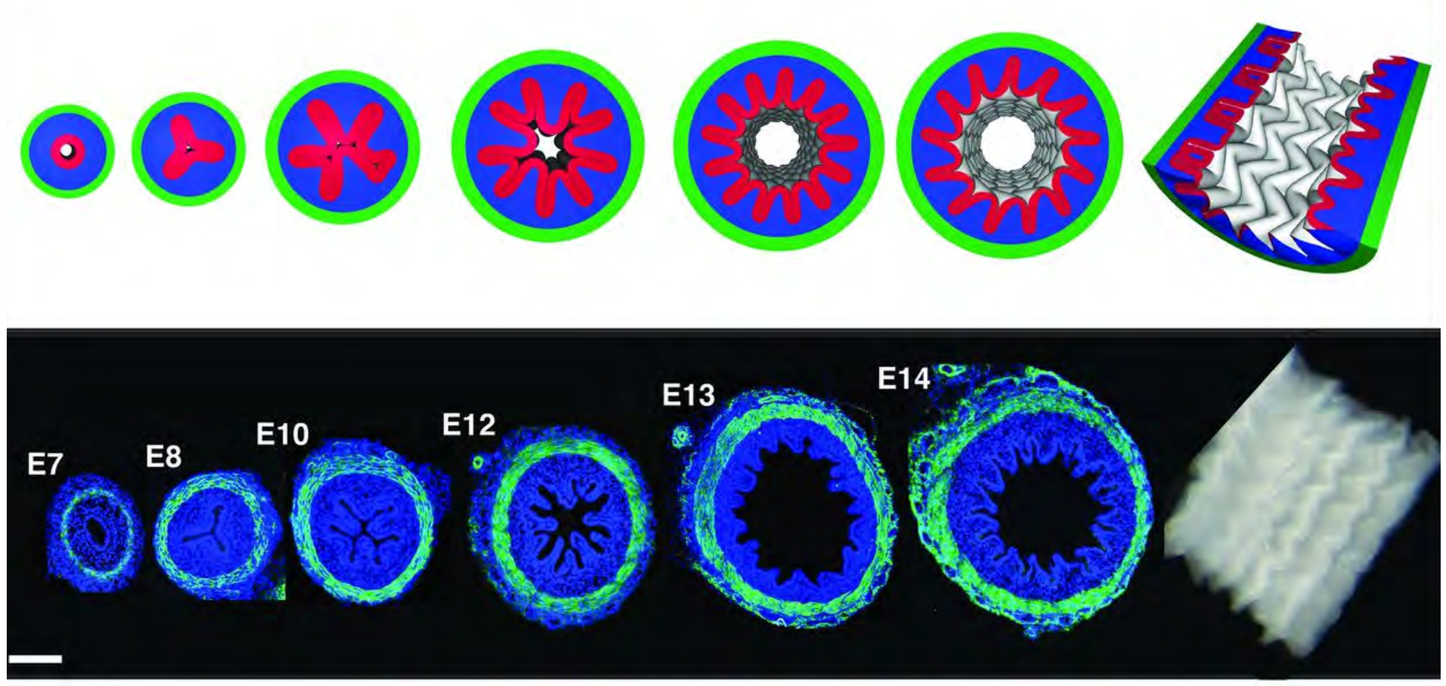

Shyer et al, *Science* 2013

Feedback from shape to transcription: 2D buckling as a mechanism for stem cell specification

Feedback from shape to fate

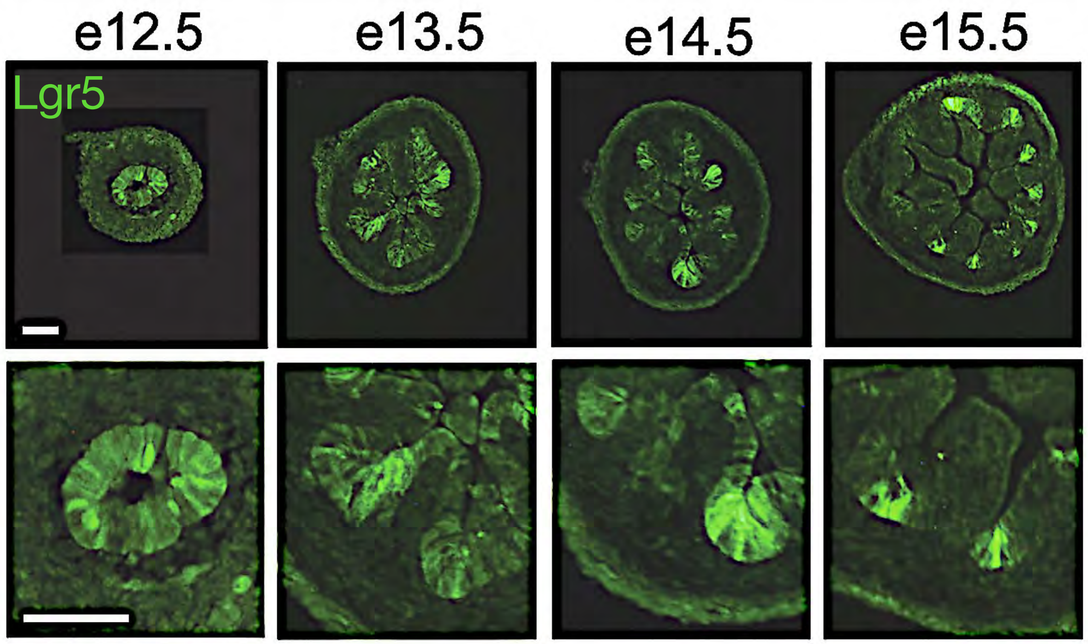

mouse intestine cross sections

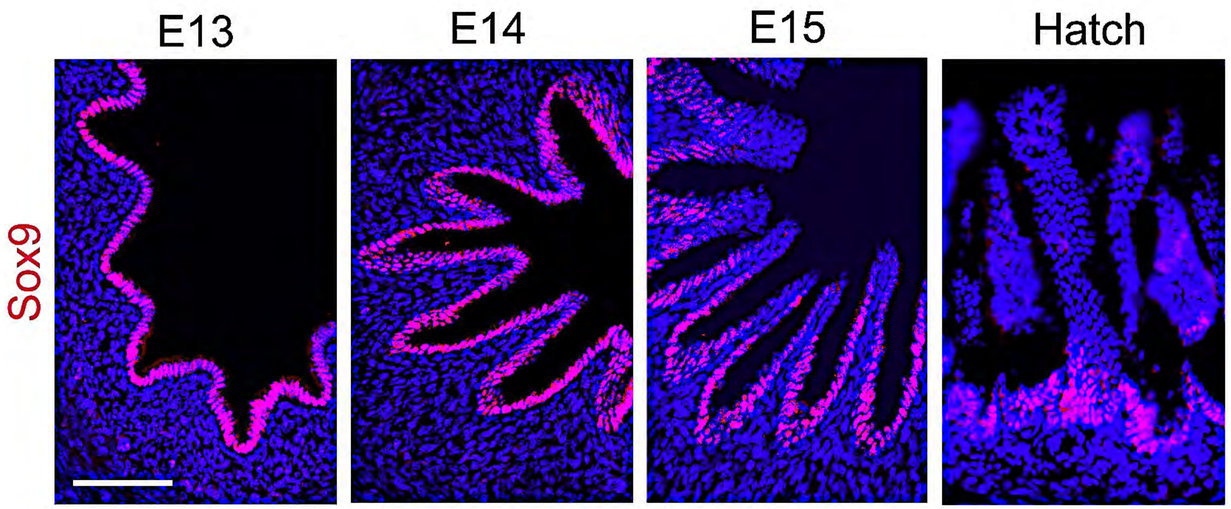

chick intestine cross sections

Intestinal stem cell markers are refined during development

Shyer et al, *Cell* 2015

Feedback from shape to transcription: 2D buckling as a mechanism for stem cell specification

Mechanical constraints from the muscle dictate stem cell identities in the endoderm through elastic effects on tissue geometry

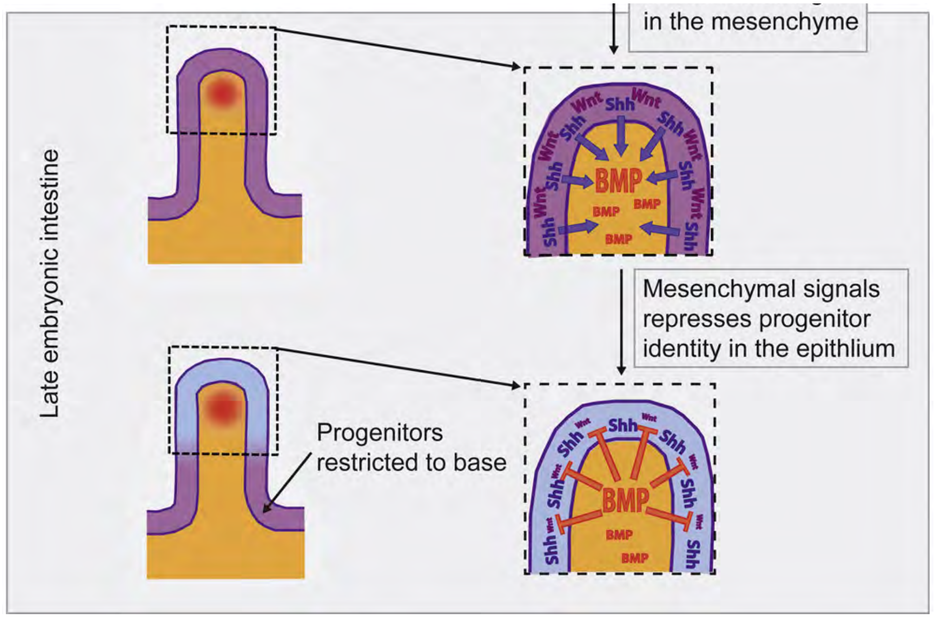

maxima of Shh from epithelium at tips

BMP inhibits Wnt in epithelium

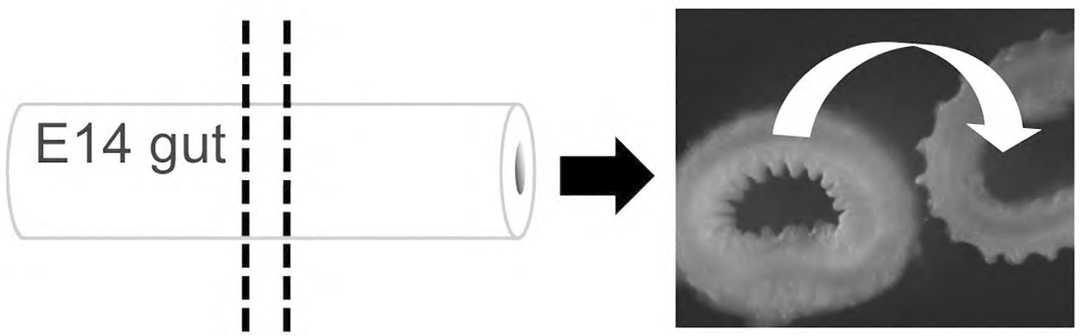

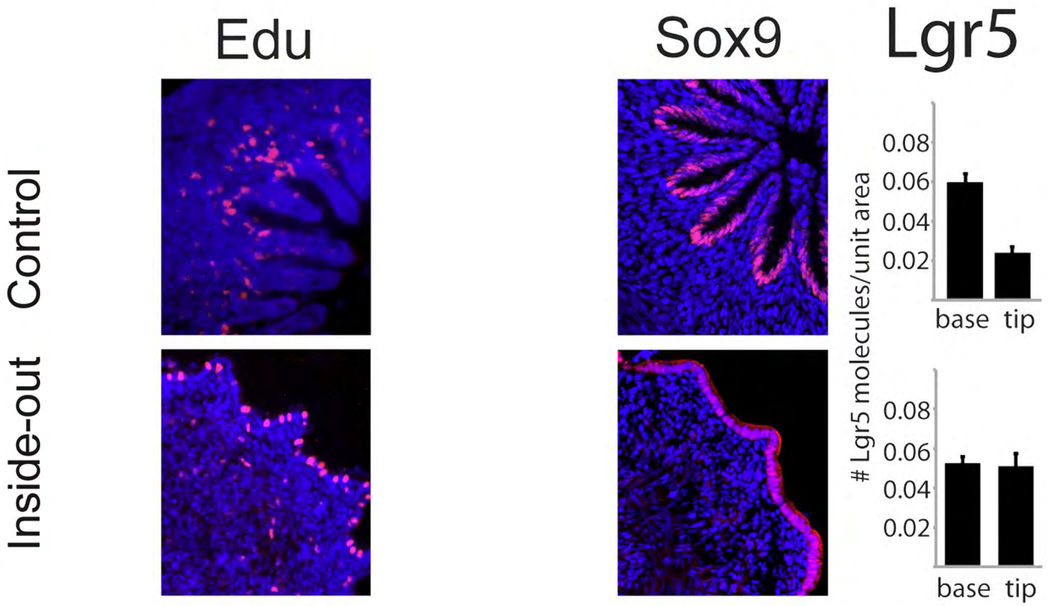

Shyer et al, *Cell* 2015

DAY 3

Mechanics of morphogenesis

Gastrulation

Morphing tissues as active solids/fluids
- Cell mechanics in convergent extension
- Tissue-scale fluid flow
- Self-organization of convergent extension

Mechanics driving tissue curvature
- Bilayer bending & ventral furrow

Organogenesis

- Wrinkling & buckling
- Programmed shape changes

Mechanics of visceral organ morphogenesis
- Midgut tissue folding in flies
- Heart morphogenesis
- branching morphogenesis

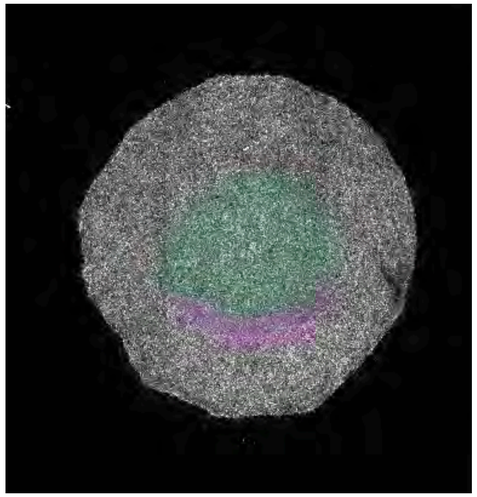

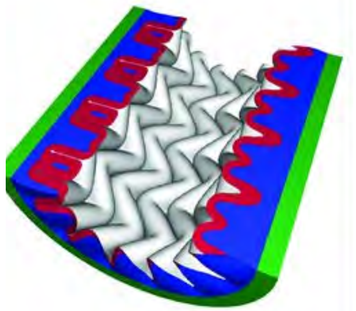

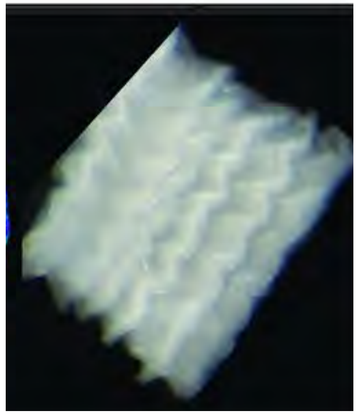

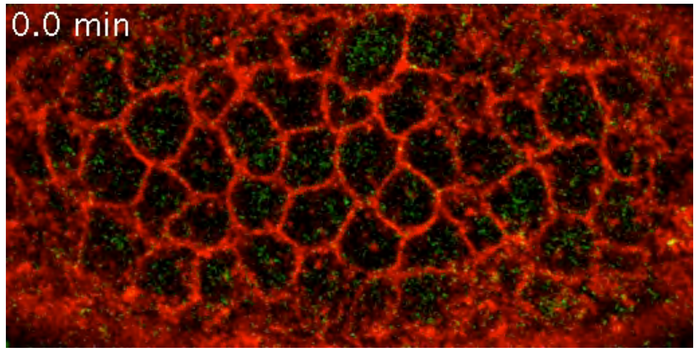

Martin *et al* (2009)

Fridtjof Brauns [KITP, UCSB]

2D non-linear incompatible elasticity in brains

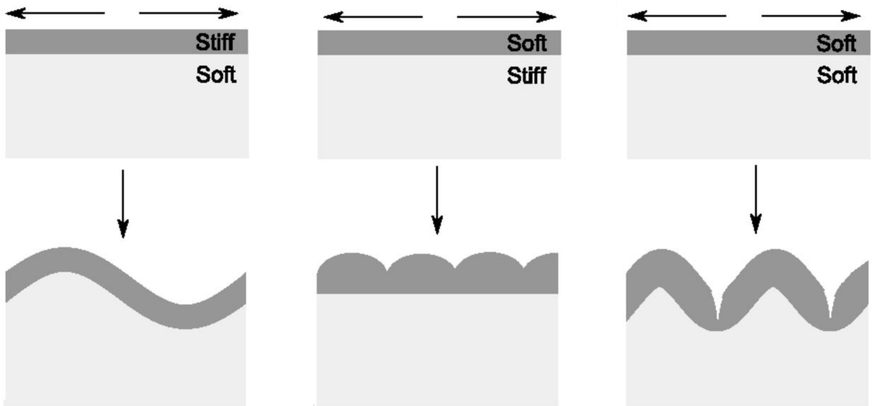

“gray matter simply grows more than the white matter”

similar stiffnesses

Difference in growth

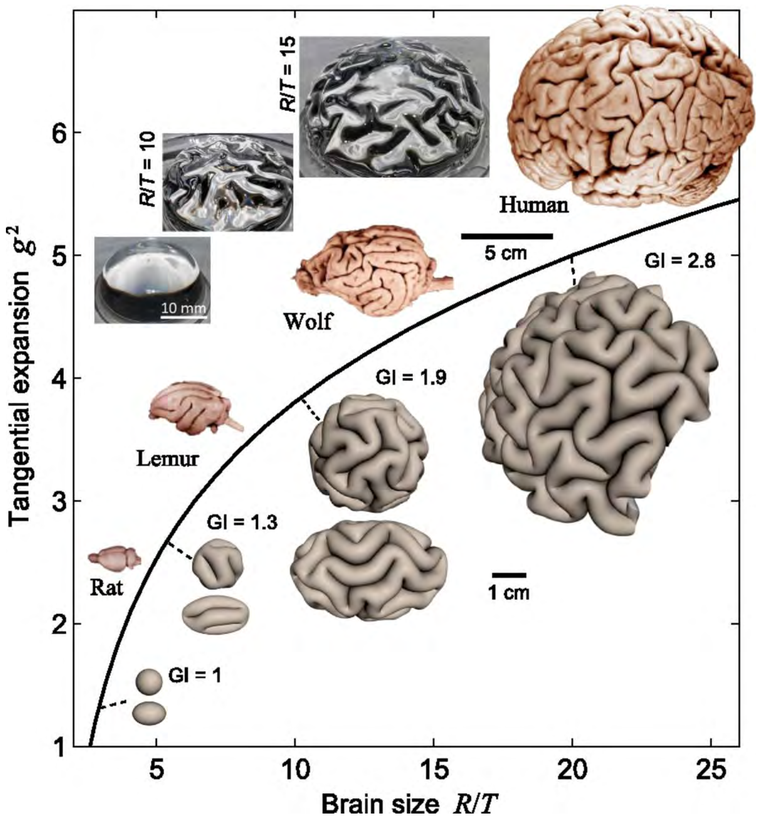

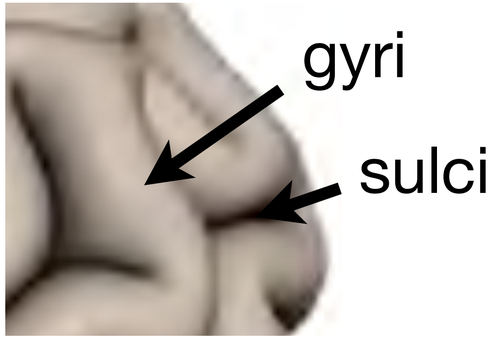

Tallinen et al. 2016
See also: Richman et al. 1975; Kaster et al. 2011; Tallinen et al. 2014

2D non-linear incompatible elasticity in brains

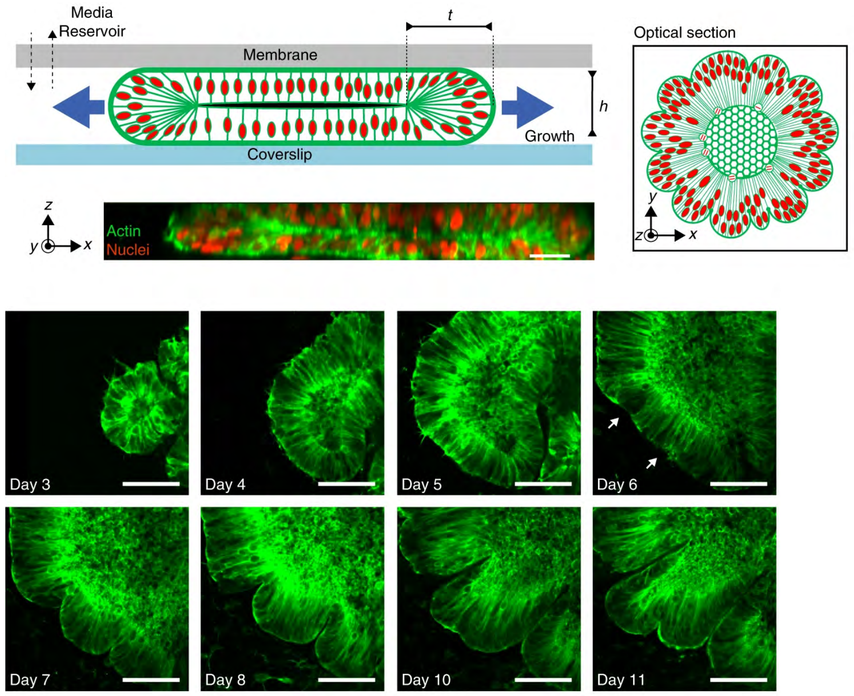

convolutions emerge at a critical cell density and maximal nuclear strain

indicative of a mechanical instability

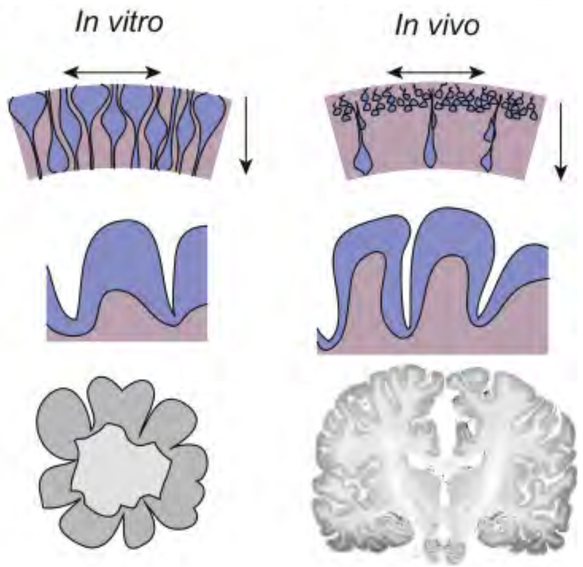

Lancaster et al *Cell Stem Cell* 201

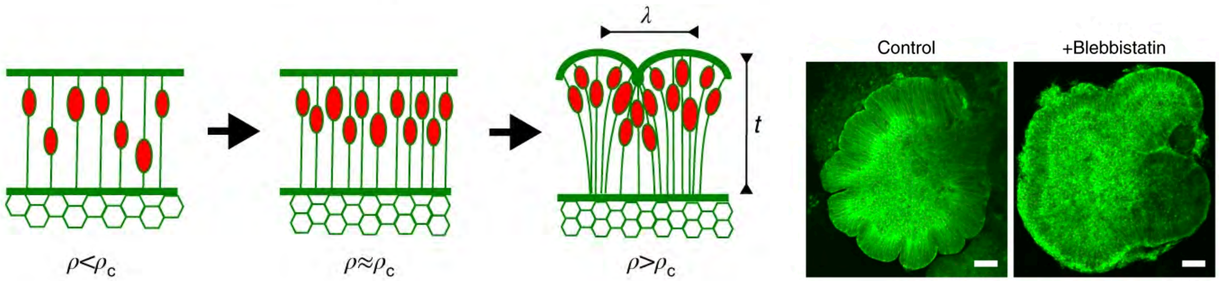

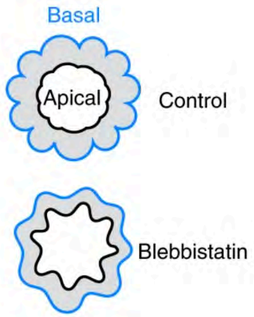

Eyal Karzbrun et al. *Nat. Phys.* 2018

2D non-linear incompatible elasticity in brains

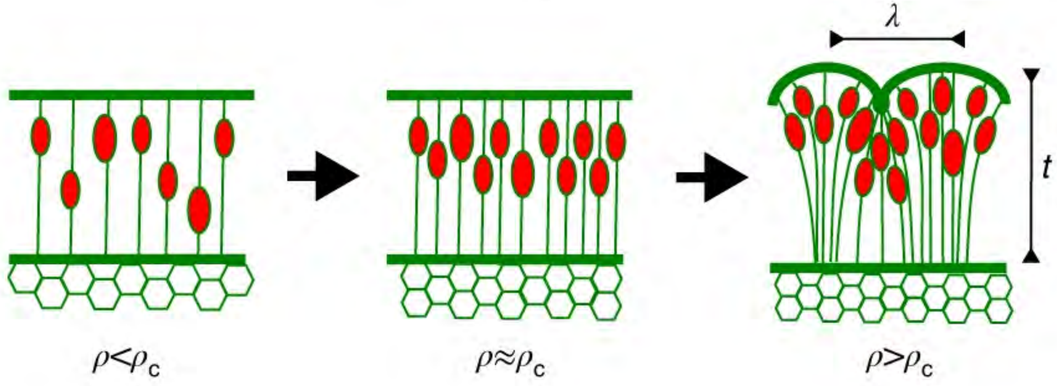

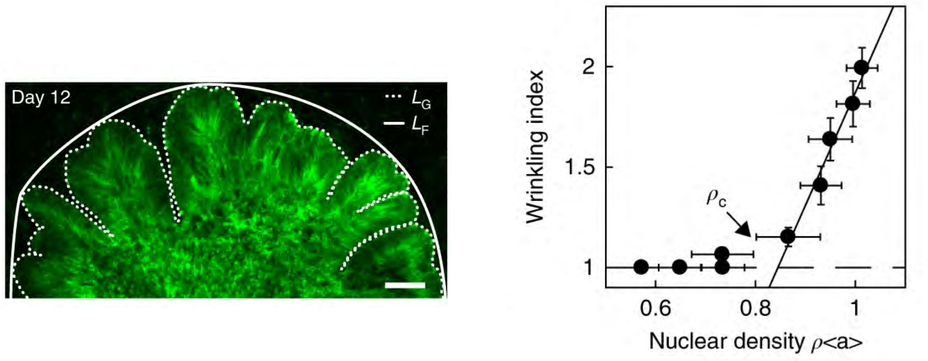

$$\lambda \propto t\left(\frac{E_{\mathrm{S}}}{E_{\mathrm{B}}}\right)^{1/3}$$

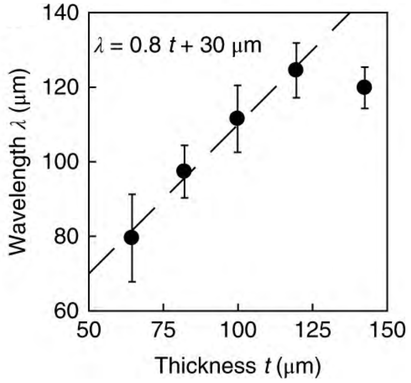

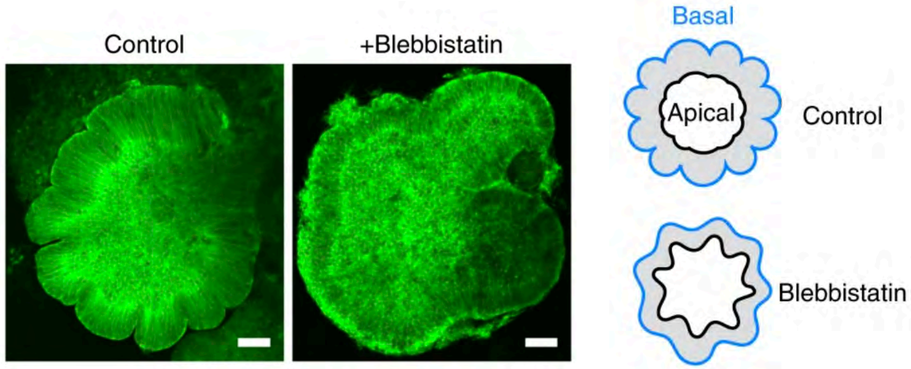

differential swelling:
+cell-cycle-dependent nuclear swelling/motion
+cytoskeleton contraction at inner surface

Eyal Karzbrun et al. *Nat. Phys.* 2018

2D non-linear incompatible elasticity in brains

artificial^

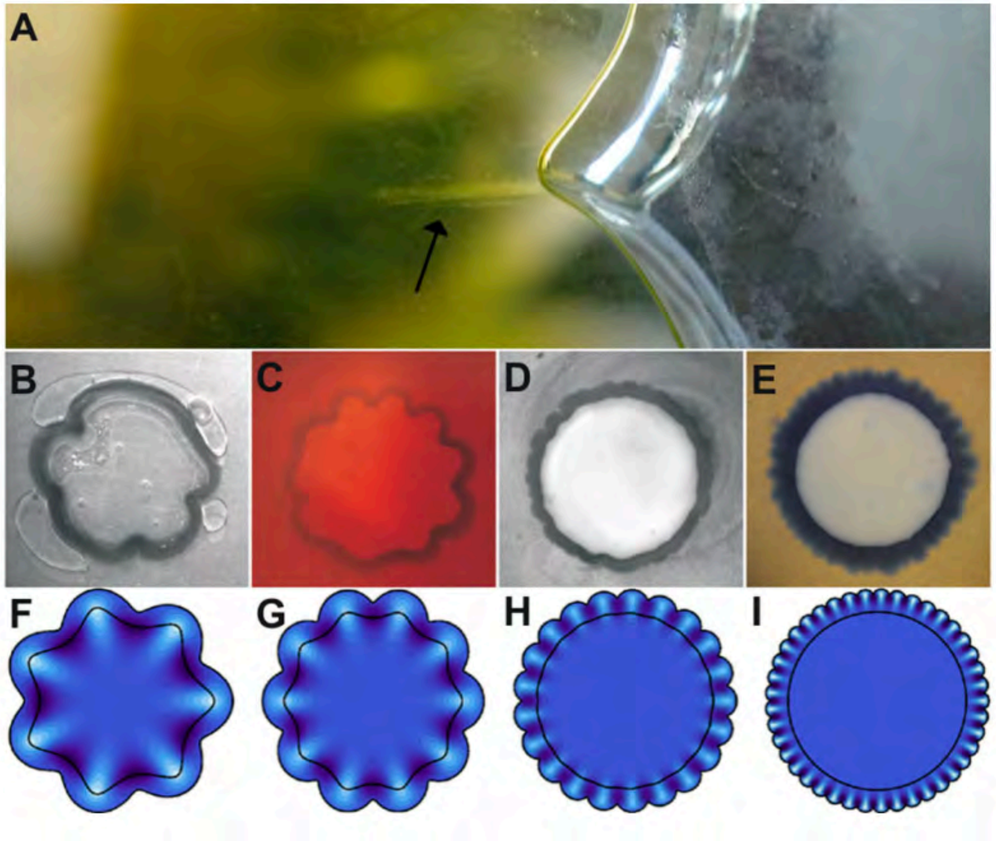

cusp formation “still resisting theoretical explanation”

Dervaux et al PRL 2011

nonuniform *in-plane* growth leads to 3D form

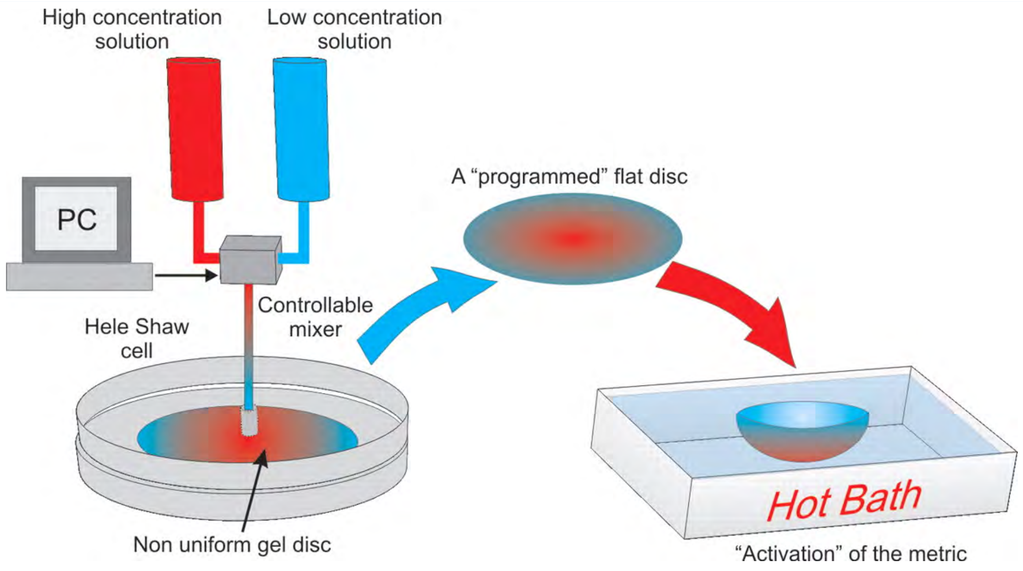

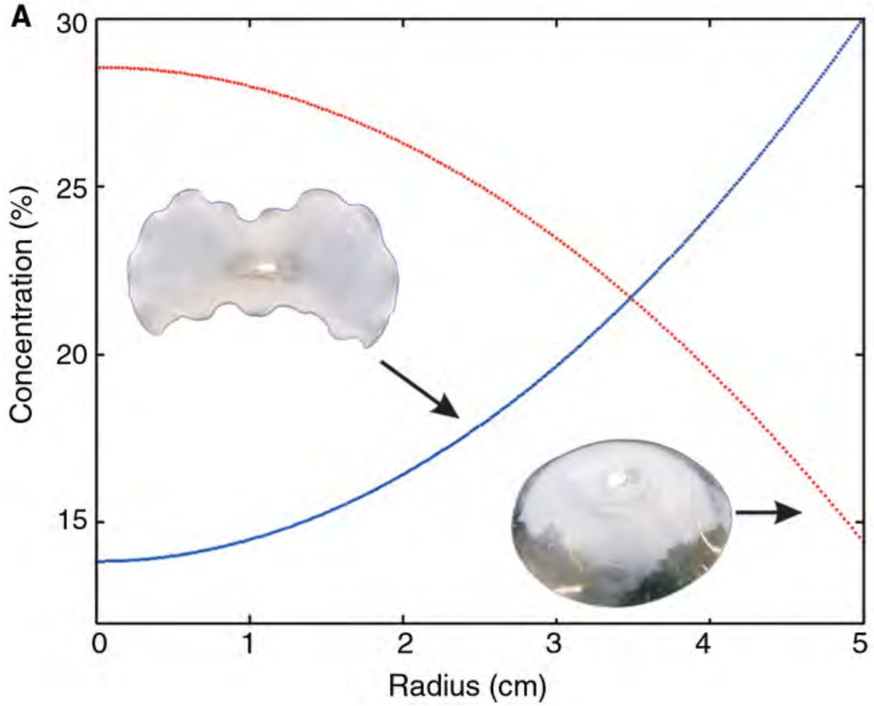

Klein, Efrati, Sharon *Science* 2007

nonuniform *in-plane* growth leads to 3D form

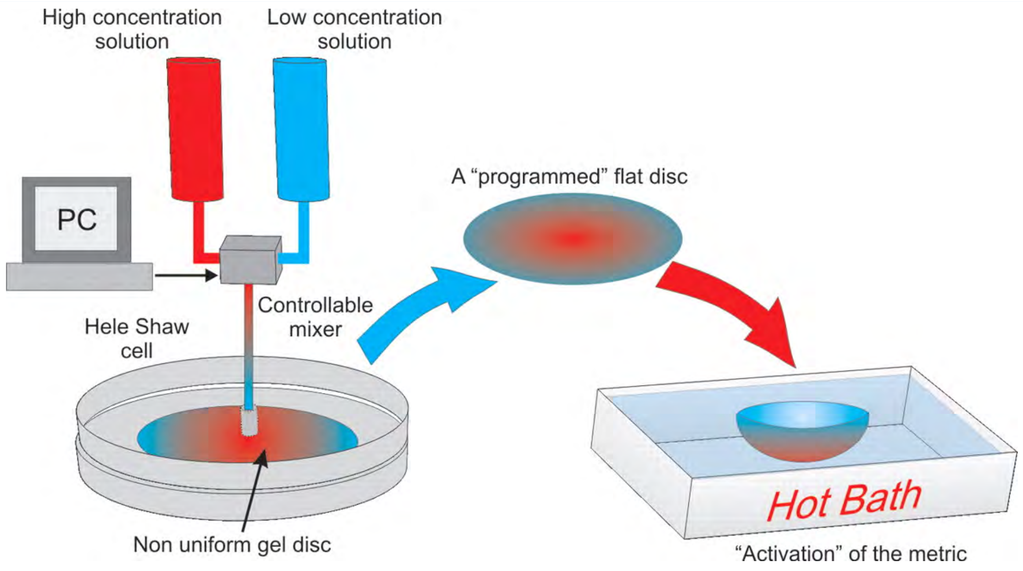

Efrati, Sharon *Soft Matter* 2010

Klein, Efrati, Sharon *Science* 2007

[On board] nonuniform *in-plane* growth leads to 3D form

Gauss-Bonnett Theorem relating growth to curvature

$$ds^2 = \Omega(x,y)(dx^2 + dy^2) \qquad K = \frac{\det b}{\det g} = -\frac{\Delta \log \Omega}{\Omega}$$

Conformal maps from a reference congifuration: embeddable shapes

Non-embeddable shapes lead to ‘incompatible elasticity’

in-plane ***anisotropy*** leads to 3D form:

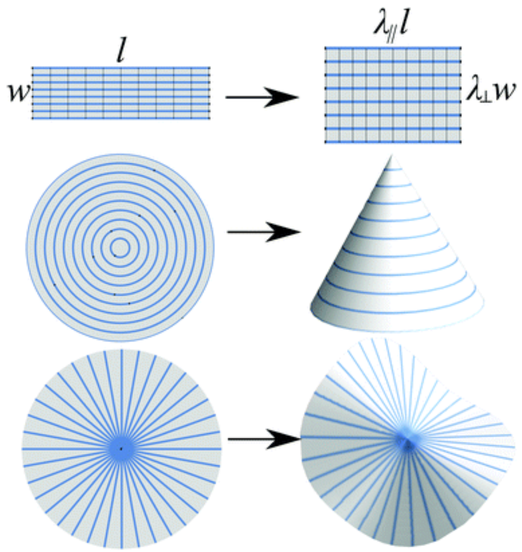

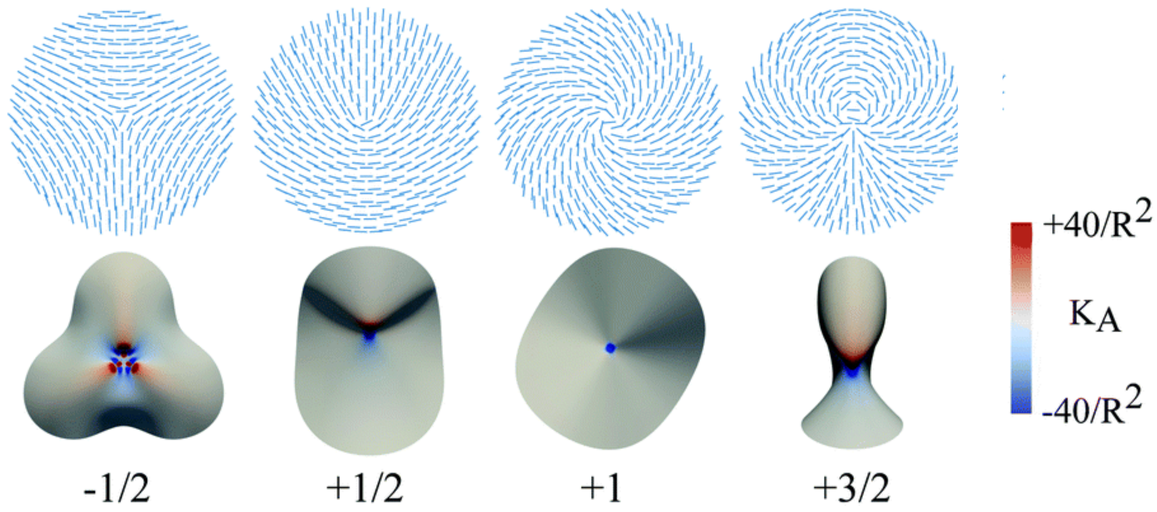

Contract along nematic lines

Duffy & Biggins, Soft Matter 2020

Outlook: Incompatibility across the thickness dimension

Incompatibility across the third dimension

Adding anisotropic growth to this picture. Turns out biology does not always use conformal maps

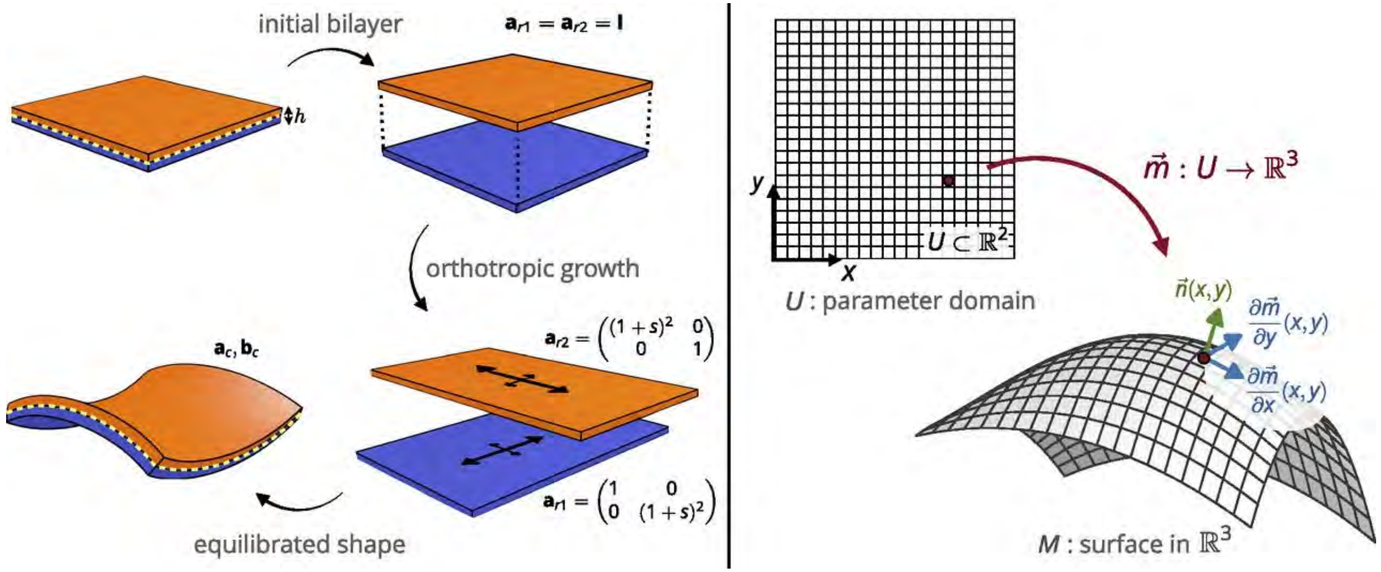

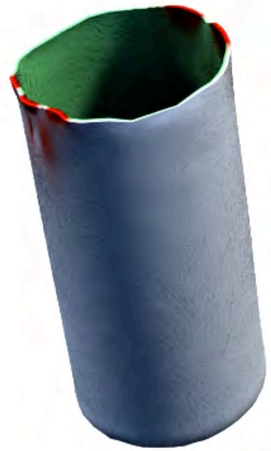

Wim M. van Rees
Etienne Vouga
L. Mahadevan

van Rees, Vouga, & Mahadevan *PNAS* (2017)

Visceral organs: complex multilayer forms

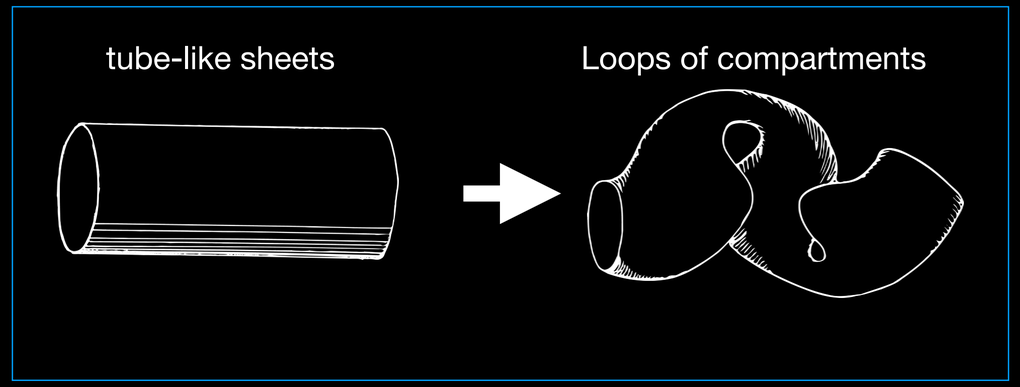

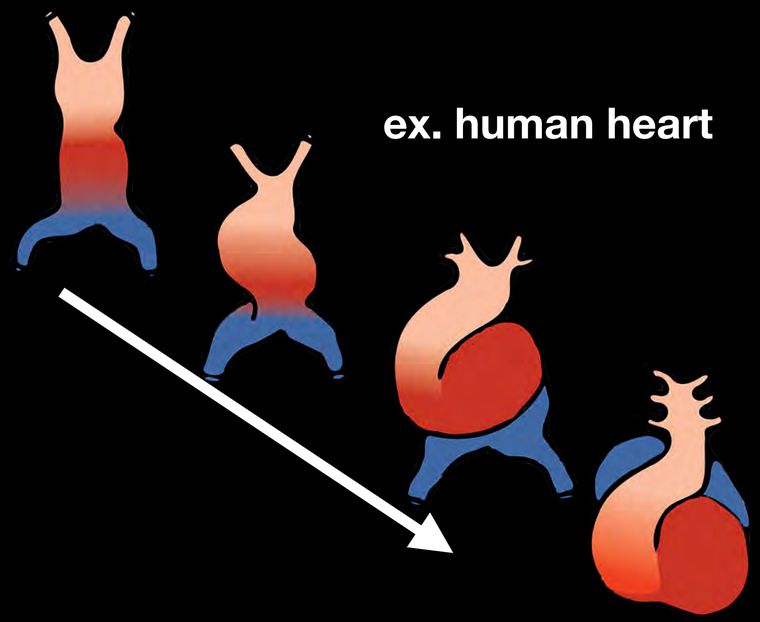

ex. human heart

chick **gut**

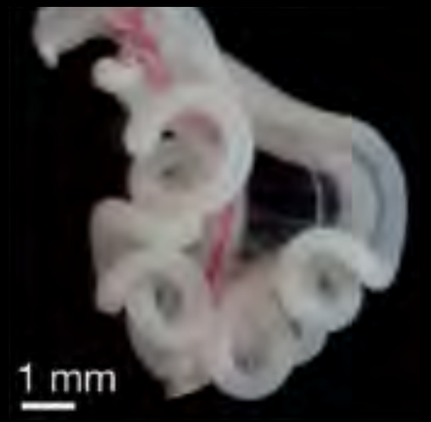

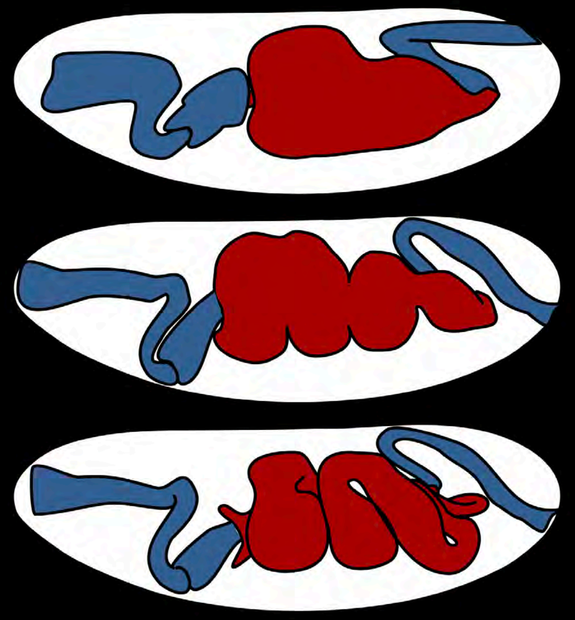

***Drosophila* gut**

- Develop deep inside living embryos
- Complex shapes make analysis challenging
- Multiple interacting layers

Gut looping & incompatible elasticity

Growth-induced buckling

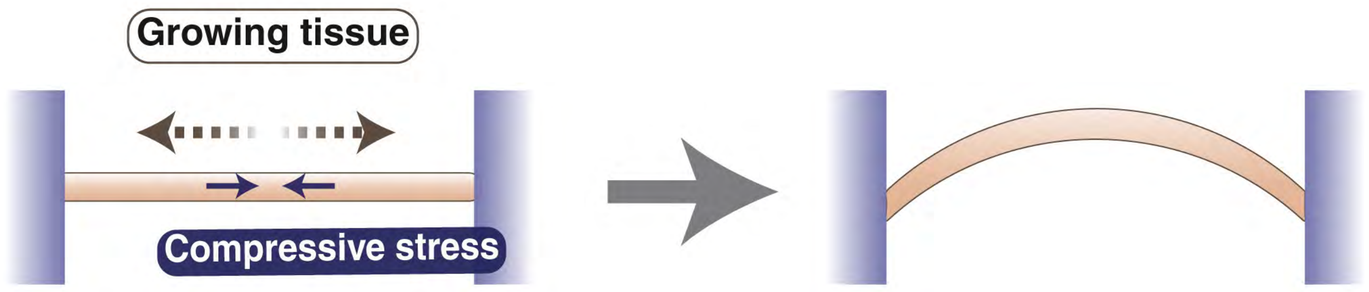

Midgut looping morphogenesis

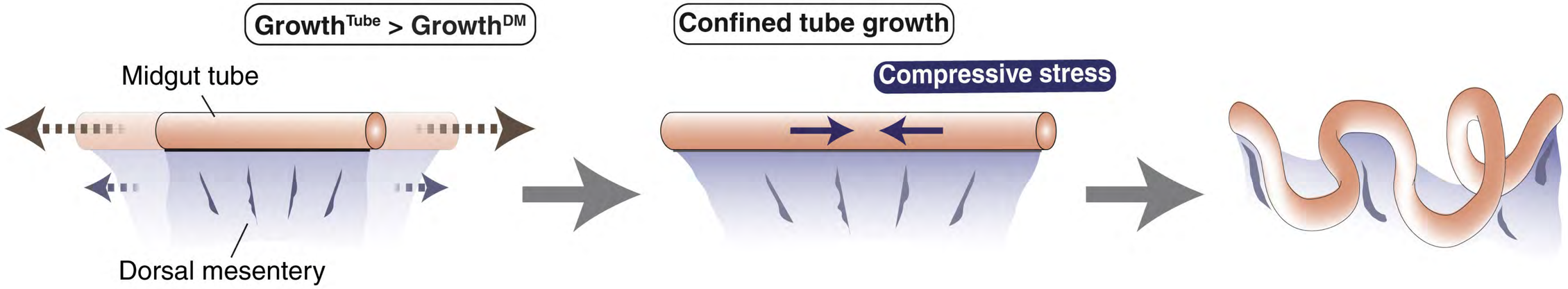

Cartoons from Houtekamer et al. (2022)

Savin *et al* Nature 2011

Gut looping & incompatible elasticity

incompatible elasticity via residual stresses in dorsal mesentery

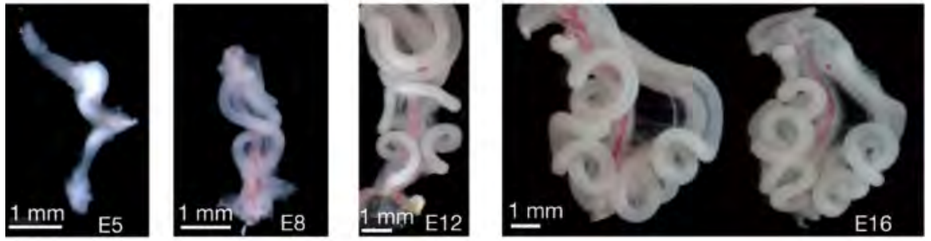

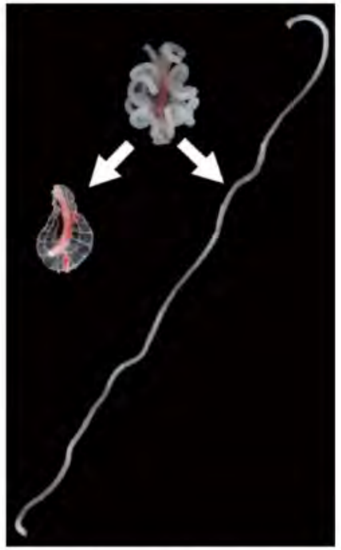

Mesentery removed *in vitro*

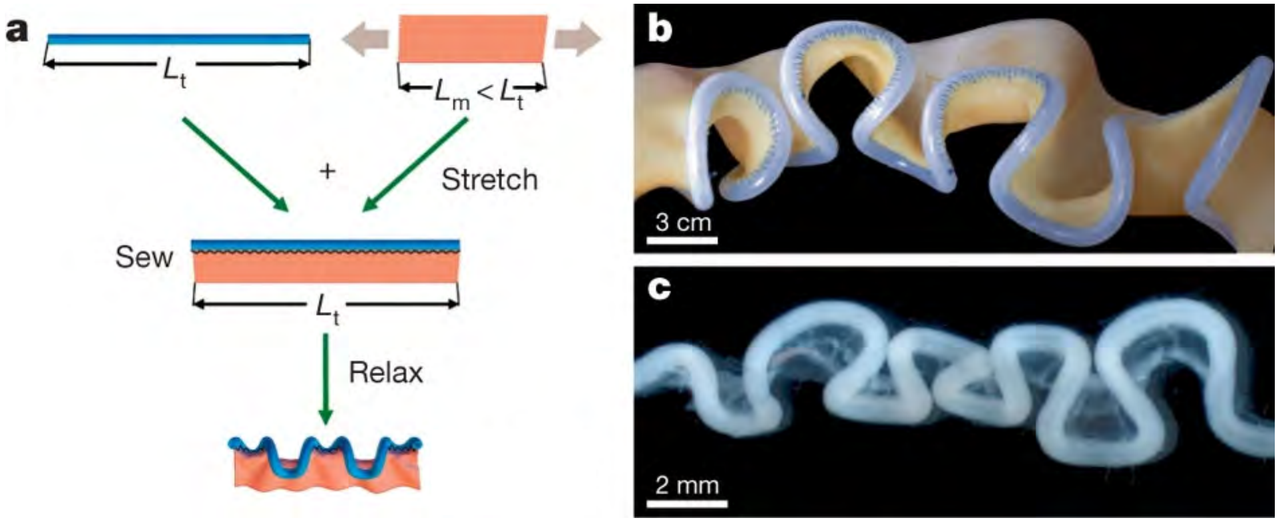

(mesenteric artery removed here)

- analogy to incompatible elasticity with negative curvature

Savin *et al* Nature 2011

Gut looping in chick/rubber

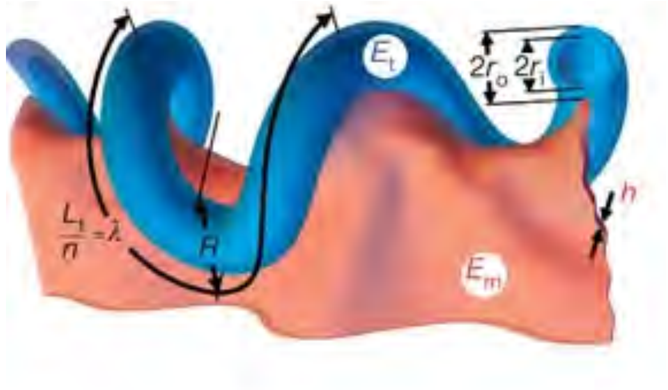

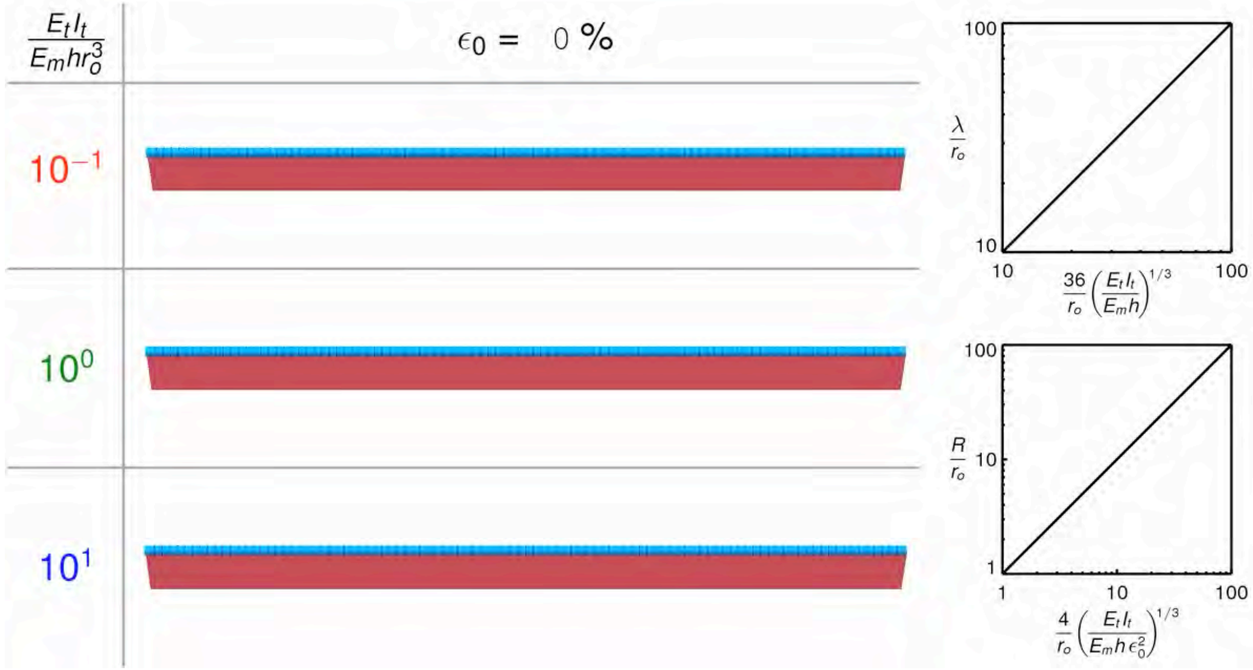

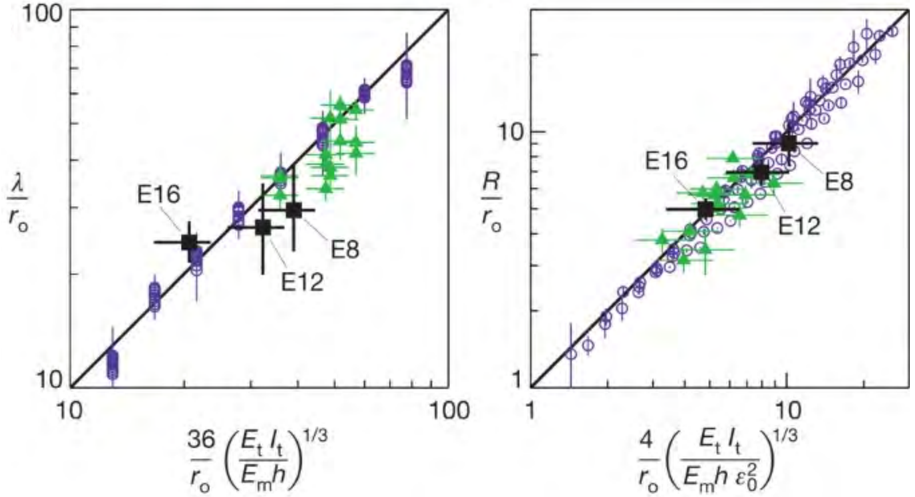

experiment
simulation
rubber (latex) model

Savin *et al* Nature 2011

Gut looping across vertebrate species

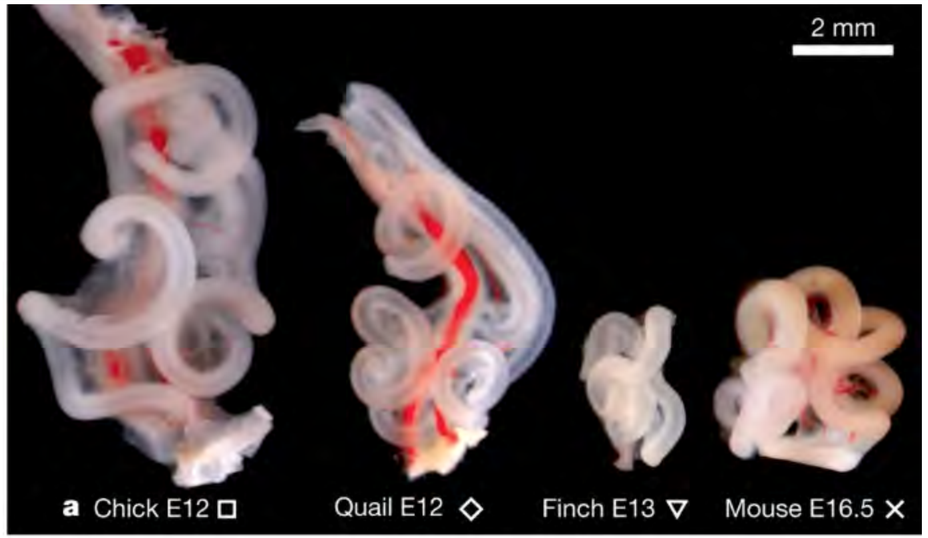

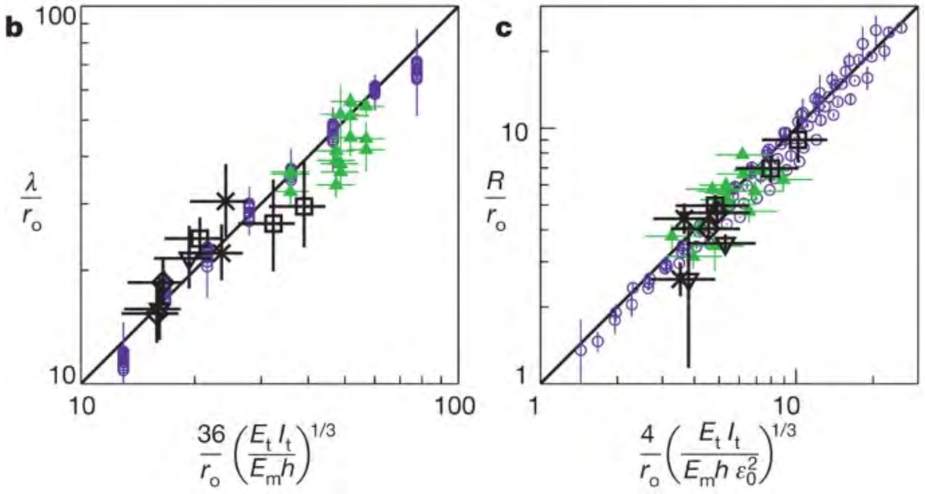

The physiological stresses in the mesentery across these species is similar…. mechanical feedback?

Savin *et al Nature* 2011

BMP in the mesentery modulates looping biomechanics

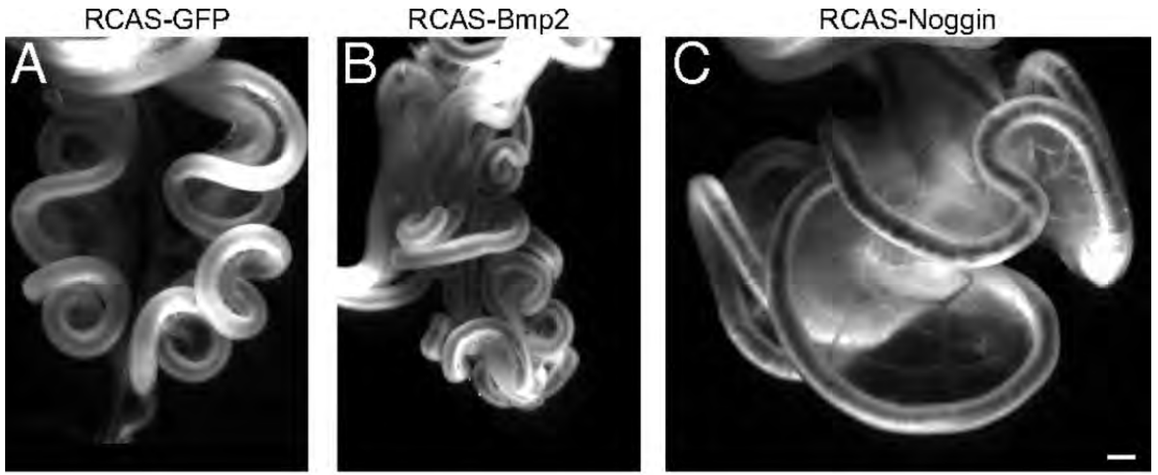

Control	More loops, Smaller wavelength Smaller radii	Fewer loops, Larger wavelength Larger radii

Nerurkar, Mahadevan & Tabin, *PNAS* 2017

Tissue folding in *Drosophila* gut morphogenesis

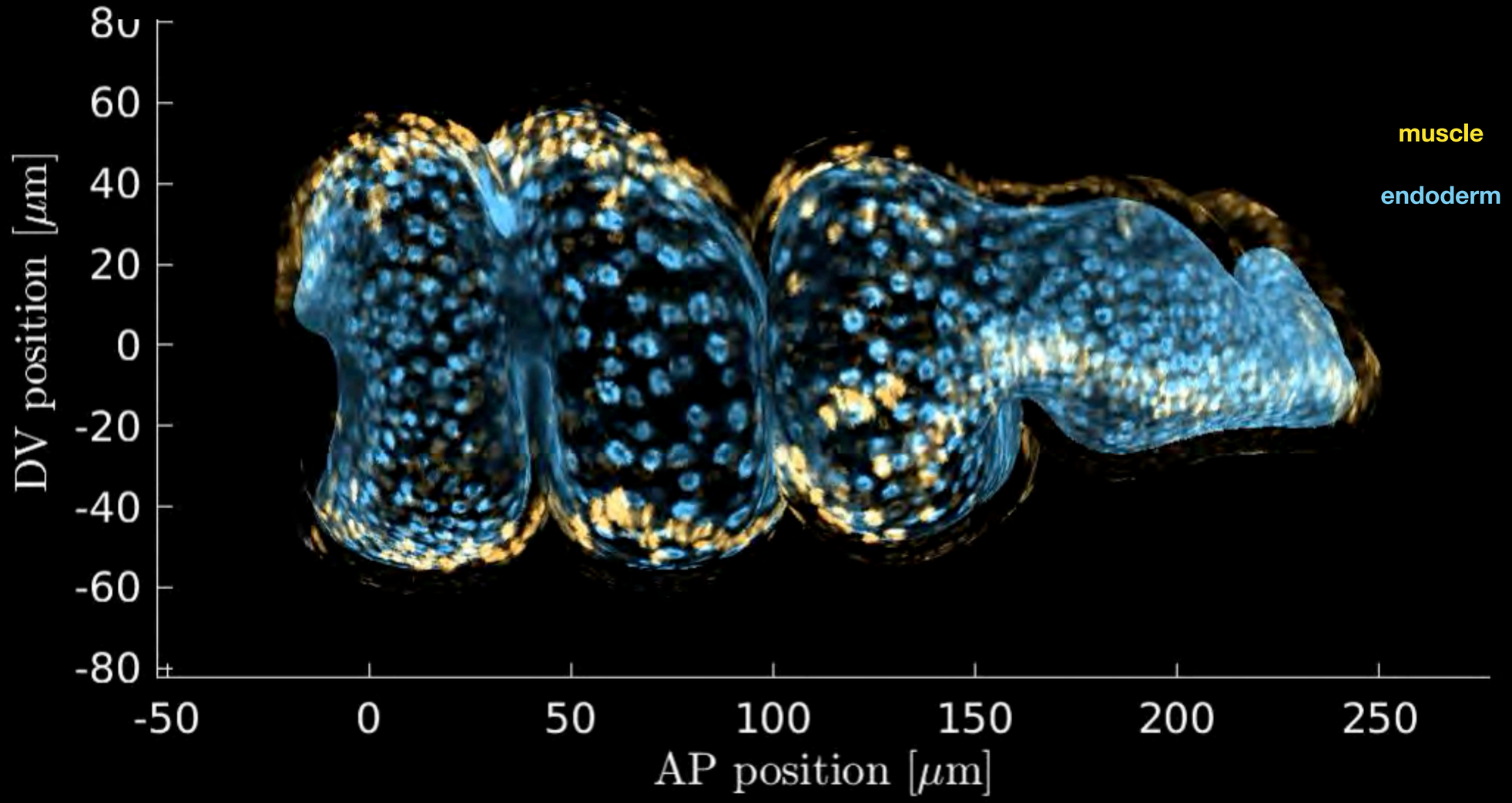

Mitchell *et al*, *eLife* 2022

Experiments: Imaging techniques for morphogenesis

multi-view confocal lightsheet microscopy

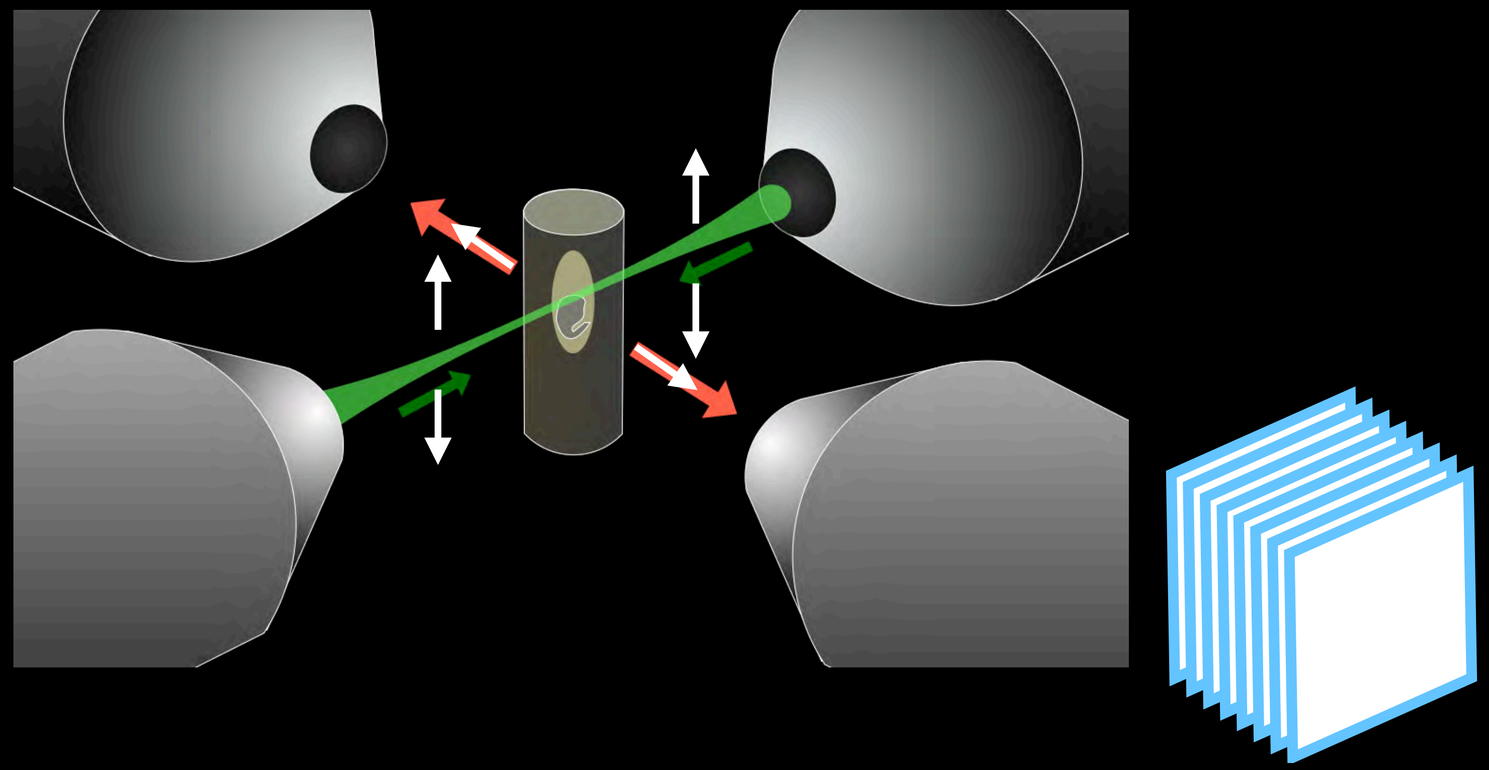

Krzic *et al*, 2012
de Medeiros *et al*, 2015

Mitchell *et al*, *eLife* 2022

Experiments: Imaging techniques for morphogenesis

multi-view confocal lightsheet microscopy

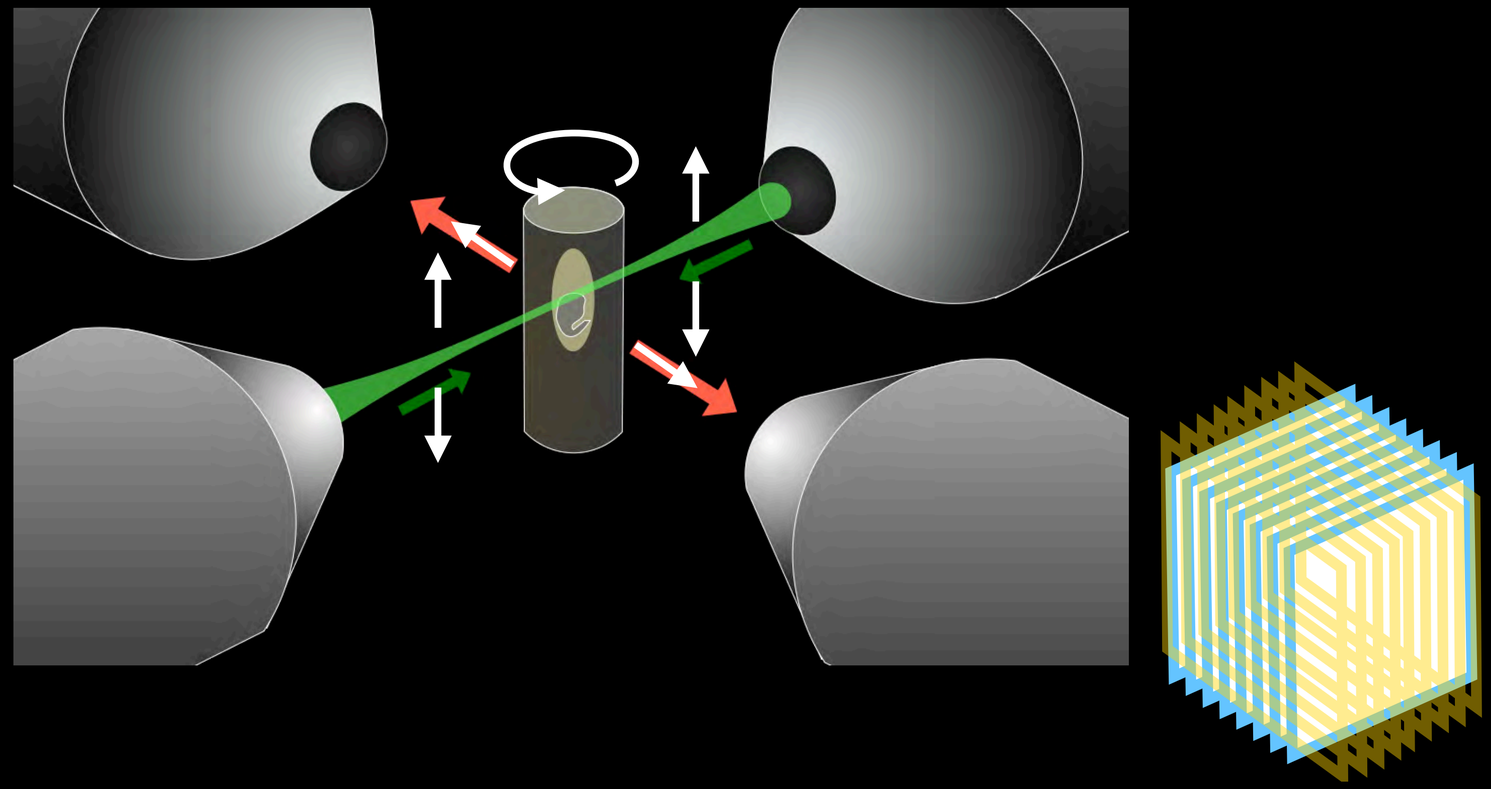

Krzic *et al*, 2012
de Medeiros *et al*, 2015

Mitchell *et al*, *eLife* 2022

Experiments: Imaging techniques for morphogenesis

multi-view confocal lightsheet microscopy

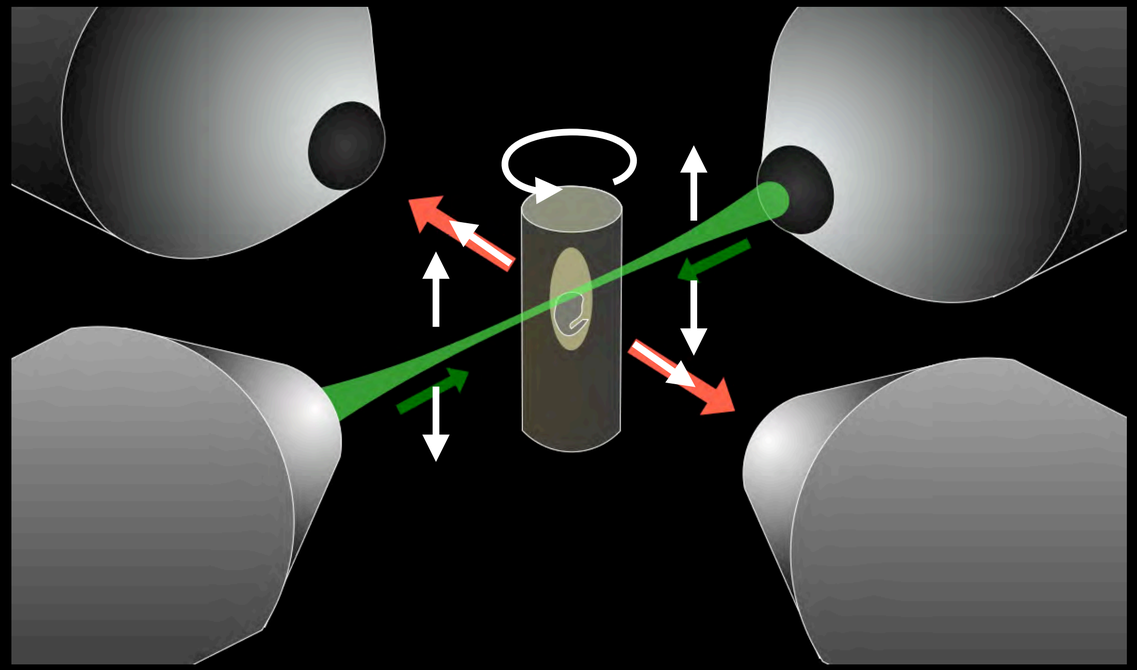

Krzic *et al*, 2012
de Medeiros *et al*, 2015

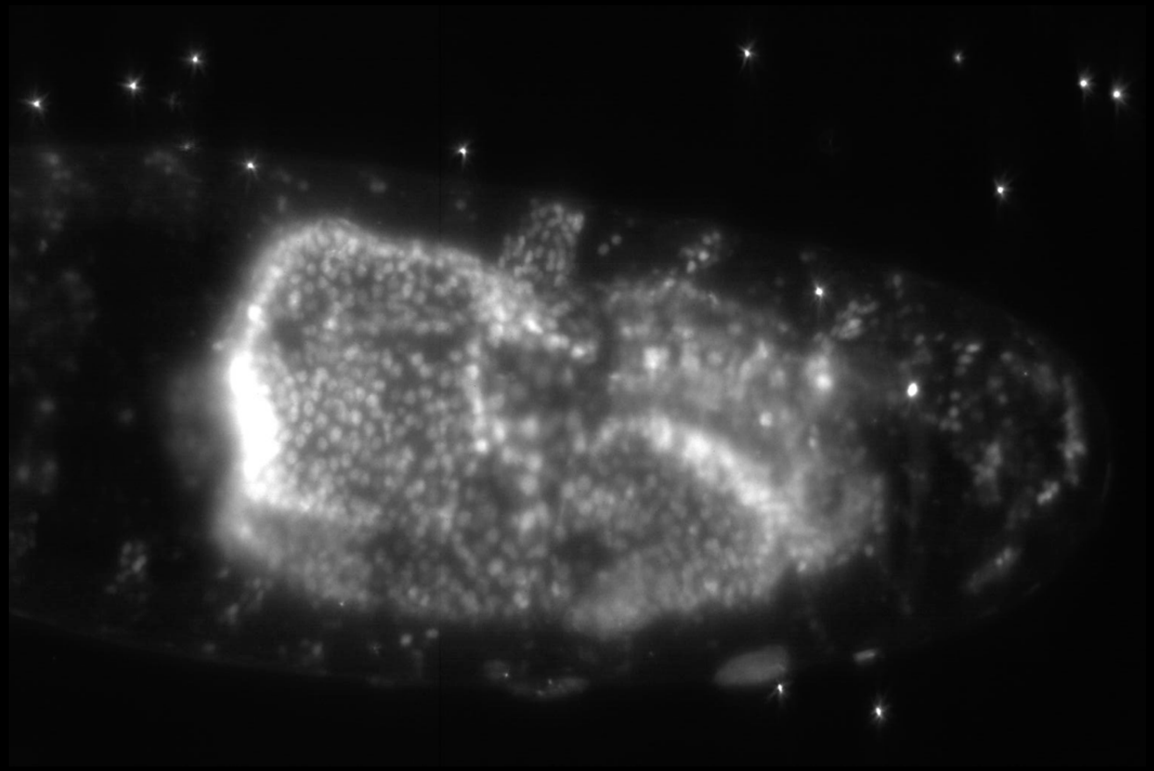

Tissue-specific markers (GAL4/UAS)

Brand & Perrimon 1993
Martin-Bermudo *et al* 1997
Riese *et al* 1997

Mitchell *et al, eLife* 2022

Experiments: Imaging techniques for morphogenesis

multi-view confocal lightsheet microscopy

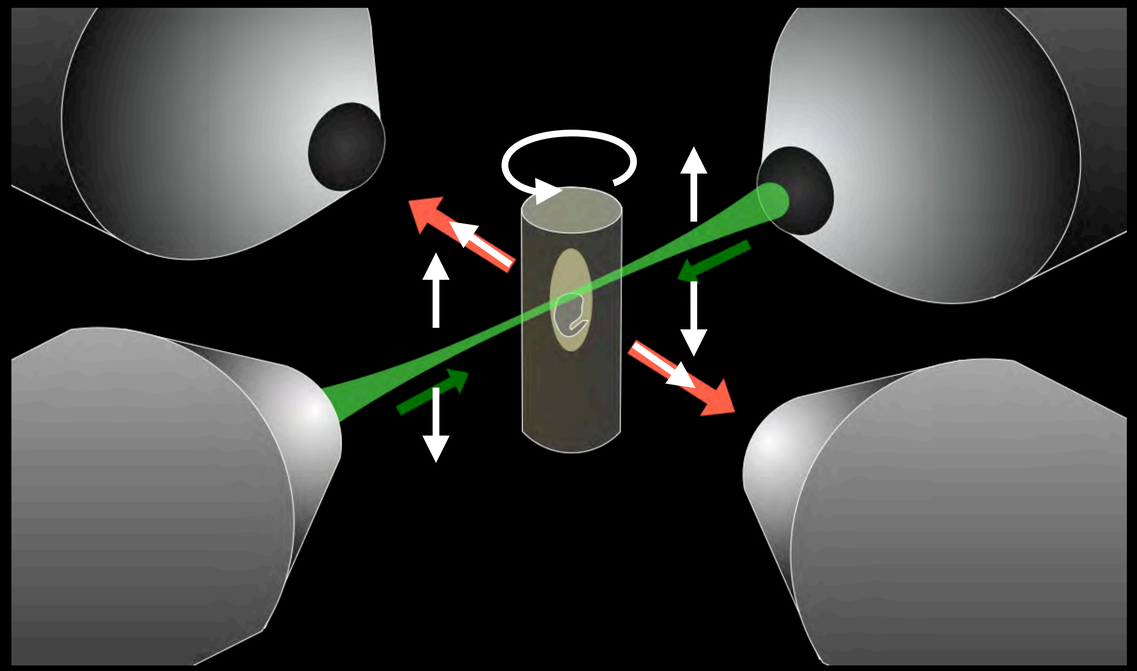

Krzic *et al*, 2012
de Medeiros *et al*, 2015

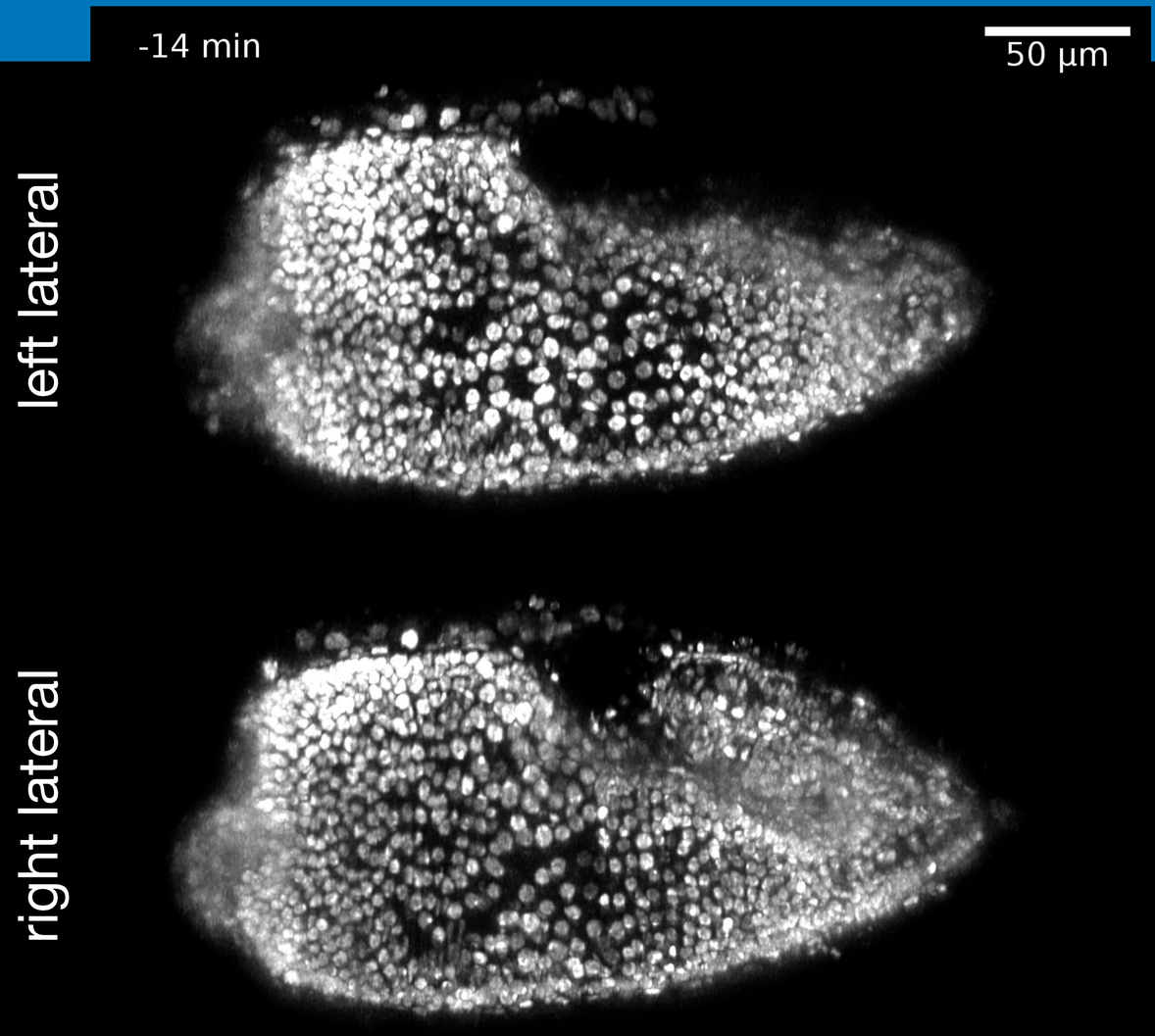

fluorescently-labeled nuclei

Mitchell *et al*, *eLife* 2022

How is genetic information translated to shape?

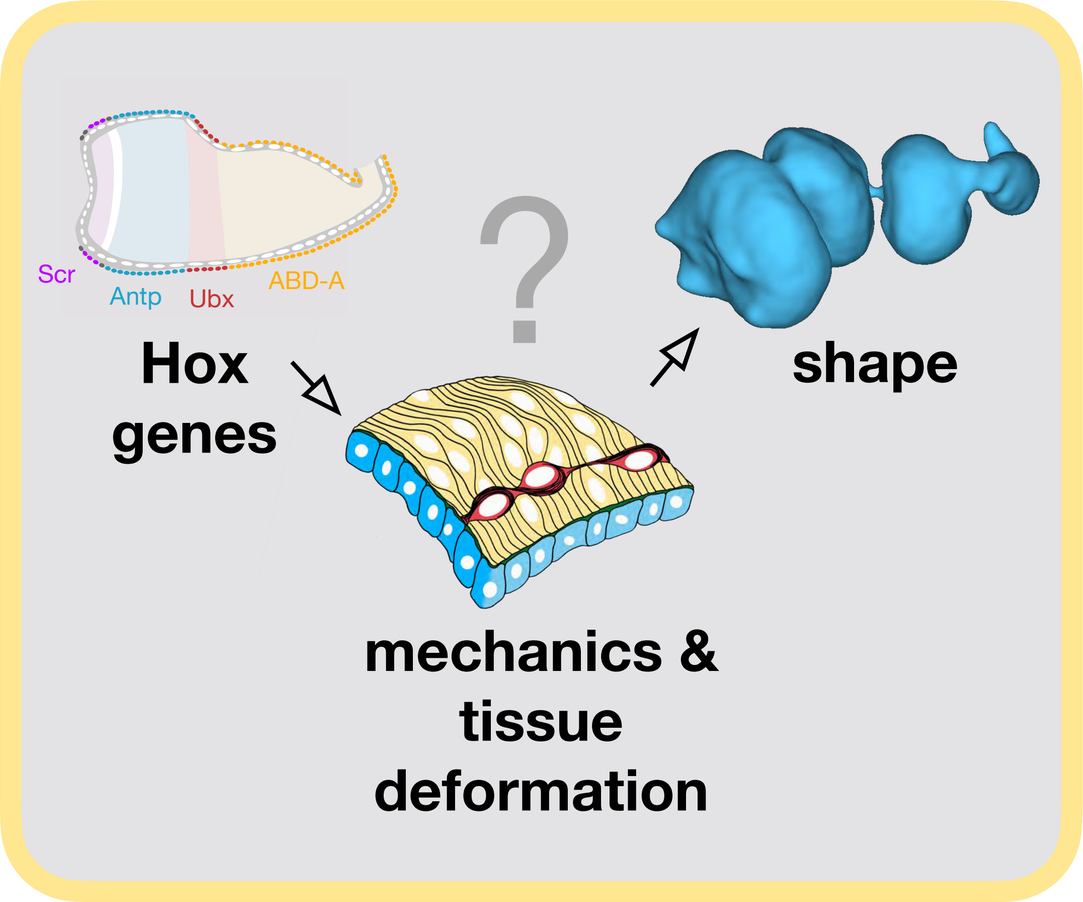

Hox genes:

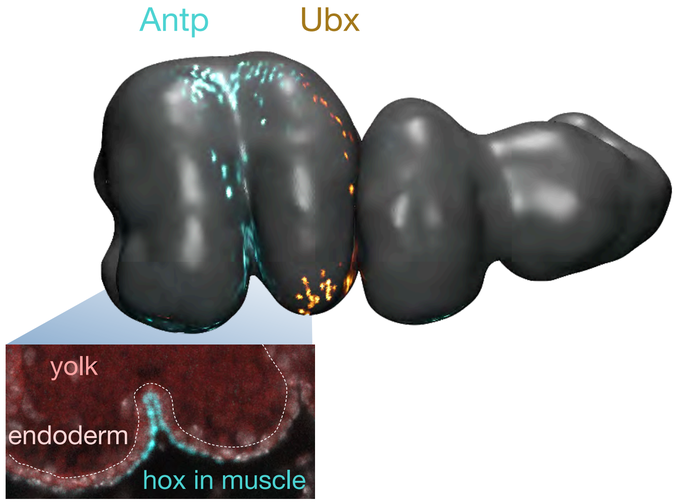

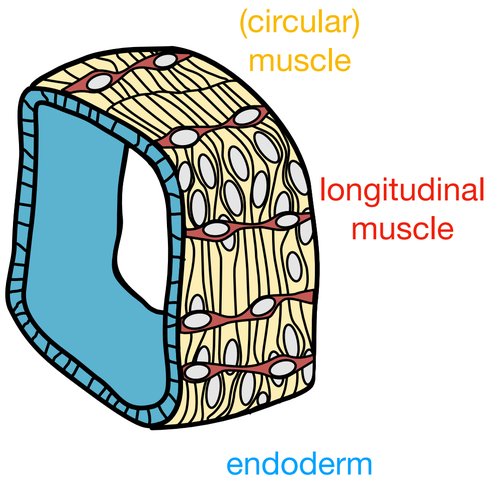

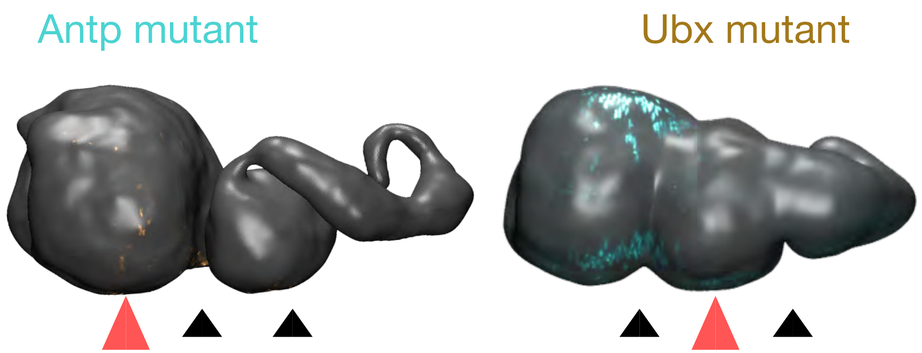

Mitchell *et al.*, eLife (2022)

Experiments: Quantifying whole-organ dynamics

TubULAR: Tube-like sUrface Lagrangian Analysis Resource

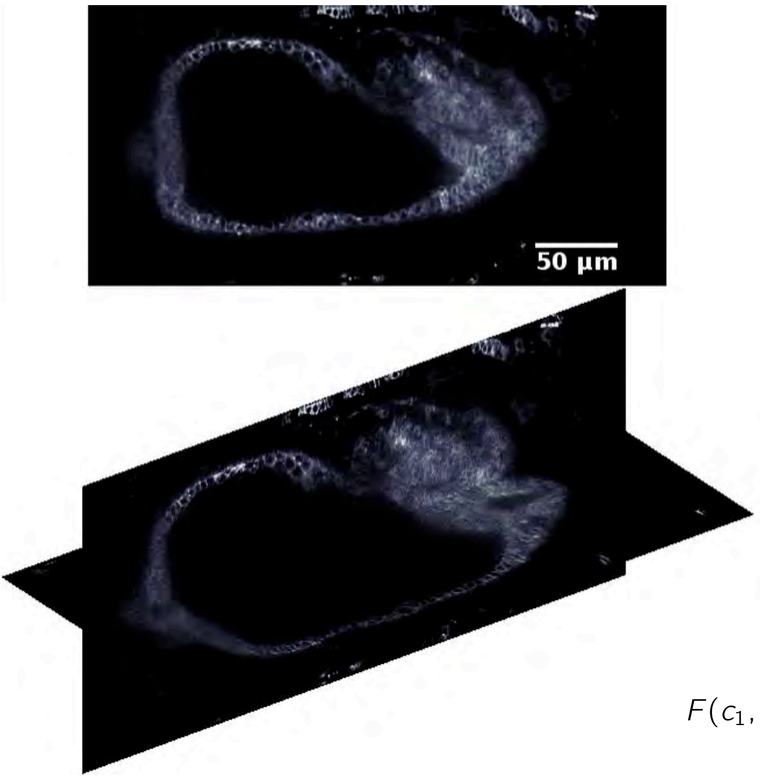

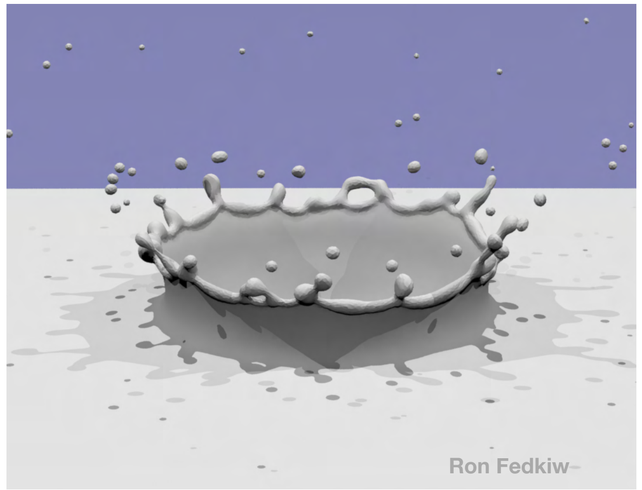

$$F(c_1, c_2, \mathcal{S}) = \sigma \int_{\mathcal{S}} ds - p \int_{\Omega} d^3\mathbf{x} + \int_{u>0} |I(\mathbf{x}) - c_1| d^3\mathbf{x} + \int_{u<0} |I(\mathbf{x}) - c_2| d^3\mathbf{x}$$

$$c_1(\mathcal{S}) = \langle I(\mathbf{x}) \rangle_{u>0}$$

$$c_2(\mathcal{S}) = \langle I(\mathbf{x}) \rangle_{u<0}$$

Mitchell & Cislo, *Nature Methods* (2023)

Experiments: Quantifying whole-organ dynamics

TubULAR: Tube-like sUrface Lagrangian Analysis Resource

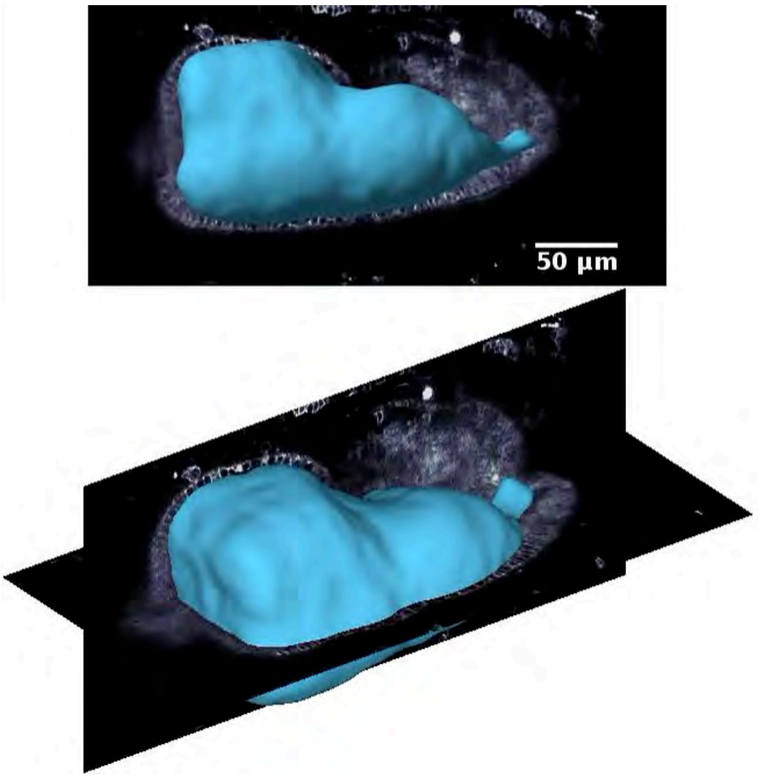

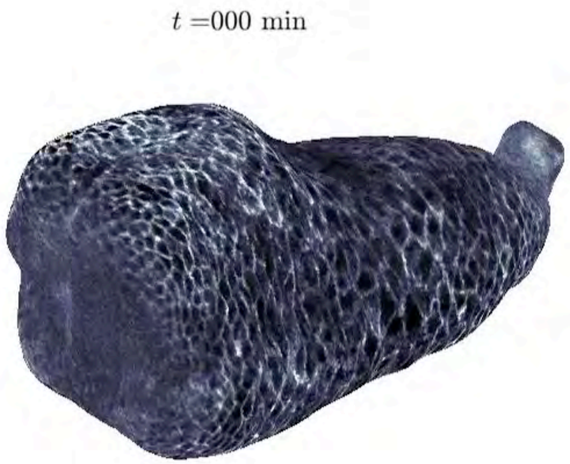

How are in-plane and out-of-plane deformations coupled?

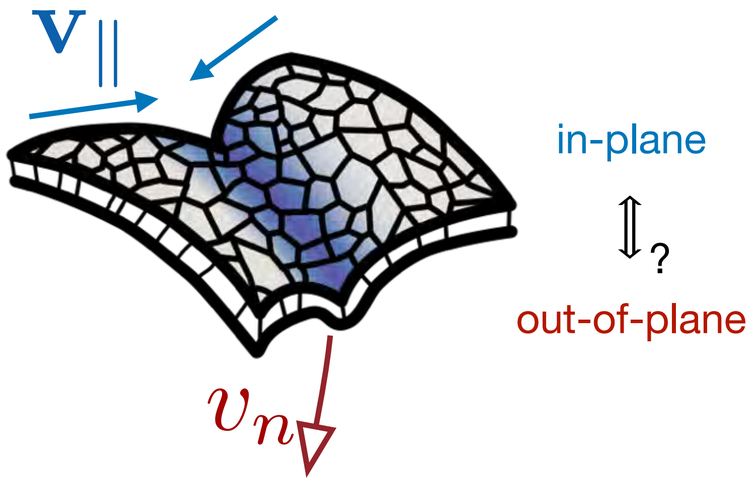

Mitchell & Cislo, *Nature Methods* (2023)

Quantifying whole-organ dynamics: Tissue cartography

TubULAR: Tube-like sUrface Lagrangian Analysis Resource

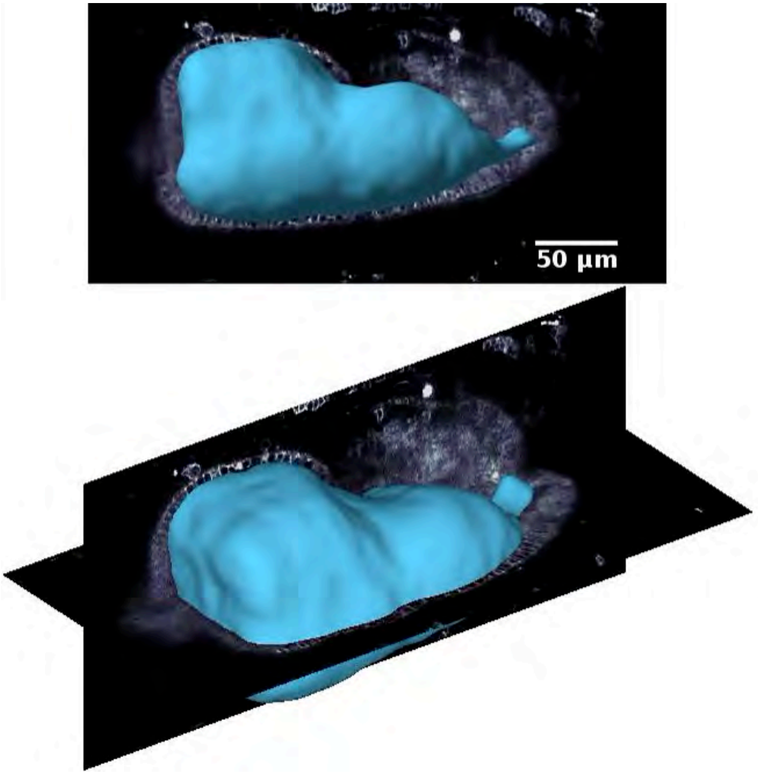

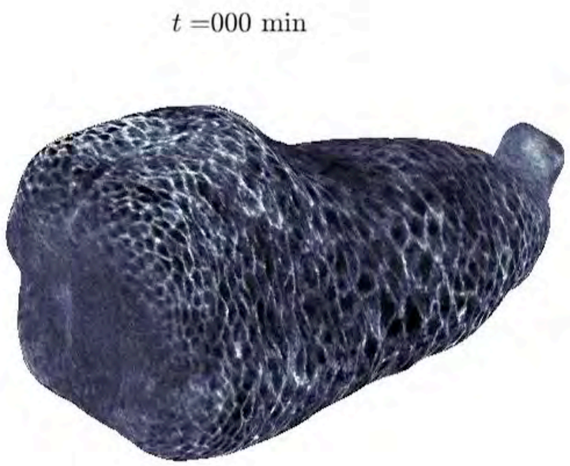

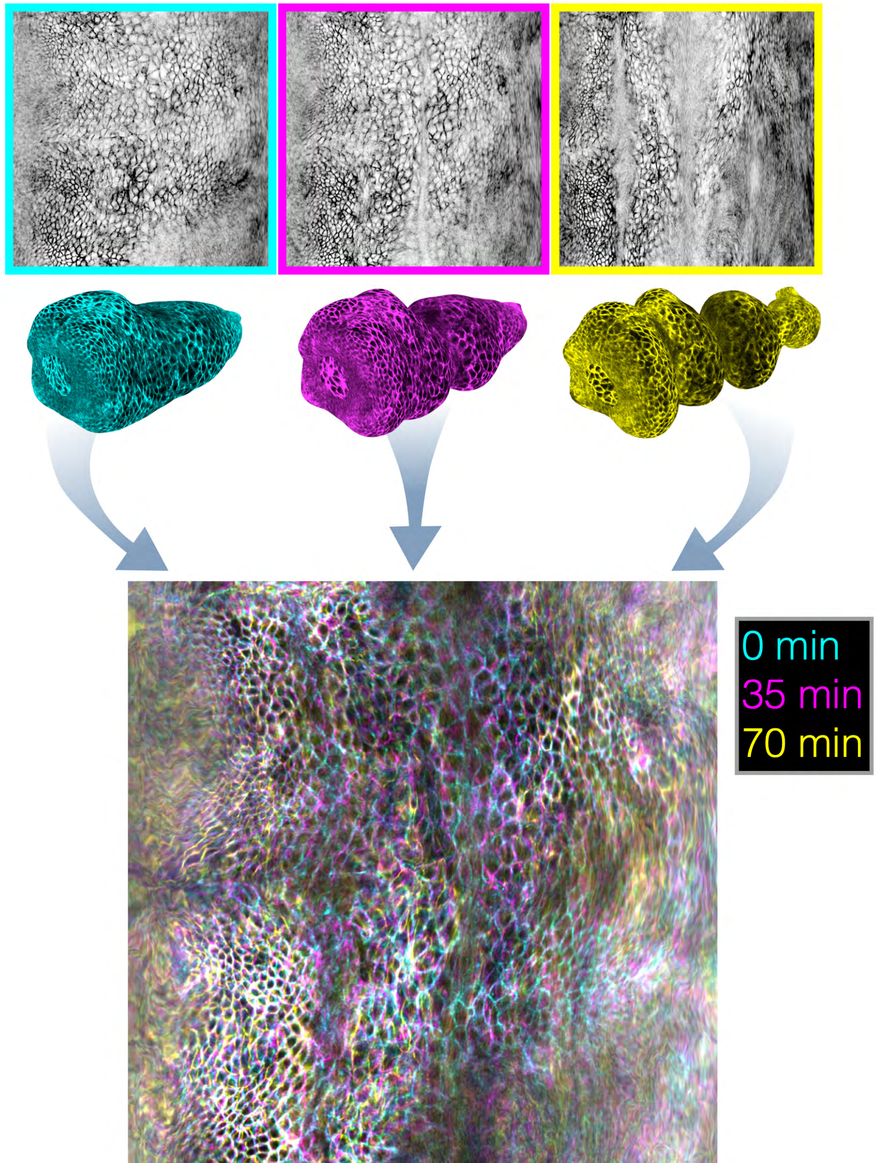

In-plane and out-of-plane kinematics

TubULAR: Tube-like sUrface Lagrangian Analysis Resource

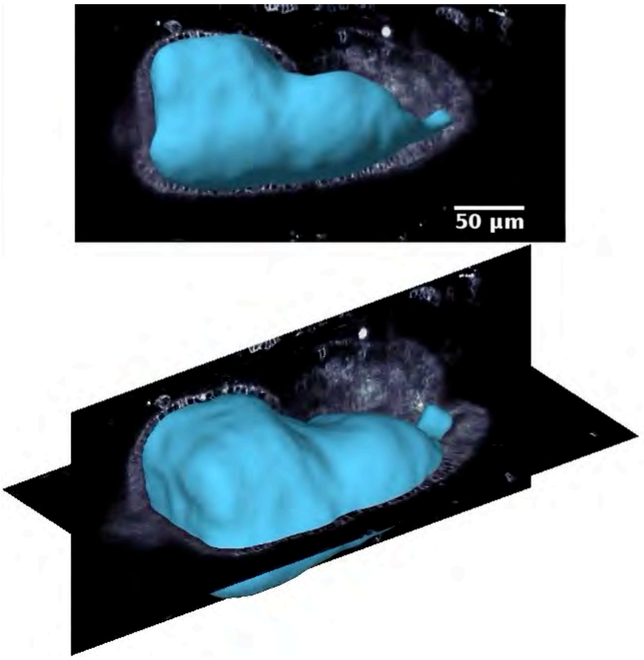

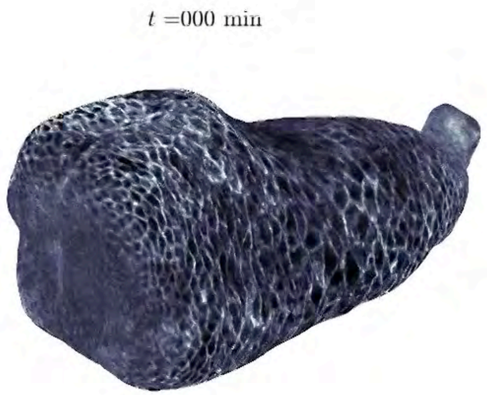

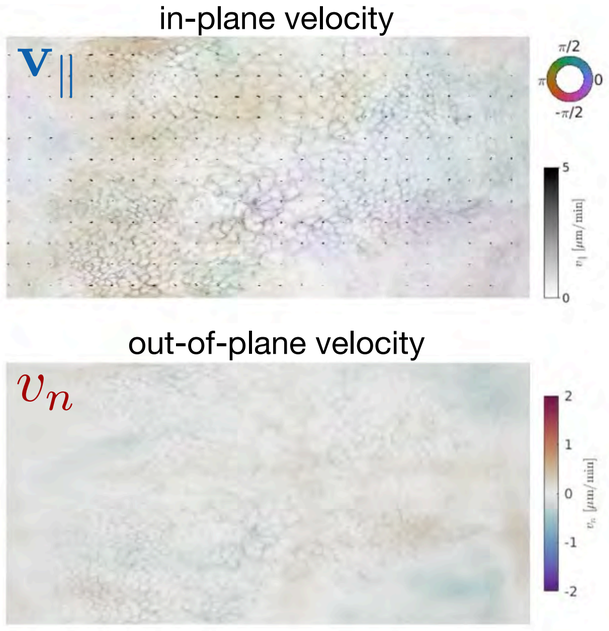

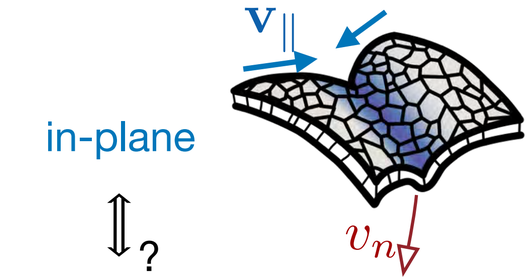

in-plane

$\Updownarrow$?

out-of-plane

Mitchell & Cislo, *Nature Methods* (2023)

[On board]

In-plane and out-of-plane deformations

4 Strain rate on a deforming surface

Denote the surface $\mathcal{S}$ embedded in $\mathbb{R}^3$ as $\mathbf{r}(x_1, x_2)$. By convention, all bold vectors will be in $\mathbb{R}^3$ in the following. The (non-normalized and not necessarily orthogonal) tangent vectors are $\mathbf{e}_i = \partial_i \mathbf{r}$, where $\partial_i := \frac{\partial}{\partial x_i}$. We also introduce the normalized normal $\mathbf{n} = \mathbf{e}_1 \wedge \mathbf{e}_2 / |\mathbf{e}_1 \wedge \mathbf{e}_2|$. Together, these define a local basis that we can use to express a vector field

$$\mathbf{v} = v^i \mathbf{e}_i + v_n \mathbf{n} \tag{5}$$

(We use Einstein summation convention for repeated indices).

We also want to express derivative operators in the surface. To that end, we first need to introduce some machinery for the surface geometry, namely the metric

$$g_{ij} := \mathbf{e}_i \cdot \mathbf{e}_j, \tag{6}$$

where the dot product is the standard inner product in $\mathbb{R}^3$. With the metric and it's inverse $g^{ij} := (g_{ij})^{-1}$ (as a matrix, not component wise!), we can raise and lower indices. In particular, we can introduce the co-tangent vectors $\mathbf{e}^i = g^{ij}\mathbf{e}_j$ which satisfy the orthonormality condition $\mathbf{e}_i \cdot \mathbf{e}^j = \delta_i^j$. The gradient operator is now defined as

$$\nabla = \mathbf{e}^i \partial_i. \tag{7}$$

This is a vector in the embedding $\mathbb{R}^3$. To derive in-plane tensors from it (like the strain rate tensor), we'll need to project onto the (co-)tangent vectors.

Let's work out the divergence of $\mathbf{v}$:

$$\begin{aligned}
\nabla \cdot \mathbf{v} &= (\mathbf{e}^i \partial_i) \cdot (v^i \mathbf{e}_i + v_n \mathbf{n}) && \text{(8a)}\\
&= \mathbf{e}^i \partial_i (v^i \mathbf{e}_i) + v_n \mathbf{e}^i \cdot \partial_i \mathbf{n} && \text{(8b)}\\
&= \mathrm{div}_{\mathcal{S}}\, v_{||} - v_n (\mathbf{e}^i \cdot \mathbf{e}^j) b_{ij} && \text{(8c)}\\
&= \mathrm{div}_{\mathcal{S}}\, v_{||} - v_n g^{ij} b_{ij} && \text{(8d)}\\
&= \mathrm{div}_{\mathcal{S}}\, v_{||} - 2 v_n H && \text{(8e)}
\end{aligned}$$

In the third line, we have introduced the surface divergence operator $\mathrm{div}_{\mathcal{S}}$ that acts on the tangential velocity field $v_{||}$. (Writing out the expression for the divergence gives the usual form with the connection). We have also used the second fundamental form $b_{ij} := -\mathbf{e}_i \cdot \partial_j \mathbf{n}$, which captures how the surface normal changes locally: $\partial_i \mathbf{n} = -b_{ij}\mathbf{e}^j$. In the last line, we have introduced the mean curvature $H := b_i^i/2 = g^{ij} b_{ij}/2$. The mean curvature describes how much the a small area element changes if it is moved (and stretched) along the surface normal. This is why it shows up in the expression for the divergence: it describes the change of area due to out-of-plane velocity v_n.

We can also define the in-plane strain rate tensor

$$2\dot{\varepsilon}_{ij} = \mathbf{e}_i \cdot \partial_j (v^k \mathbf{e}_k) + \mathbf{e}_j \cdot \partial_i (v^k \mathbf{e}_k), \tag{9}$$

which has the trace $\mathrm{tr}\dot{\varepsilon} = \dot{\varepsilon}_i^i = g^{ij}\varepsilon_{ij} = \mathrm{div}_{\mathcal{S}}\, v_{||}$, as expected. It's traceless part is the deviatoric strain rate

$$\dot{\bar{\varepsilon}}_{ij} = \dot{\varepsilon}_{ij} - g_{ij}\dot{\varepsilon}_k^k/2 \tag{10}$$

[The total strain rate tensor (including the out-of-plane contribution) is $\frac{1}{2}\partial_t g_{ij} = \dot{\varepsilon}_{ij} - v_n b_{ij}$. The area-element rate of change is

$$\frac{\partial_t \sqrt{g}}{\sqrt{g}} = \frac{\partial_t g}{(2g)} = \frac{1}{2} g^{ij} \partial_t g_{ij} = g^{ij}\dot{\varepsilon}_{ij} - 2Hv_n = \mathrm{div}_{\mathcal{S}}\, v_{||} - 2v_n H \tag{11}$$

where $g = \det(g_{ij})$ and we used the Jacobi formula for the variation of the determinant.]

In-plane and out-of-plane kinematics

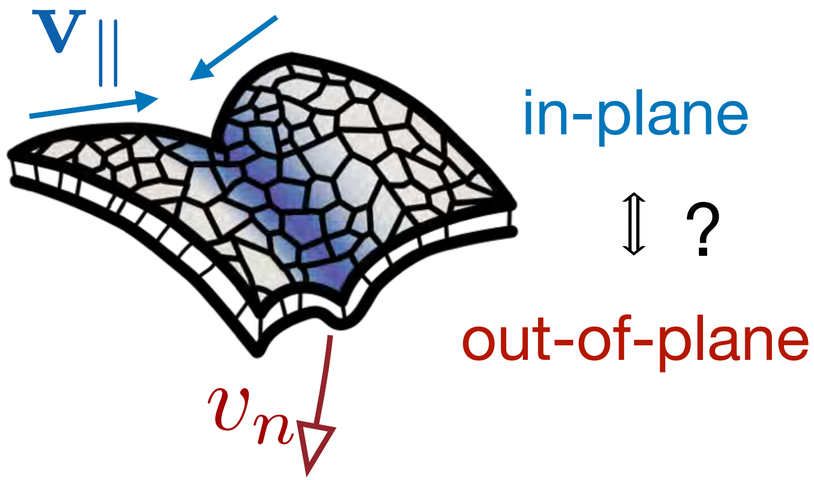

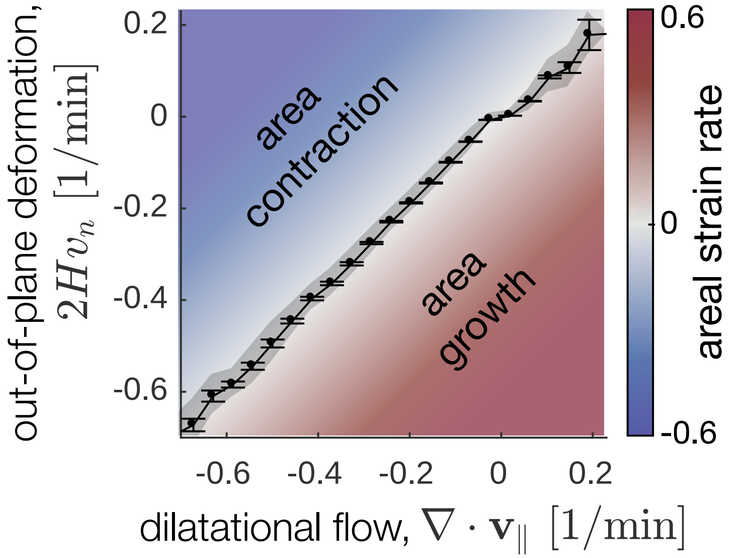

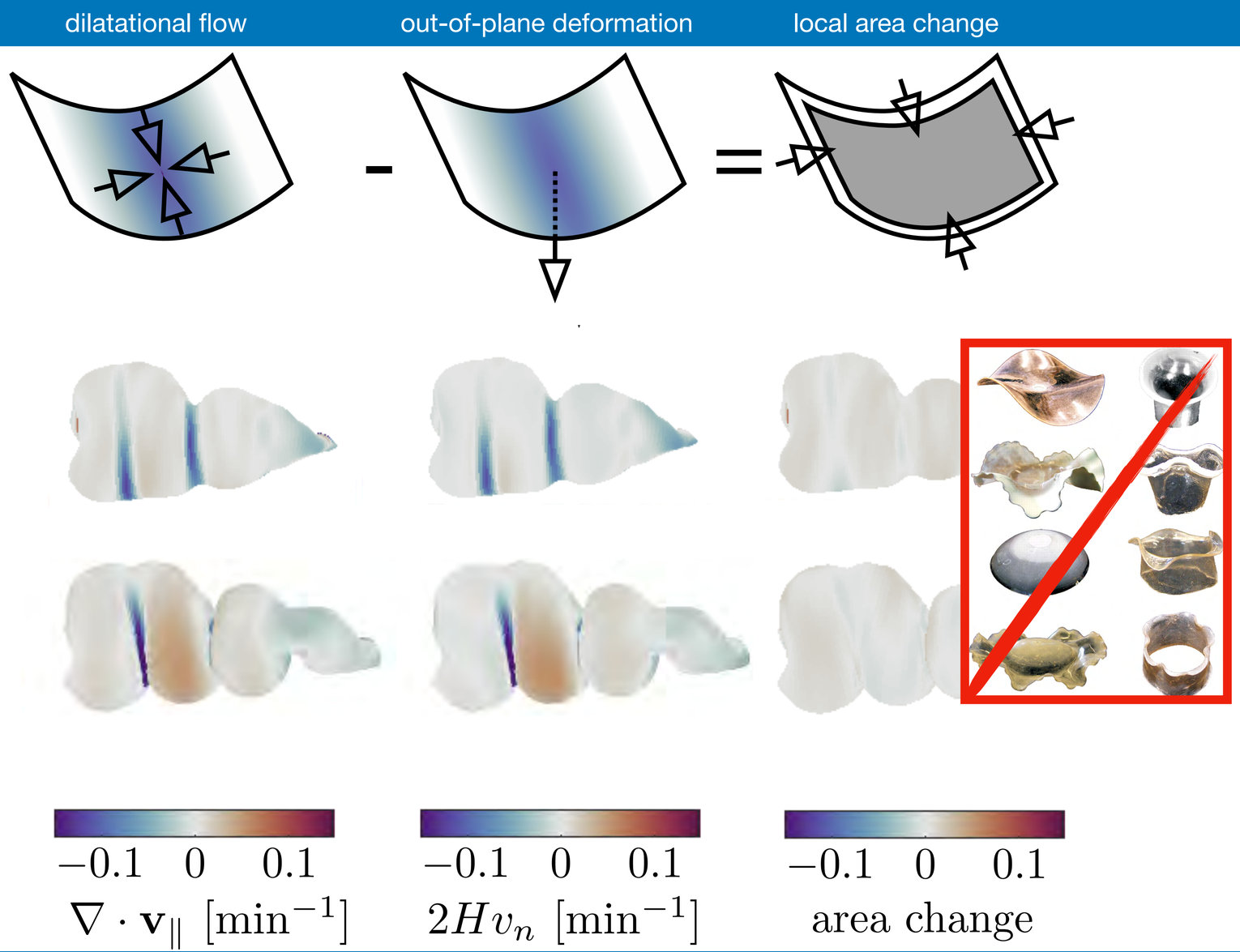

Mitchell *et al.*, *eLife* (2022)

Incompressibility + geometry couple convergent extension to constriction

folding ⇔ tissue shear

incompressibility

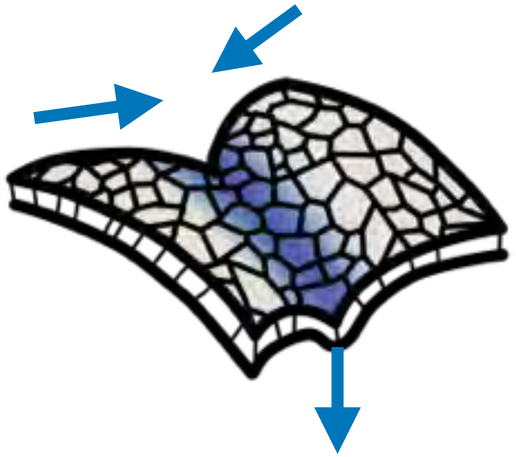

areas are nearly preserved

+

curvature

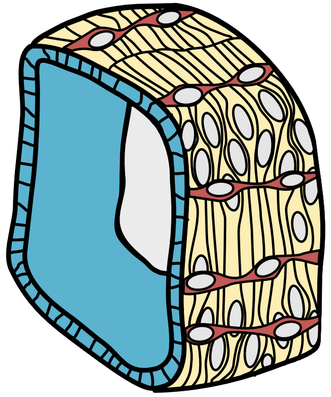

⇒

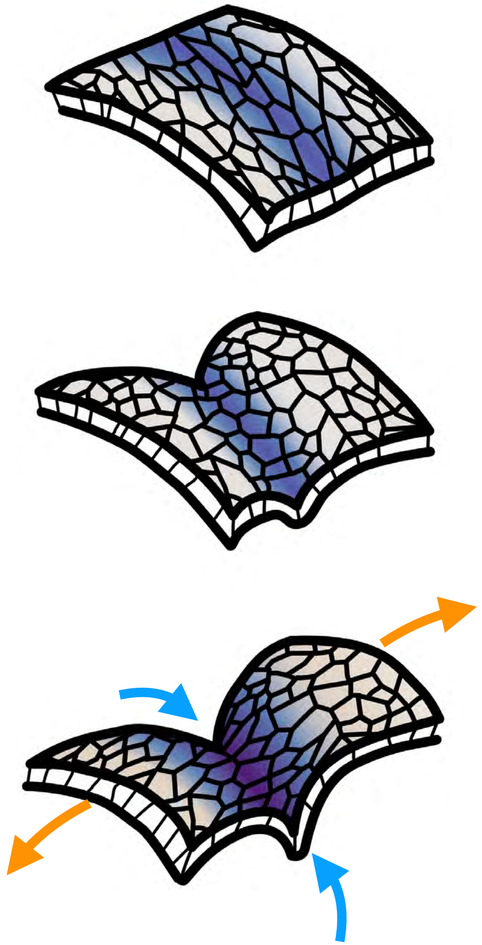

Mitchell *et al.*, *eLife* (2022)

Incompressibility + geometry couple convergent extension to constriction

incompressibility

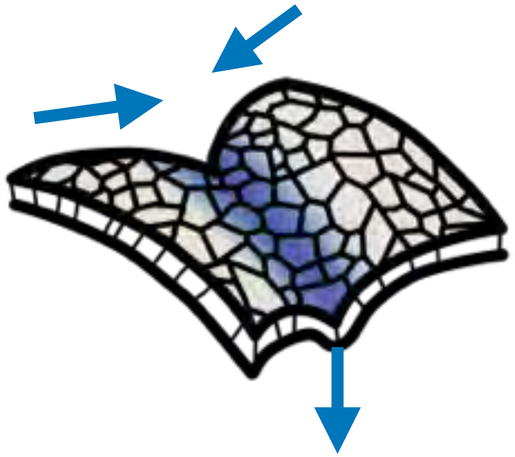

areas are nearly preserved

+

curvature

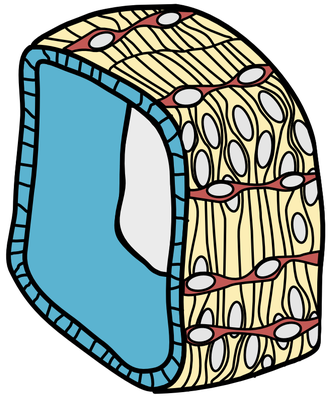

folding ⇔ tissue shear

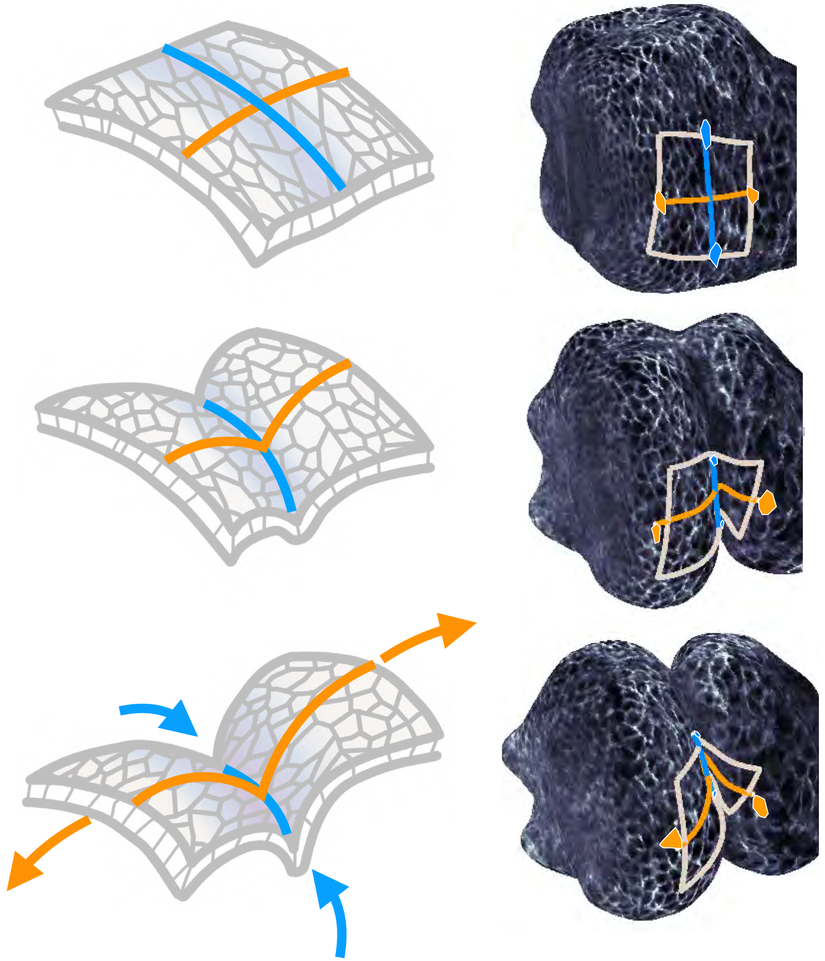

Mitchell *et al.*, *eLife* (2022)

Incompressibility + geometry couple convergent extension to constriction

folding ⇔ tissue shear

incompressibility

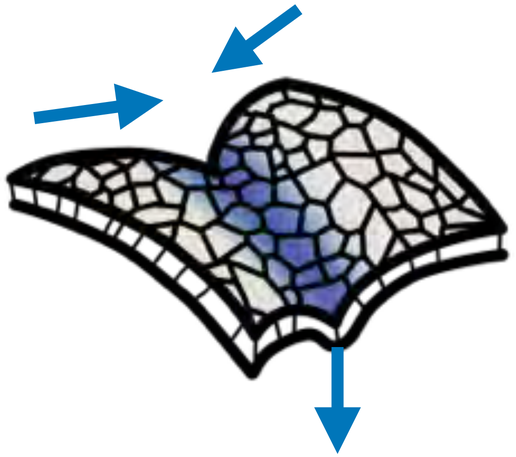

areas are nearly preserved

+

curvature

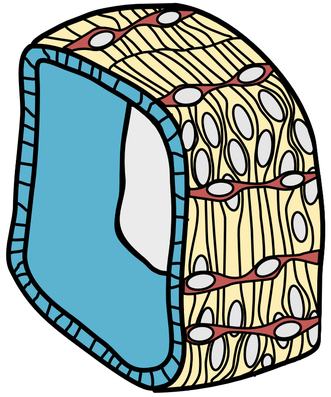

⇒

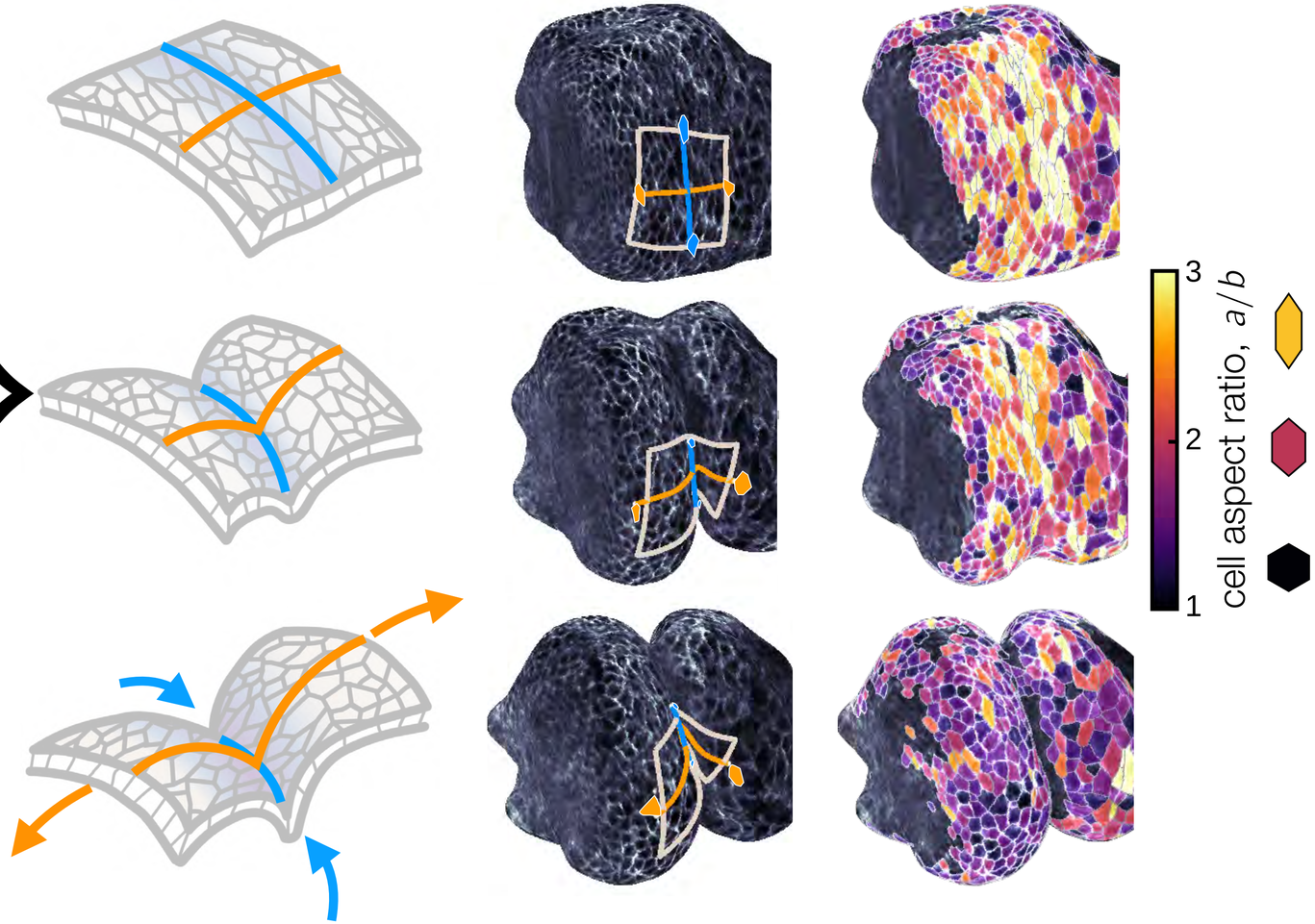

Mitchell *et al.*, *eLife* (2022)

Incompressibility + geometry couple convergent extension to constriction

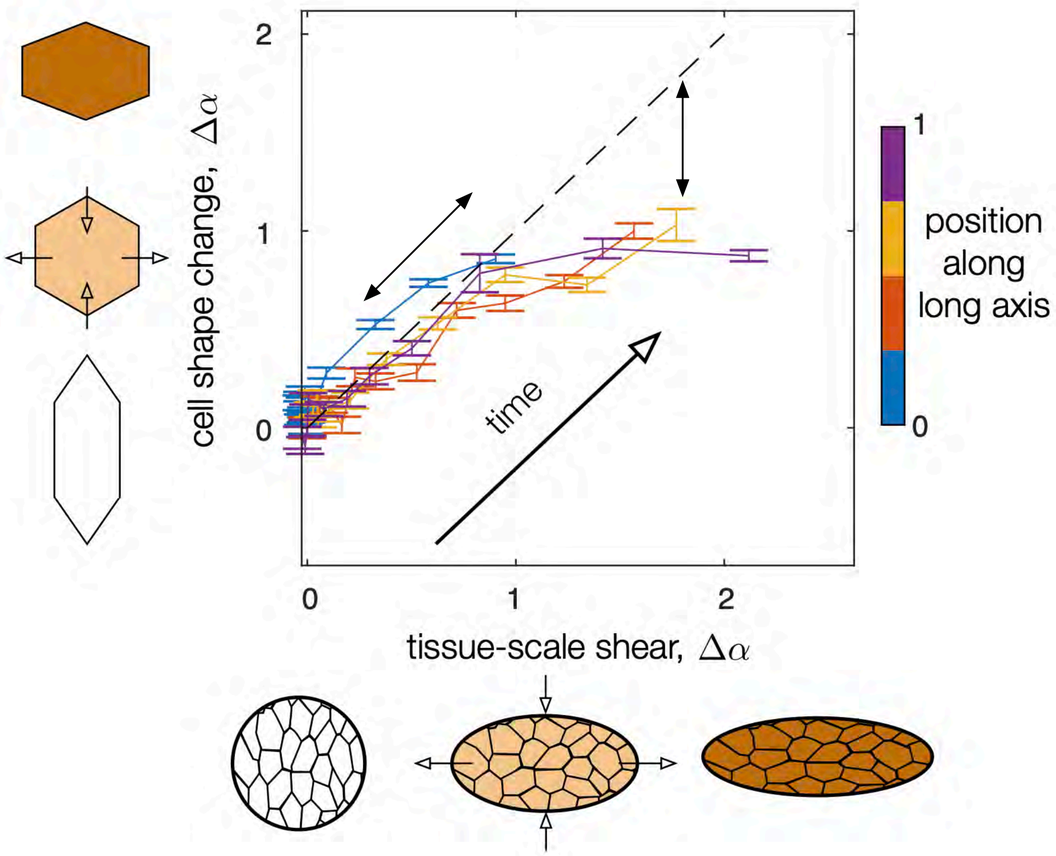

folding ⇔ tissue shear

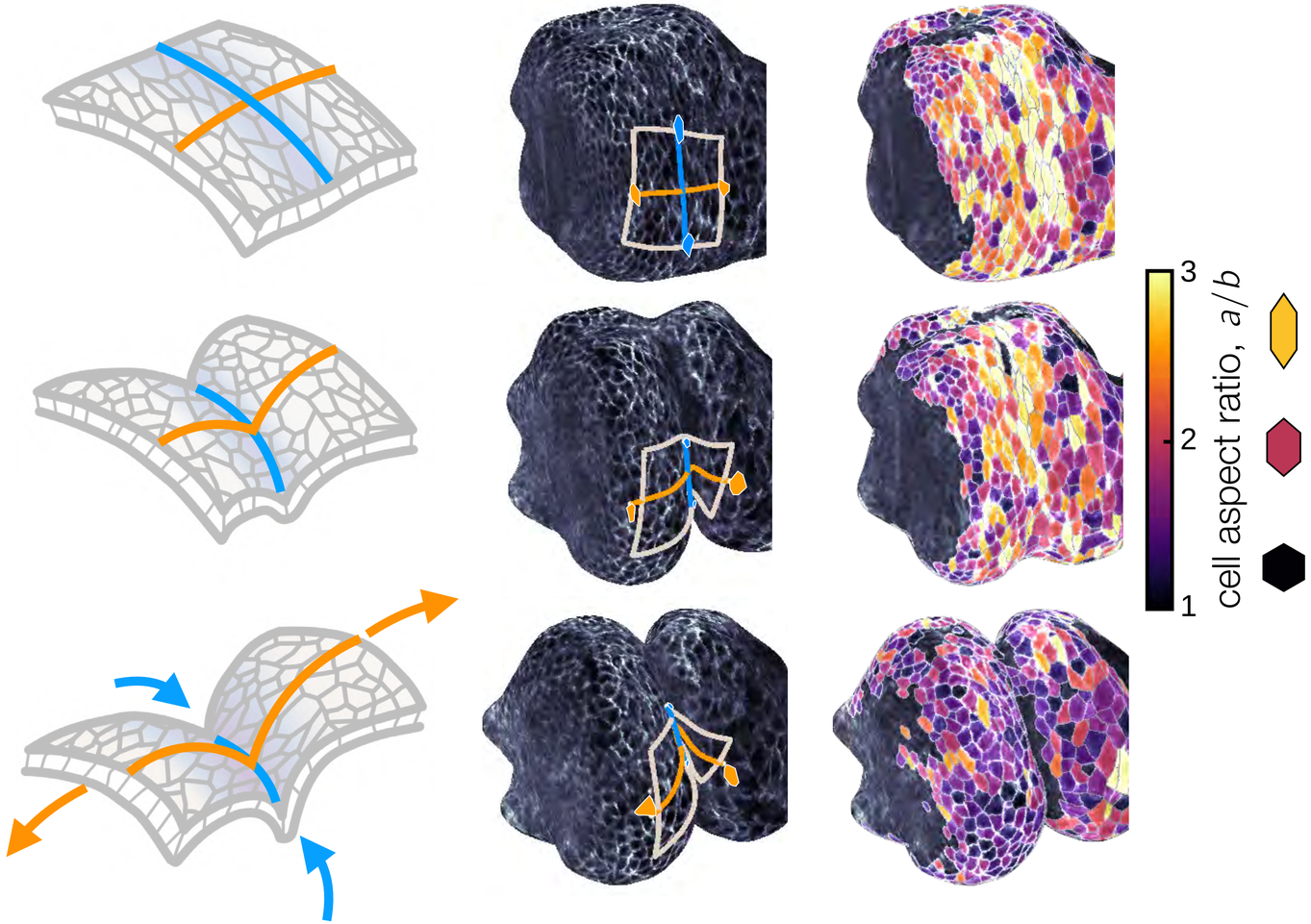

Mitchell *et al.*, *eLife* (2022)

Cell shape change collectively generates patterned convergent extension + constrictions

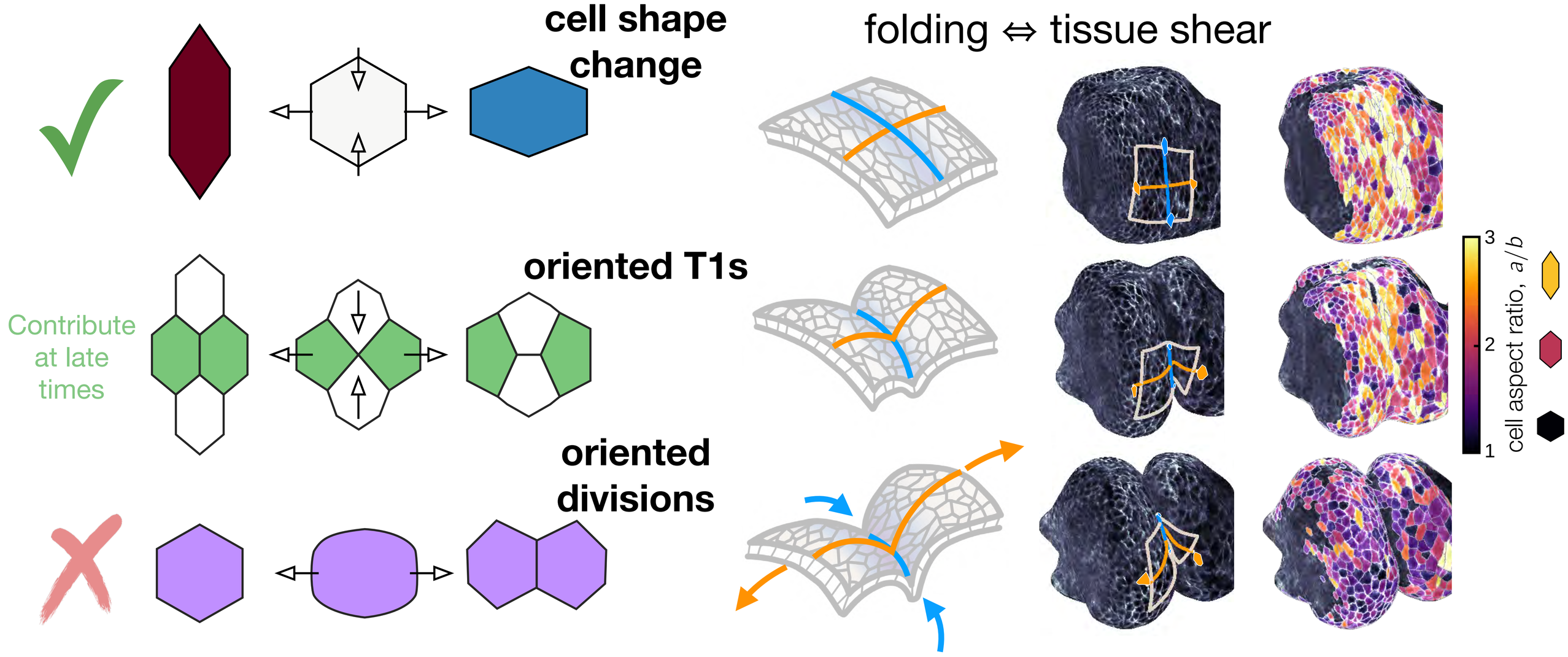

Mitchell *et al.*, *eLife* (2022)

Muscle contraction generates organ constrictions

Perturb muscle contractility with **optogenetics**

Antp GAL4

t= 0

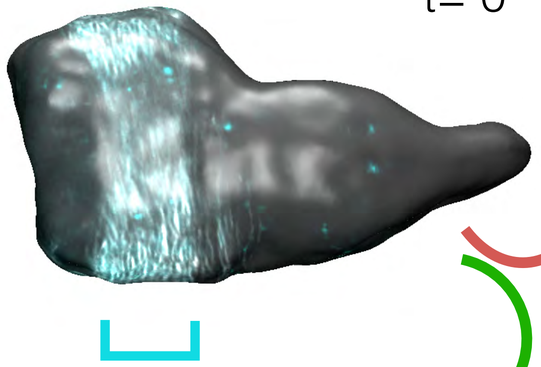

inhibit muscle contraction

t=1.5 hr

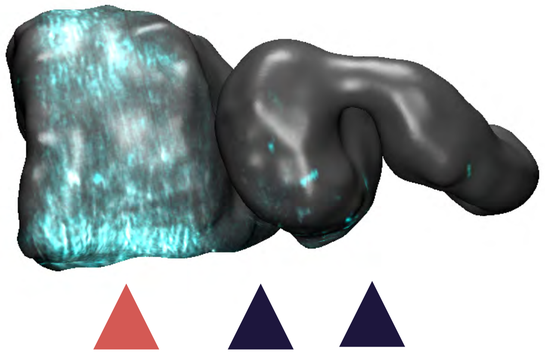

induce muscle contraction

t=10 min

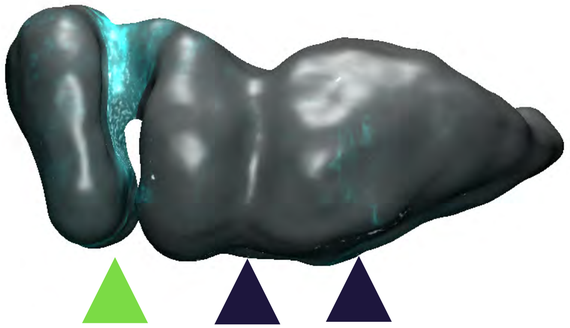

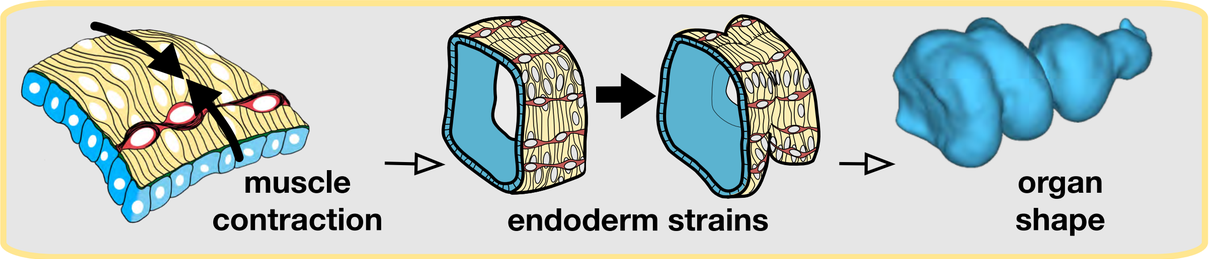

Mitchell *et al.*, *eLife* (2022)

High-frequency calcium pulses are localized near constrictions

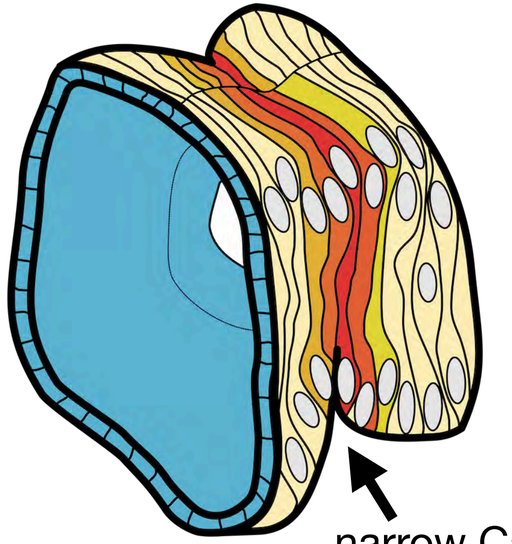

narrow Ca pulses

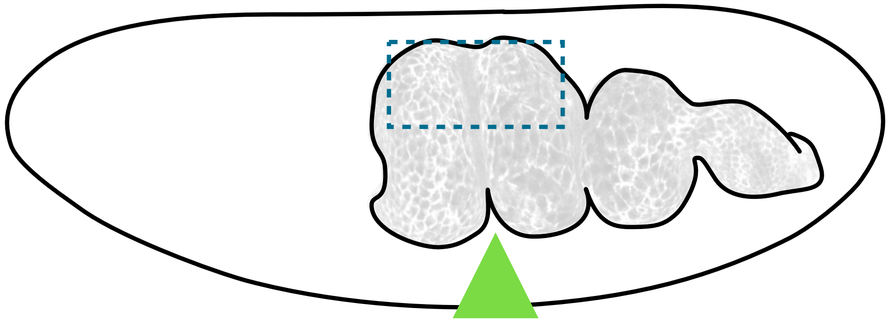

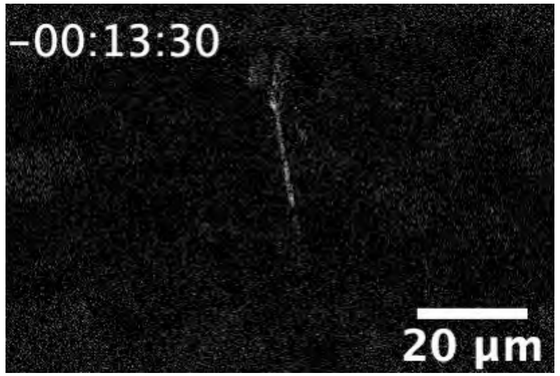

stochastic calcium pulses

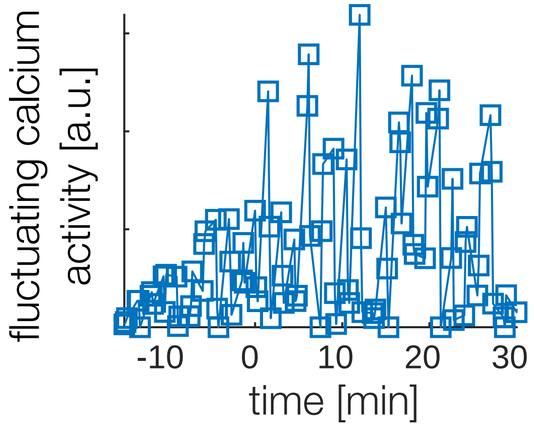

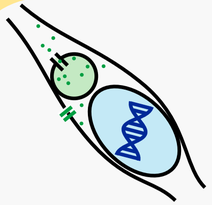

hox genes

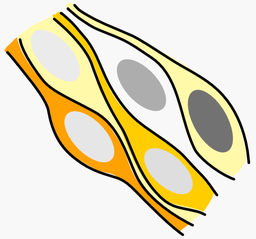

calcium signaling

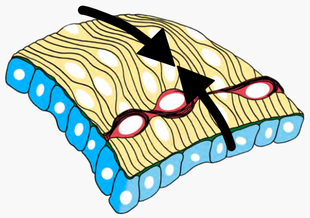

muscle contraction

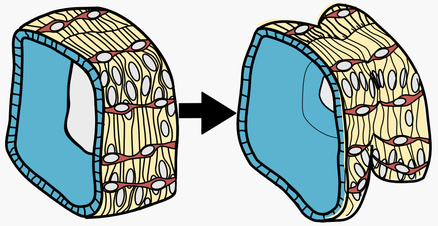

endoderm strains

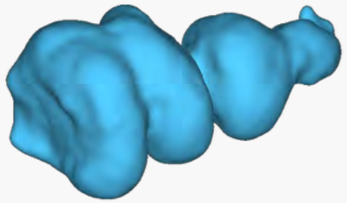

organ shape

Mitchell *et al.*, *eLife* (2022)

High-frequency calcium pulses are localized near constrictions

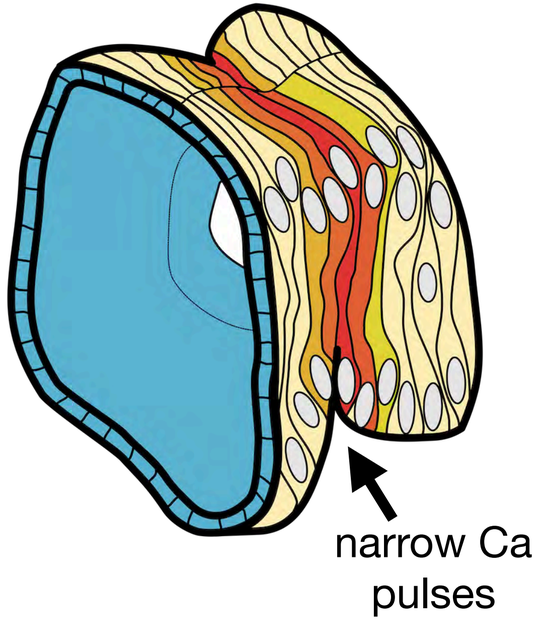

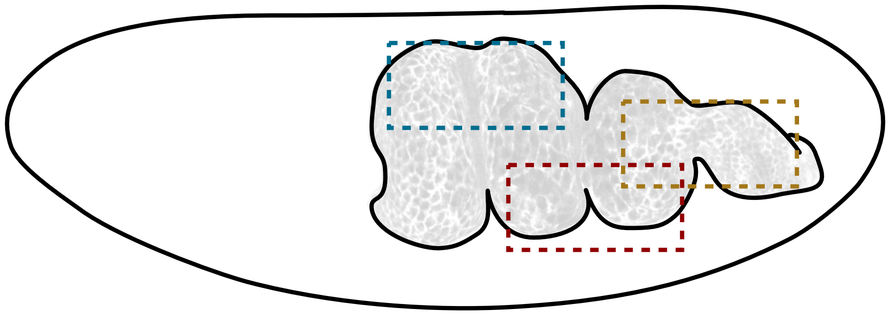

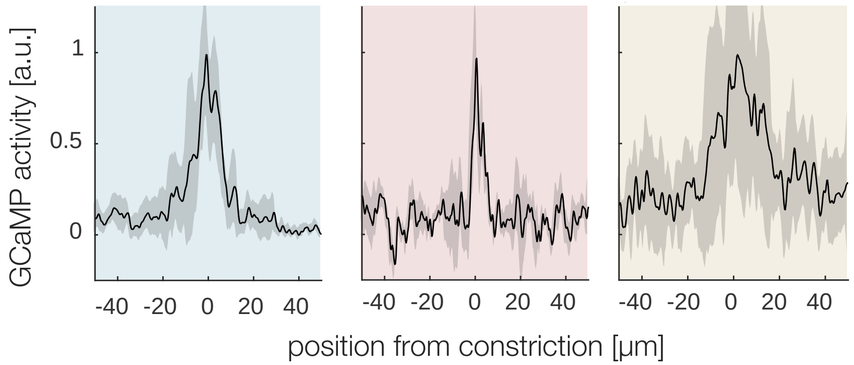

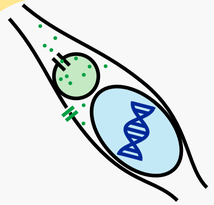

hox genes

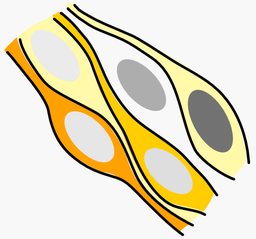

calcium signaling

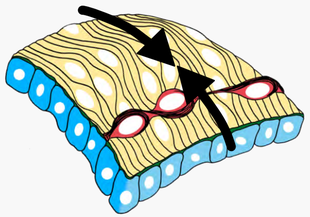

muscle contraction

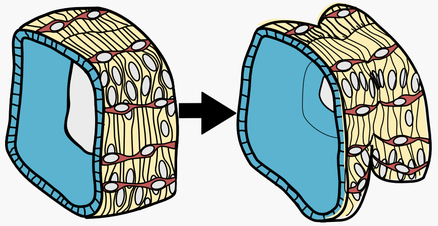

endoderm strains

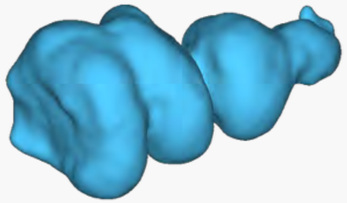

organ shape

Mitchell *et al.*, *eLife* (2022)

Chiral organ morphogenesis

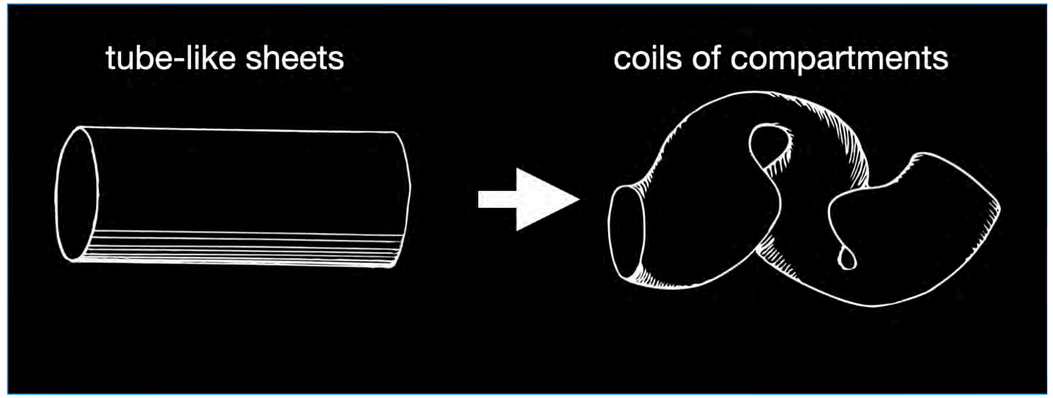

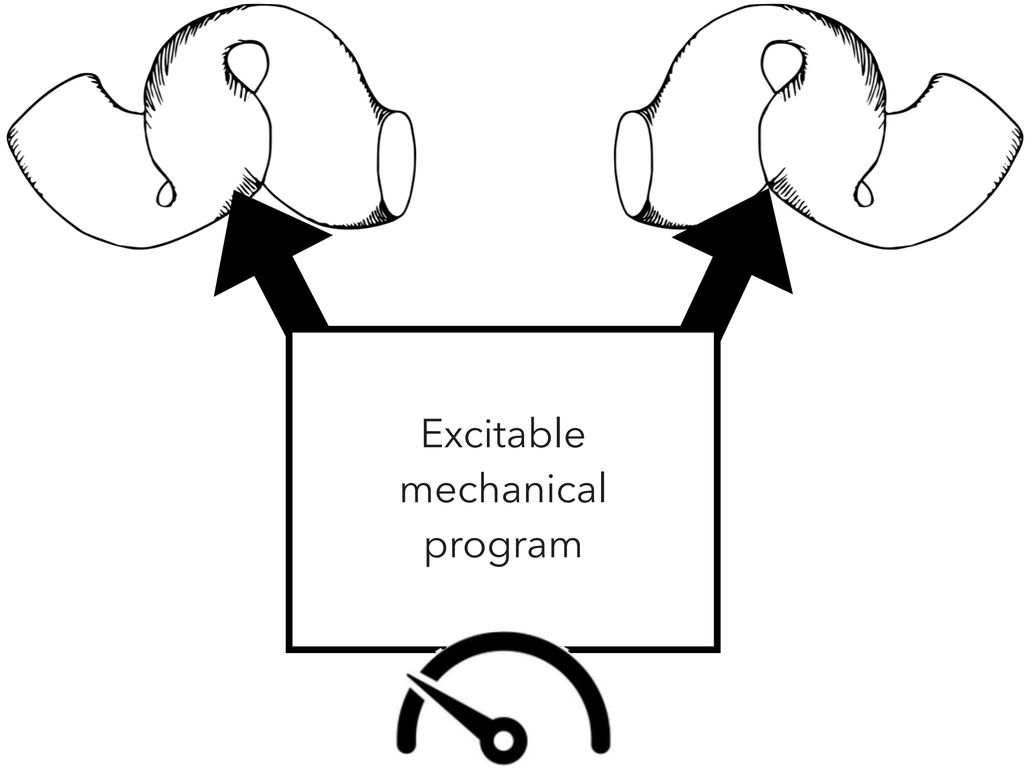

(1) a symmetry-breaking event (molecular chirality⇒ left-right bias)

(2) organ-specific mechanical program ("generator" + "interpreter")

Brown and Wolpert (1990)

Tube demo

Chiral organ morphogenesis

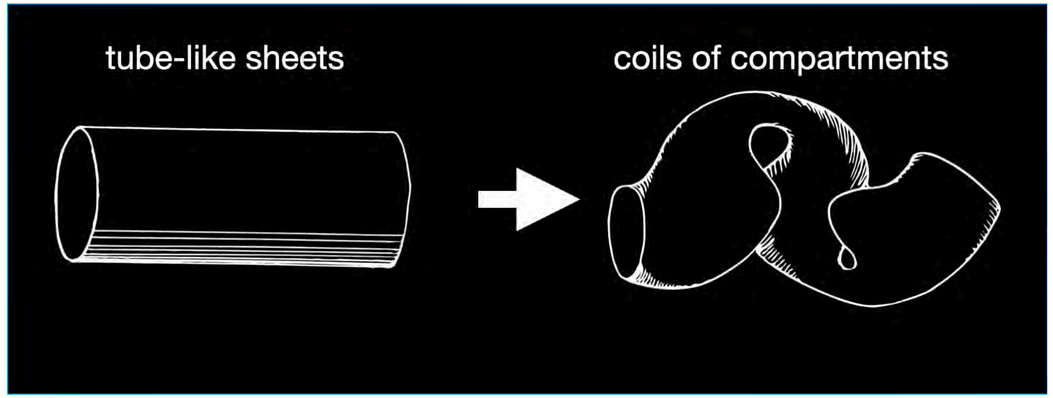

(1) a symmetry-breaking event (molecular chirality⇒ left-right bias)

(2) organ-specific mechanical program ("generator" + "interpreter")

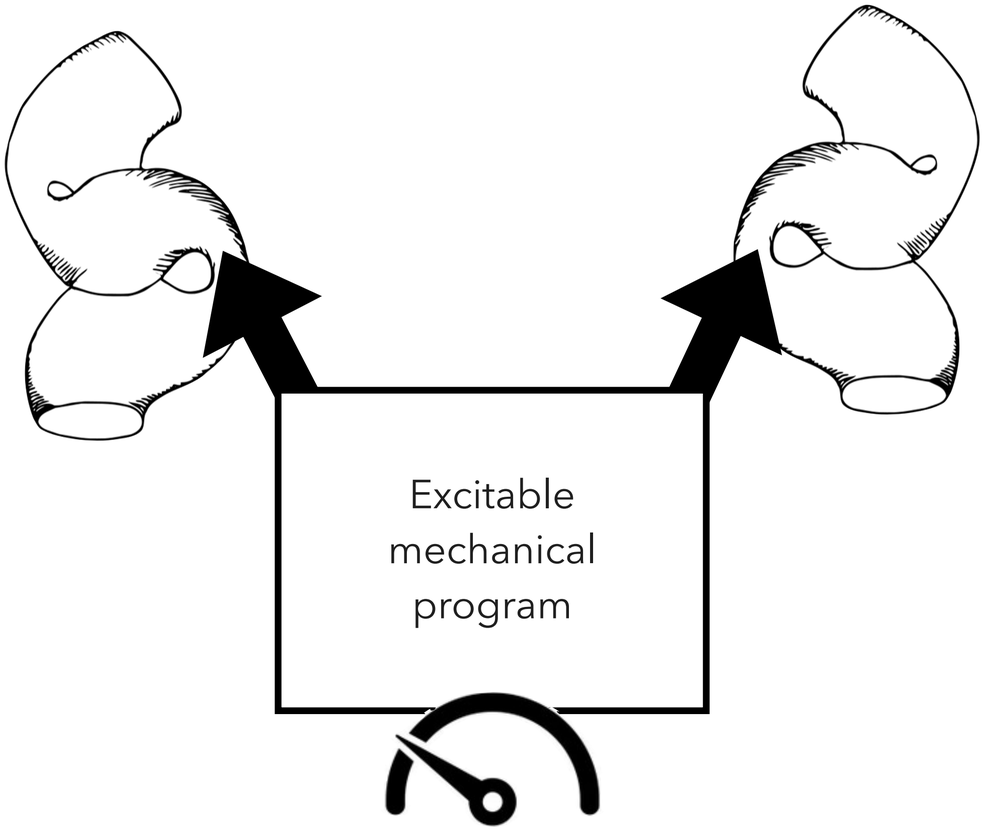

Brown and Wolpert (1990)

Early Left-Right asymmetry in morphogenesis

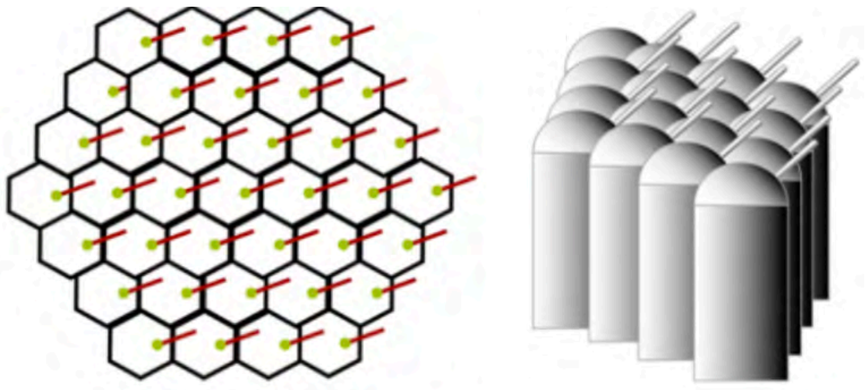

Lee & Anderson *Dev. Dyn.* 2008

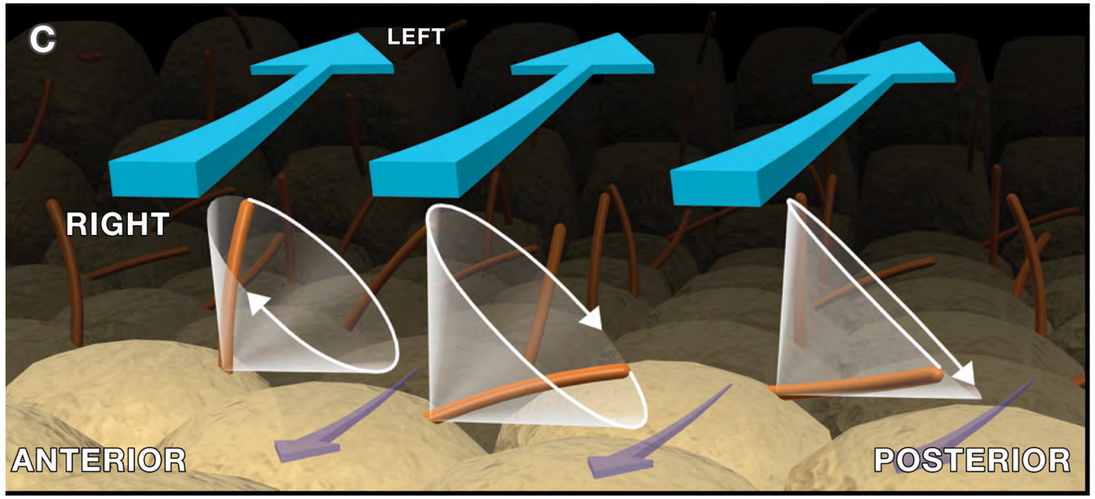

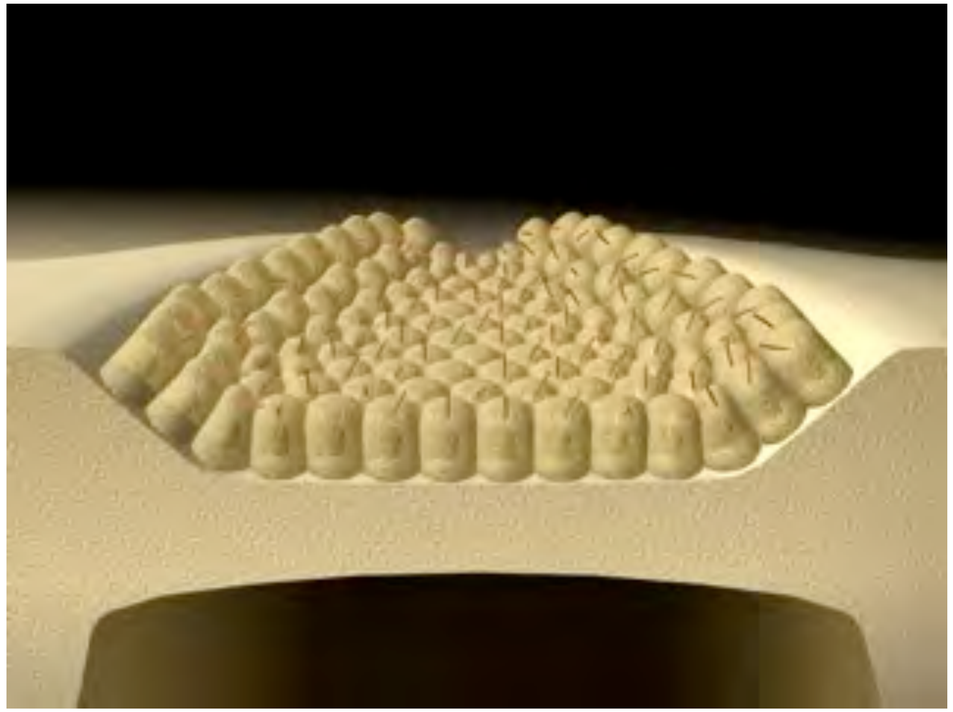

Lee & Anderson *Dev. Dyn.* 2008

Early Left-Right asymmetry in morphogenesis

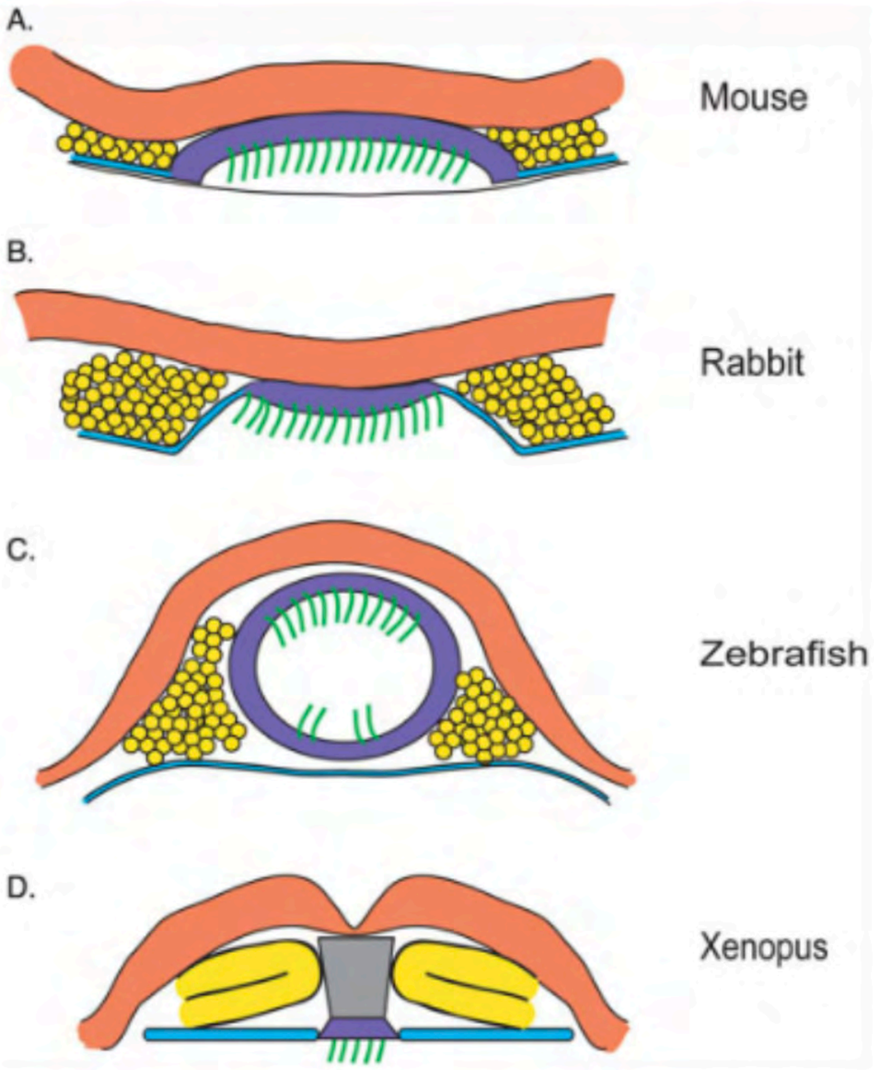

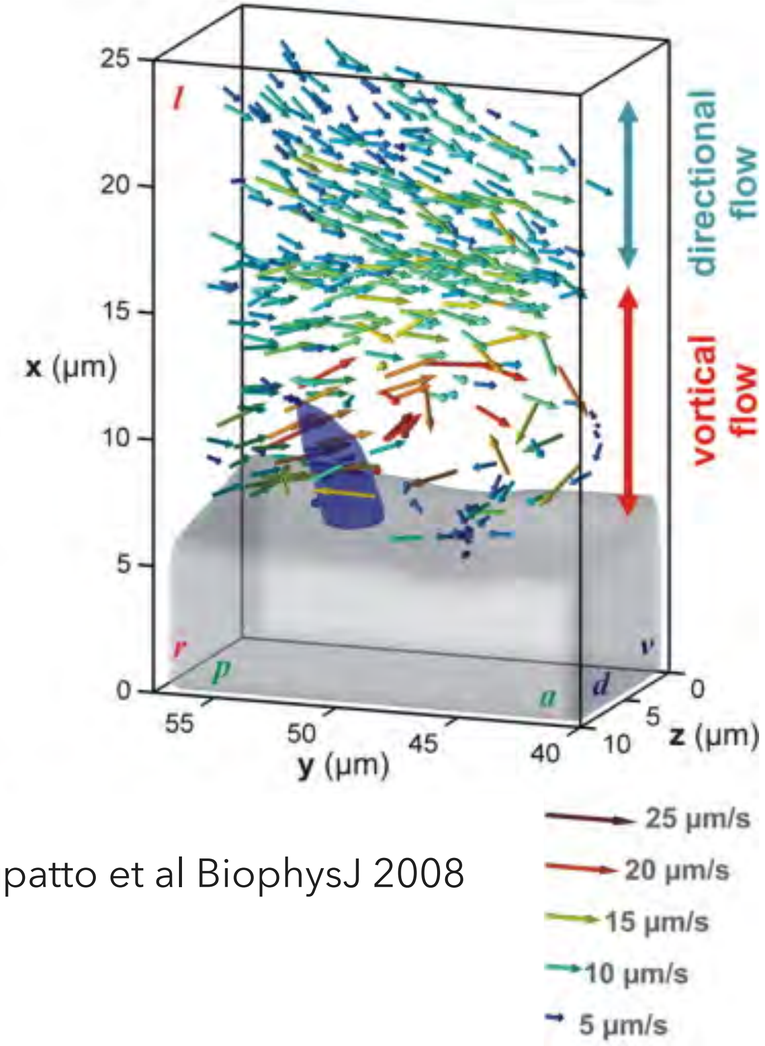

Supatto et al BiophysJ 2008

A system ripe for modeling?

see Cartwright et al *PNAS* 2004

Cell-intrinsic chirality plays a central role in heart morphogenesis

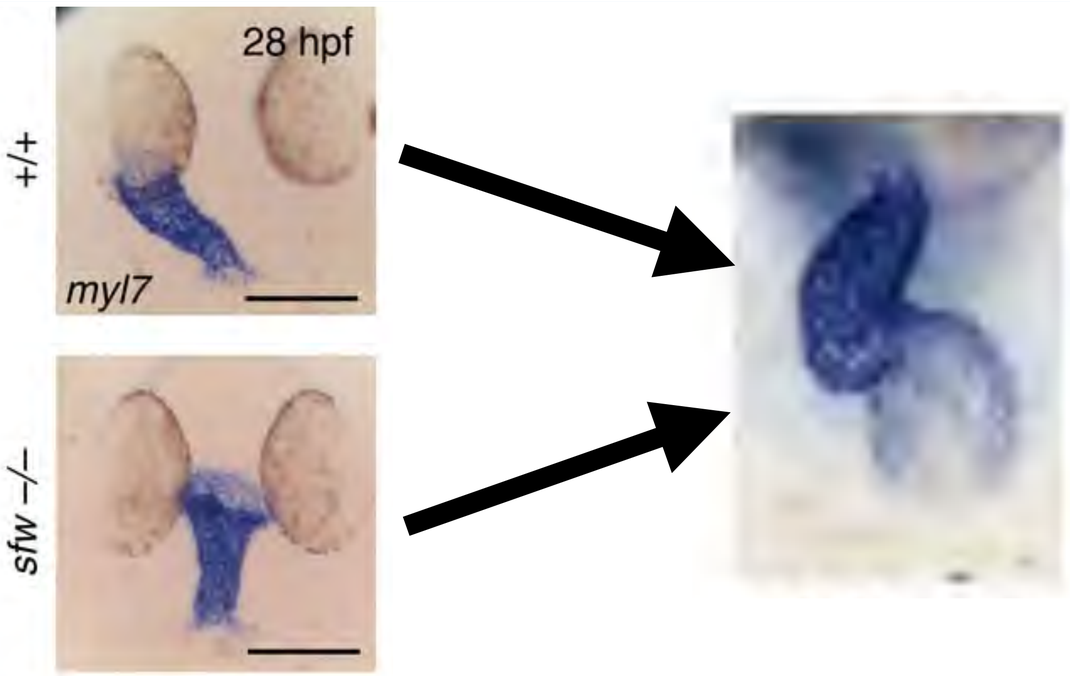

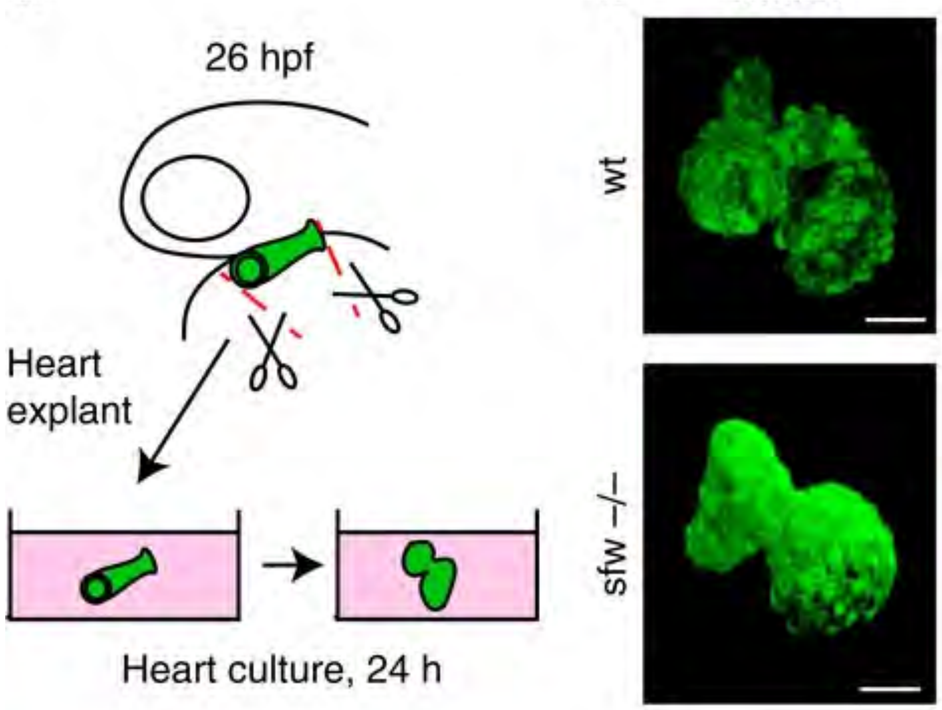

- mutant for the Nodal-related *southpaw*: dextral heart, but gut and brain are random.
- Genetic and pharmacological inhibition of Nodal does not abolish heart asymmetry
- tissue intrinsic: *ex vivo* hearts have chiral looping
- Nodal may amplify tissue-intrinsic looping mechanism

Noël et al. *Nat Comm.* 2013

Left-Right asymmetry in heart morphogenesis

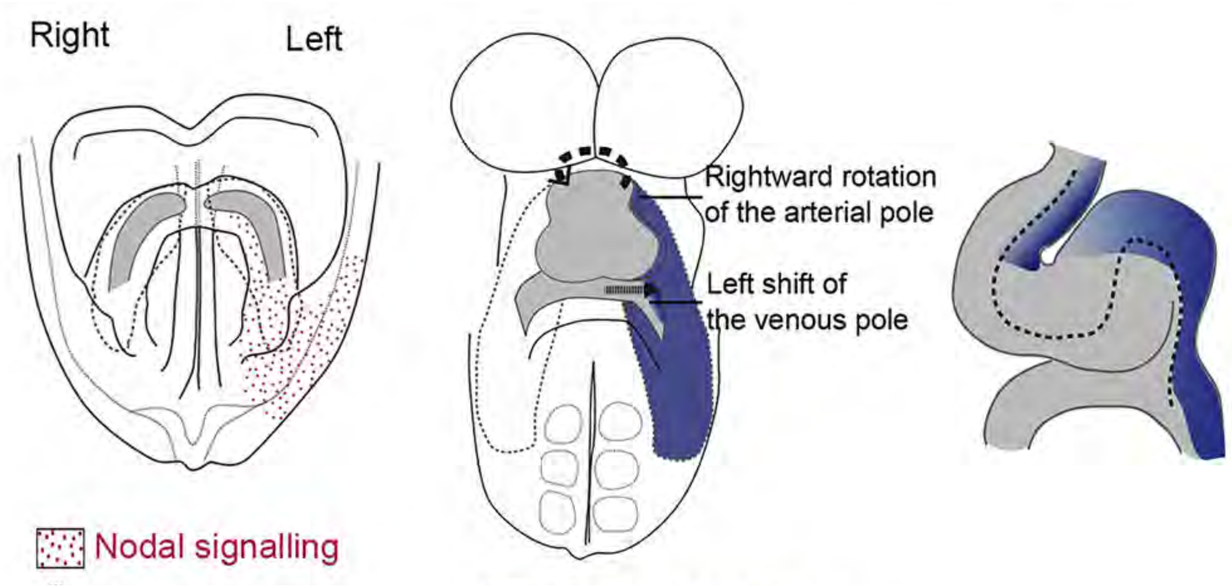

"We provide evidence of a heart-specific **random generator of asymmetry** that is independent of Nodal."

Nodal functions as a bias of this mechanism: amplify and coordinate opposed left-right asymmetries at the heart tube poles

Desgrange et al, *Dev Cell* 2020

Left-Right asymmetry in heart morphogenesis

Is cell intrinsic asymmetry in the cytoskeleton generating asymmetric biomechanical forces?
Or is the laterality pathway providing asymmetric cues to the cells?

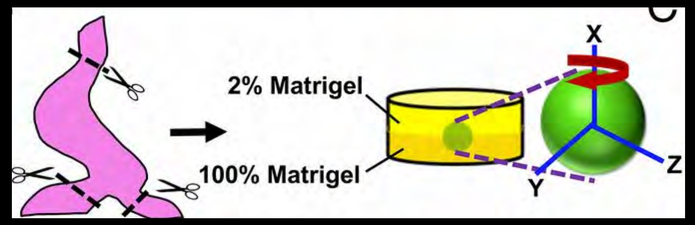

Ray et al., *PNAS* 2018

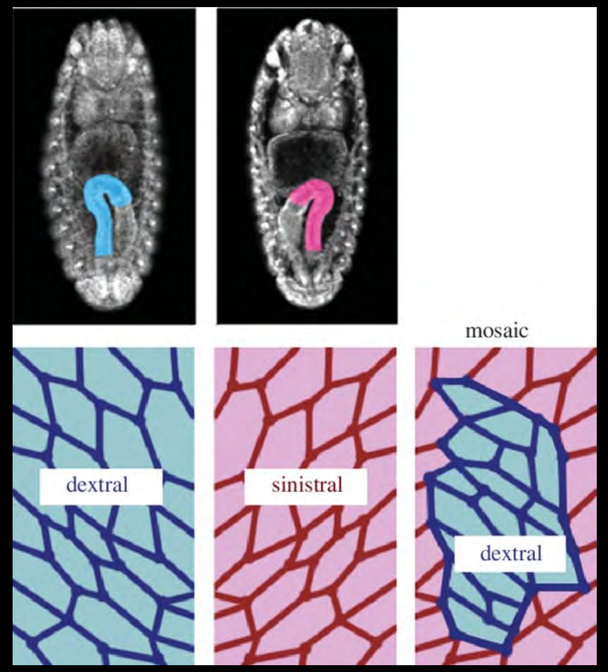

Matsuno group

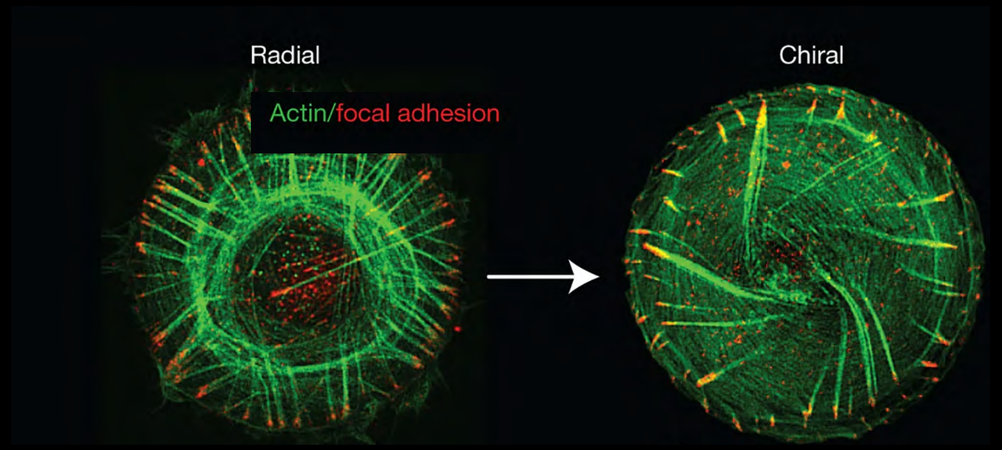

Tee et al., *Nat Cell Bio* 2015

Left-Right asymmetry in heart morphogenesis

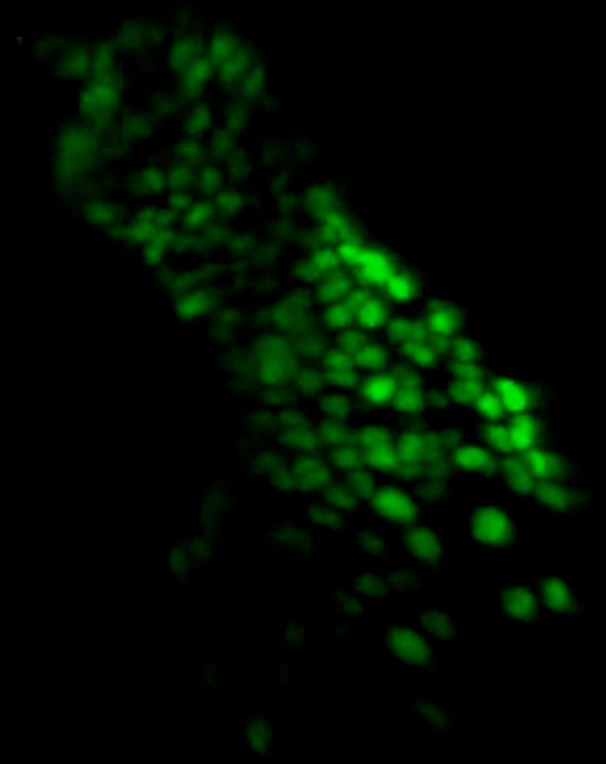

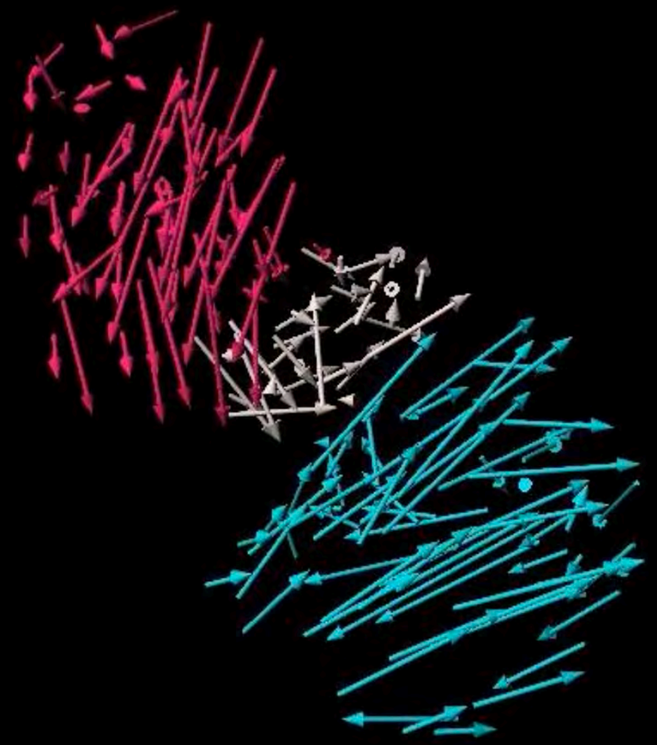

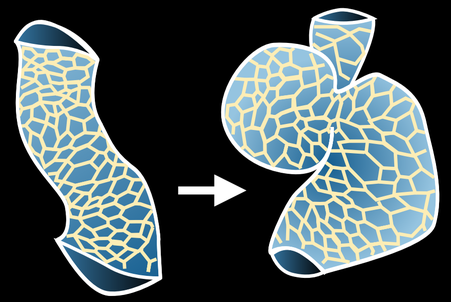

Strains? Strain rates?
Stresses?

tnnt2a morpholino blocks heart beat
(Sehnert et al., 2002)

Tessadori et al, *eLife* 2021

Outlook: supracellular biophysics of visceral organ morphogenesis

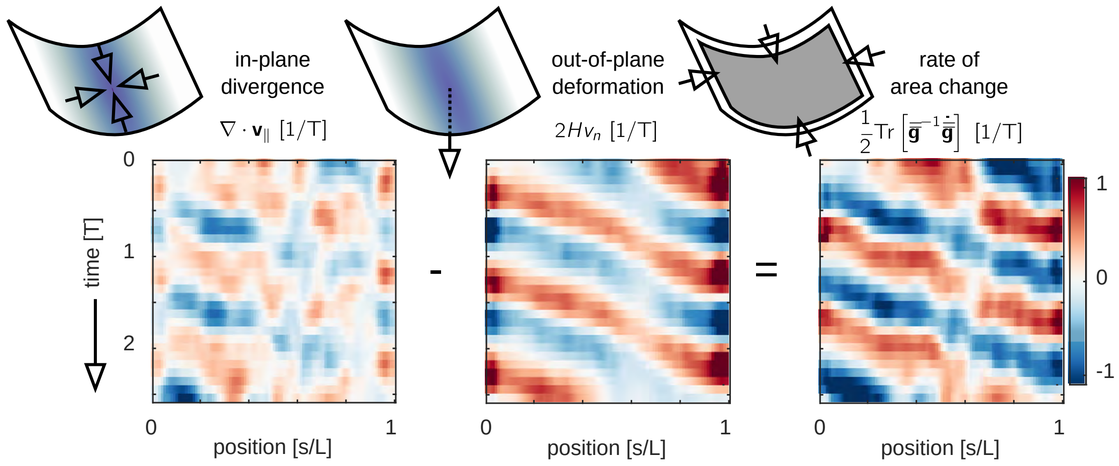

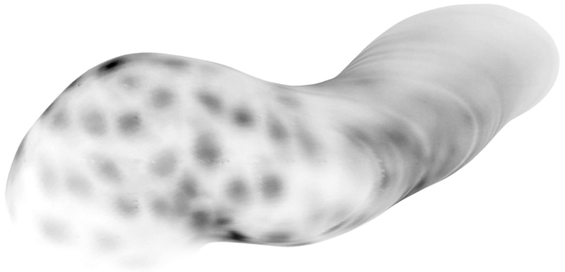

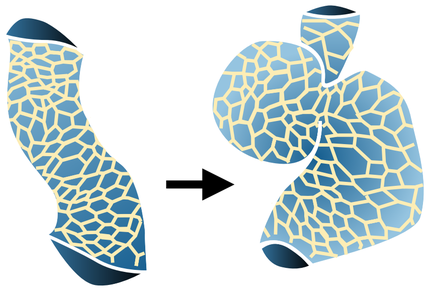

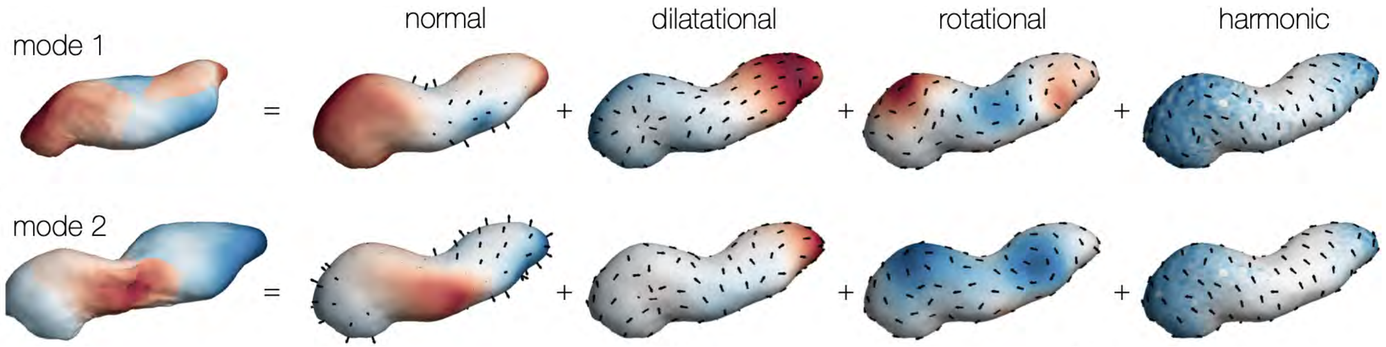

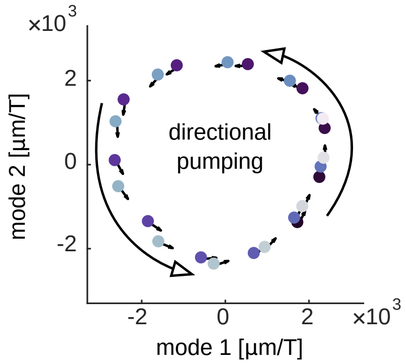

Strains? Strain rates?
Stresses?

Left-Right asymmetry in heart morphogenesis

linear tube twists around a fixed hinge

The two chambers rotate in opposite directions

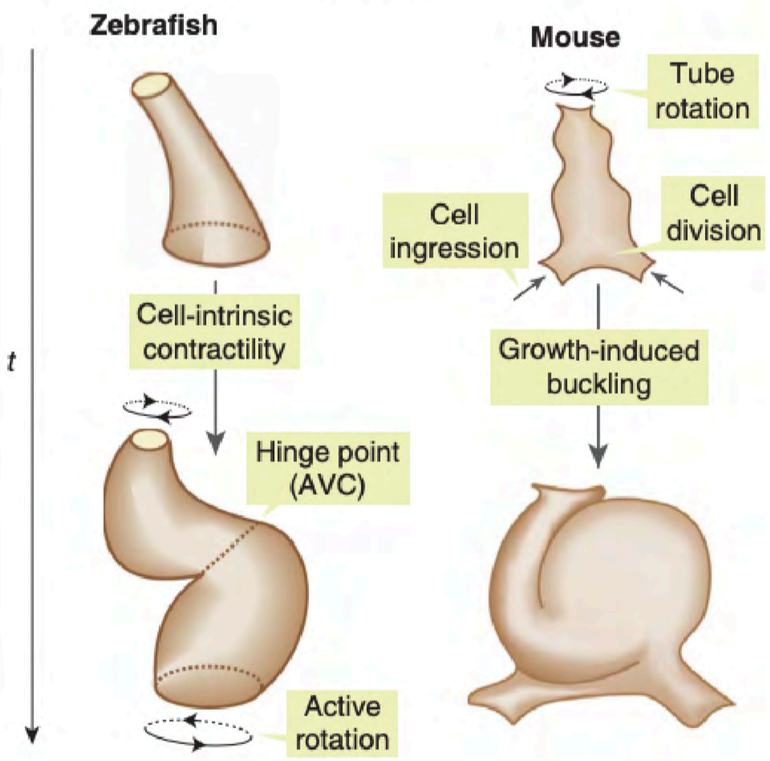

Andrews & Priya, Cold Spring Harb Perspect Biol. 2024

human

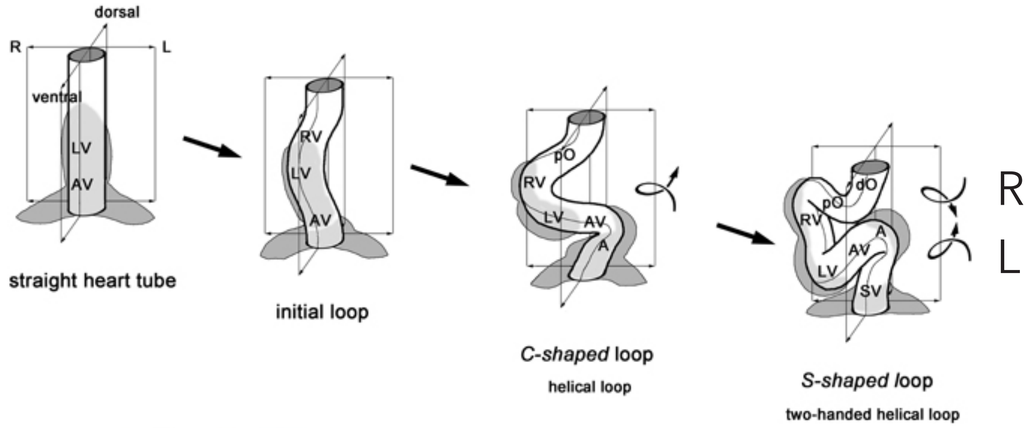

R
L

perversion

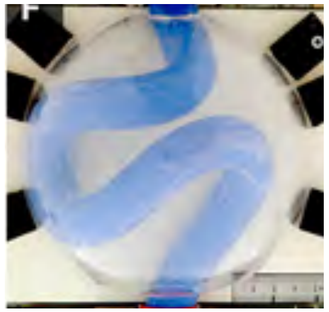

buckling deformations

Bayraktar & Männer *Frontiers* 2014

Open Challenges

- **Feedback**: post-translational loops, mechanics > gene expression
- Cell **intrinsic** vs extrinsic forces
- **Linking scales**: molecules > cells > tissues > organ shape
- **Complex 3D forms** with tissue layer interactions
- Repurposed mechanisms: development > **physiology**
- Coupled **pulsatile oscillators** (actomyosin pulses, calcium pulses…)
- **Learning** and adaptive material behavior: cells & tissues as computing agents
- **Computational tools** for quantitative analysis of experimental data
- How tissue **rheology** influences morphogenetic processes
- **Synthetic morphogenesis**: creating controllable models to sweep morphospace and dissect development
- **Evolutionary Perspectives**: how mechanisms have evolved and diversified across different organisms

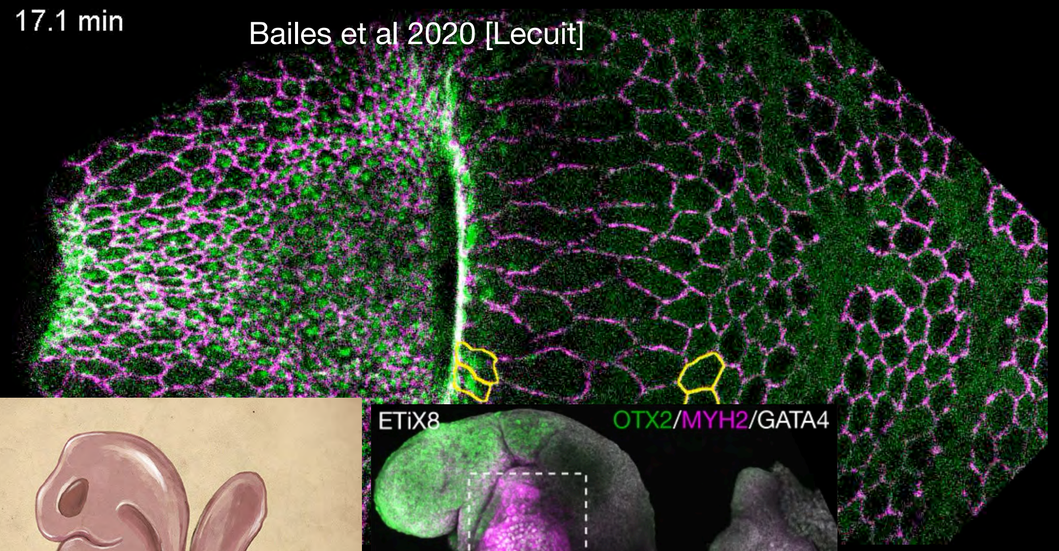

Bailes et al 2020 [Lecuit]

Magdalena Zernicka-Goetz , Jacob Hannah

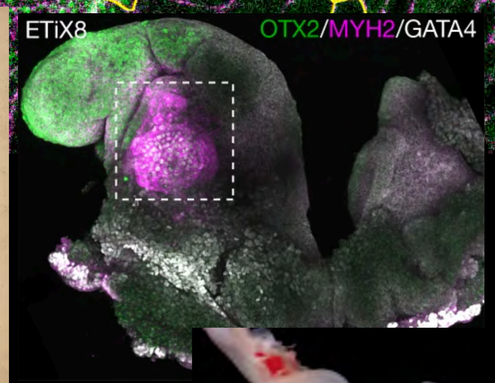

Savin et al 2011

Mechanics of morphogenesis

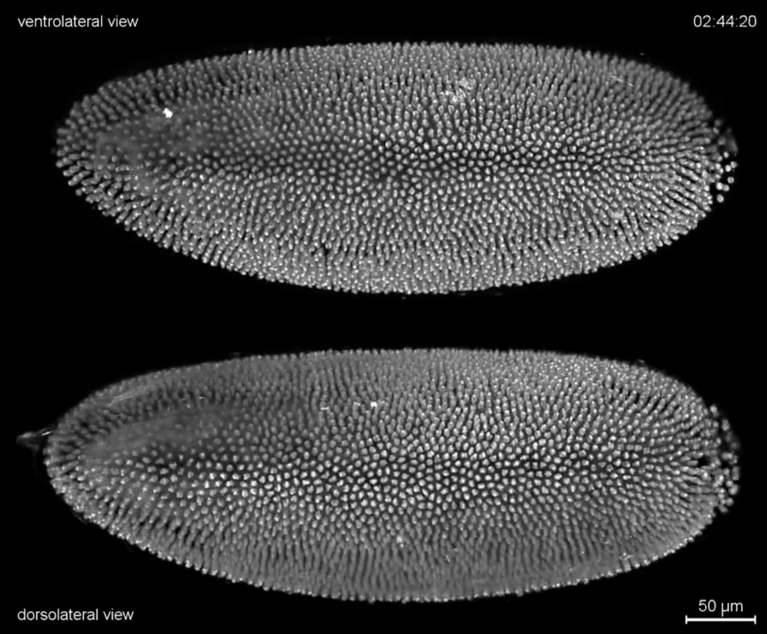

Tomer *et al* (2012)

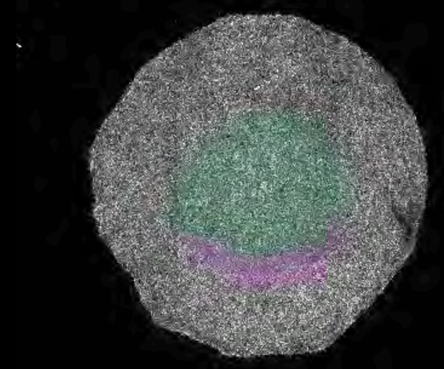

Saadhoui et al, 2018

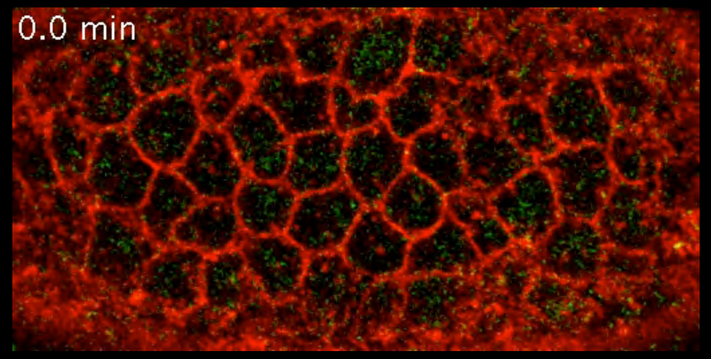

Martin *et al* (2009)

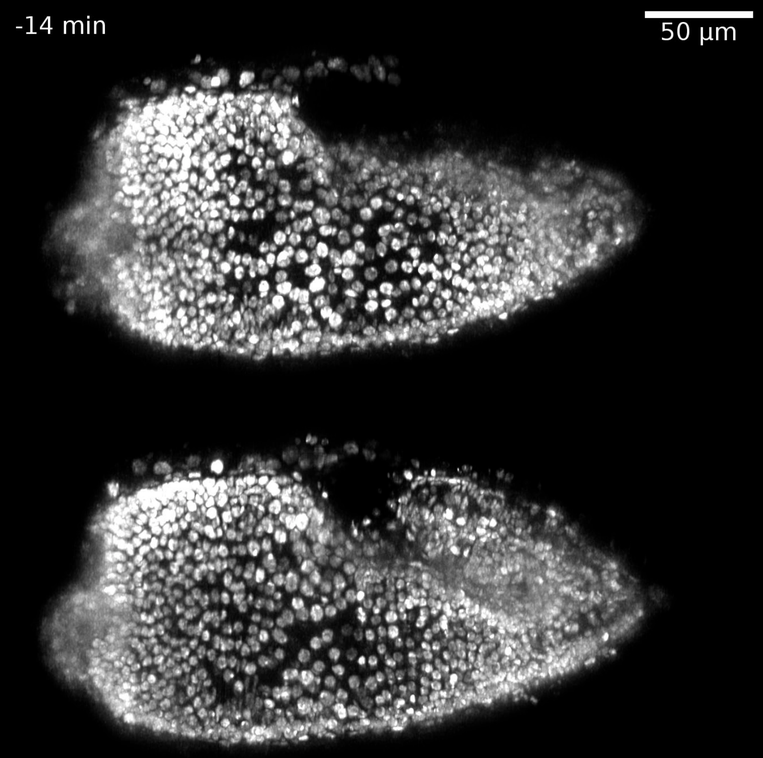

Mitchell *et al* (2022)

Fridtjof Brauns [KITP, UCSB]

Concrete problem

The tissue of a tube-shaped organ constricts to pinch off into two chambers. The tissue is incompressible.

a) Consider a step function for the constriction. How does each segment deform to maintain area? (Ie what is the motion of cells on the surface that results?)

b) Consider an advancing Gaussian profile for the constriction. What is the flow field on the surface that results?

c) Is the tissue flow aligned with (or perpendicular to) the local axis of elongation?

d) What makes this solution counter-intuitive?

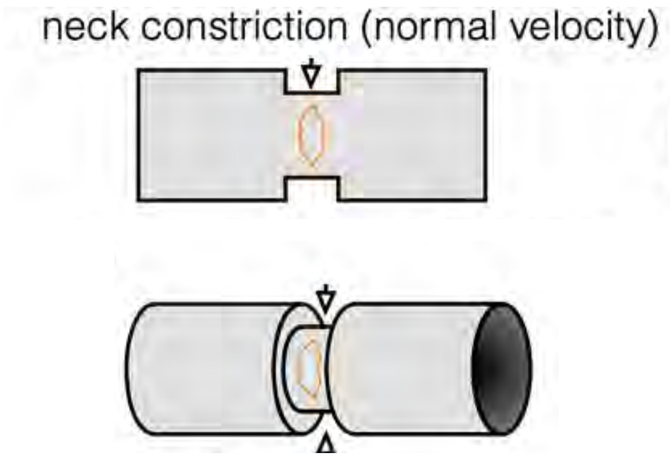

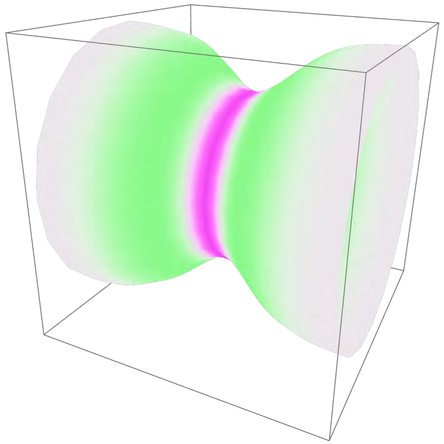

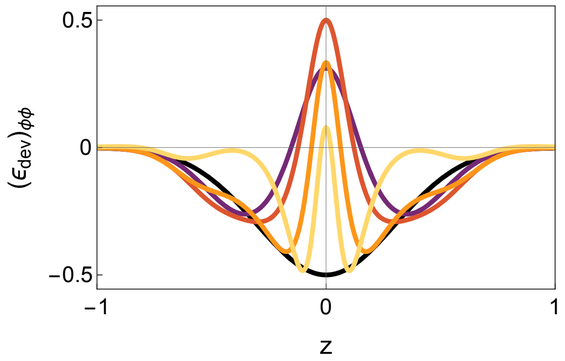

Open-ended question

Consider an elongated organ with a lumen inside, such as the embryonic gut tube containing yolk. The tube contorts into a chiral geometry akin to a helical tube.

a) What are in-plane deformations of a tube that generate intrinsic chirality – ie, coiling – of the tube's centerline?

b) What cellular (mechanical) mechanisms could drive such kinematics?

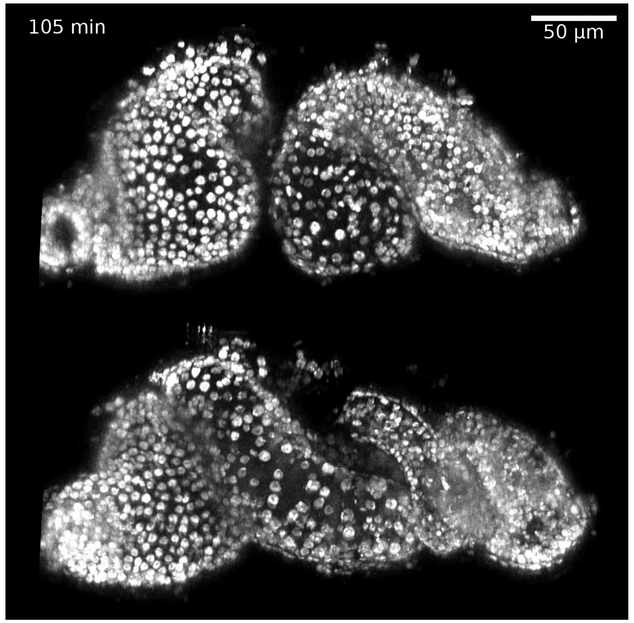

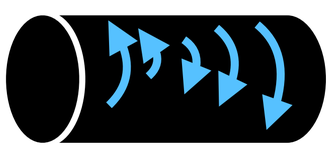

Bend + twist

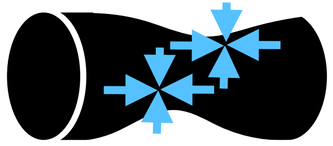

Dilation along a helix

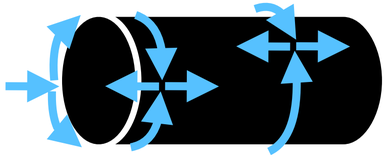

Convergent extension along a helix

Concrete problem:

Solution

Setup:

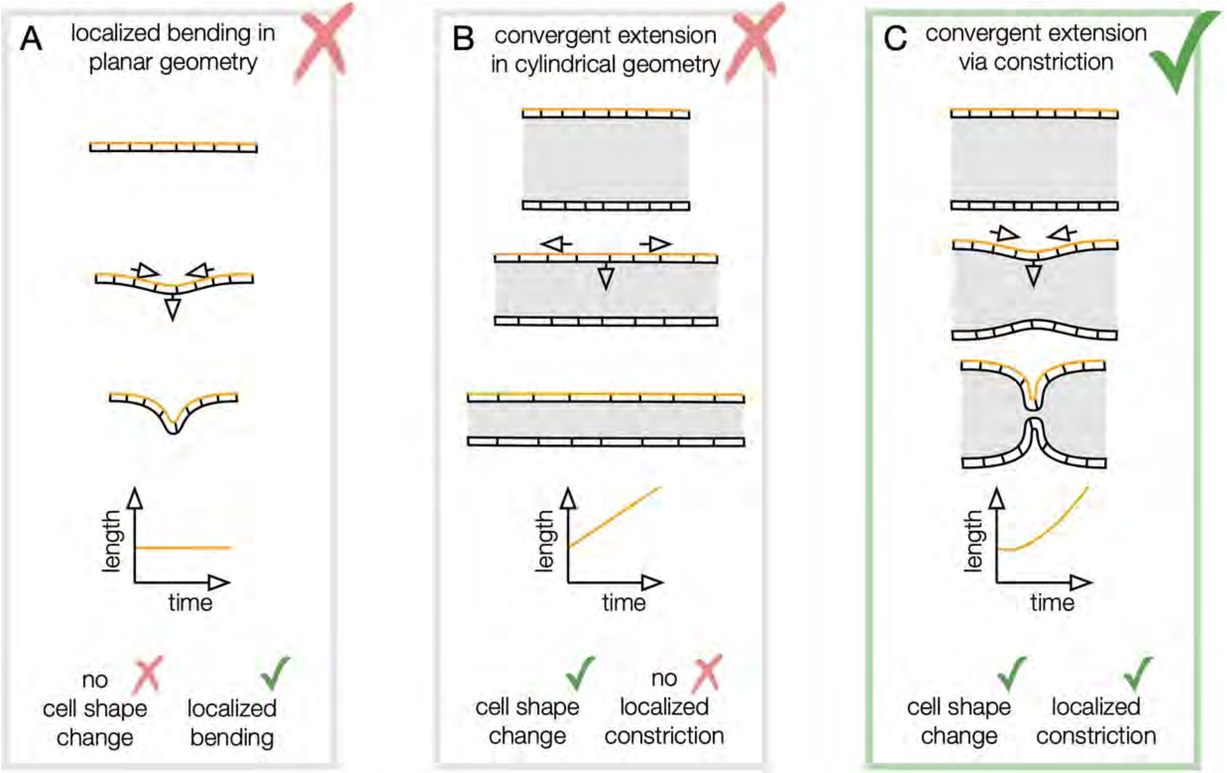

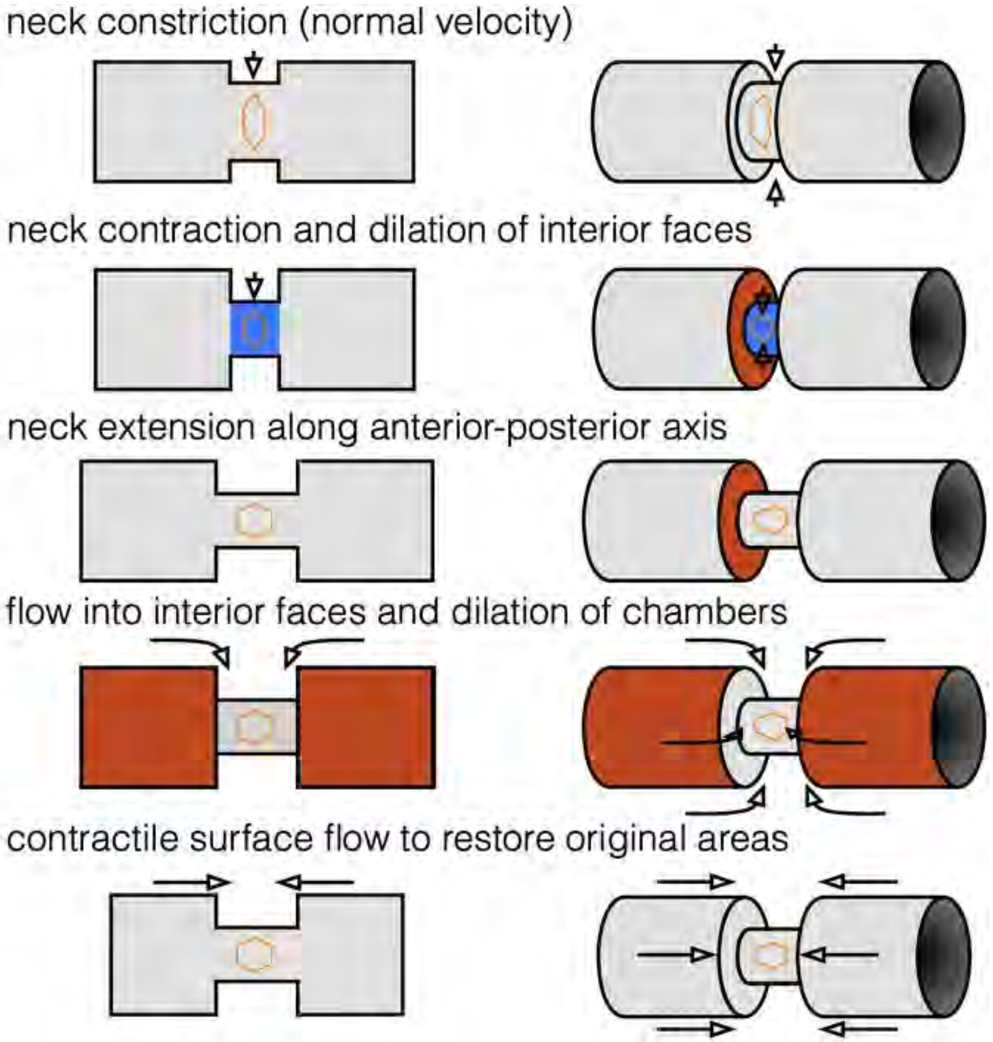

Concrete problem:

Solution